University of Louisville
ThinkIR: The University of Louisville's Institutional Repository

Electronic Theses and Dissertations

8-2021

Develop a multi-functional green pervious concrete (MGPC) pavement with polycyclic aromatic hydrocarbons (PAHs) removal function.

Hong Shang
University of Louisville

Follow this and additional works at: https://ir.library.louisville.edu/etd

 Part of the Civil Engineering Commons, Environmental Engineering Commons, Geochemistry Commons, Geotechnical Engineering Commons, and the Hydraulic Engineering Commons

Recommended Citation

Shang, Hong, "Develop a multi-functional green pervious concrete (MGPC) pavement with polycyclic aromatic hydrocarbons (PAHs) removal function." (2021). *Electronic Theses and Dissertations.* Paper 3681.
Retrieved from https://ir.library.louisville.edu/etd/3681

This Doctoral Dissertation is brought to you for free and open access by ThinkIR: The University of Louisville's Institutional Repository. It has been accepted for inclusion in Electronic Theses and Dissertations by an authorized administrator of ThinkIR: The University of Louisville's Institutional Repository. This title appears here courtesy of the author, who has retained all other copyrights. For more information, please contact thinkir@louisville.edu.

DEVELOP A MULTI-FUNCTIONAL GREEN PERVIOUS CONCRETE (MGPC) PAVEMENT WITH POLYCYCLIC AROMATIC HYDROCARBONS (PAHS) REMOVAL FUNCTION

By
Hong Shang
B.S., Tongji University, China, 2006
M.S., University of Louisville, USA, 2015

A Dissertation
Submitted to the Faculty of the
J. B. Speed School of Engineering of the University of Louisville
in Partial Fulfillment of the Requirements
for the Degree of

Doctor of Philosophy
in Civil Engineering

Civil and Environmental Engineering Department
University of Louisville
Louisville, Kentucky

August 2021

Copyright 2021 by Hong Shang

All rights reserved

DEVELOP A MULTI-FUNCTIONAL GREEN PERVIOUS CONCRETE (MGPC) PAVEMENT WITH POLYCYCLIC AROMATIC HYDROCARBONS (PAHS) REMOVAL FUNCTION

By

Hong Shang
B.S., Tongji University, China, 2006
M.S., University of Louisville, USA, 2015

A Dissertation Approved on
April 16, 2020

By the following Dissertation Committee

_____
Dr. Zhihui Sun (Dissertation Director)

_____
Dr. Nageshwar R. Bhaskar

_____
Dr. Thomas D. Rockaway

_____
Dr. Noppadon Sathitsuksanoh

DEDICATION

This dissertation is dedicated to my beloved parents

Mr. Lin Shang

and

Mrs. Lianhui Liu

For their love, support, and encouragement

ACKNOWLEDGEMENTS

To begin with, I would like to convey my sincere gratitude to my dissertation advisor, Professor Dr. Zhihui Sun, the chair of the Civil and Environmental Engineering Department, for her tremendous help, invaluable support, constructive guidance, inspiring encouragement, and financial aid throughout my whole Ph.D. study. As an "old" guy pursuing an advanced degree abroad after working in the industry for more than eight years, I always struggled for my academic progress. Dr. Sun strategized all the significant training for me, such as technical writing, classroom teaching, off-campus training, and conference presentations, etc. She also advised me on going through all the details timely and smoothly. Long story short, it is hard to find words to express the full measure of my appreciation to my dear advisor Dr. Zhihui Sun. So please accept my vehement gratitude here!

Next, I extend my appreciation to my dissertation committee members, Dr. Nageshwar R. Bhaskar, Dr. Thomas D. Rockaway, and Dr. Noppadon Sathitsuksanoh (Tik) for their elaborate guidance, scientific suggestion, and academically challenging. It is a great horror for me to work as a teaching assistant for Dr. Bhaskar for multiple courses. It was really a joyful experience. Dr. Rockaway is a real gentleman helping me settle down from day one here and advised me to adapt to the new academic life. Dr. Tik is an enthusiastic researcher having a lot of formal and informal discussions with me that helped me further consolidate my knowledge with critical thinking skills.

I would also like to acknowledge Dr. J. P. Mohsen, the former chair of the Civil and Environmental Engineering Department and the current associate dean of J.B. Speed Engineering School, for his generosity and endless help.

I would like to appreciate Mr. Bernie Miles, our great technician, for helping me in solving all the technical issues in the lab.

I also want to thank Dr. Biyun Shi from the Chemical Engineering Department of UofL and Sihang Chen from the Department of Chemical Engineering, Tianjin Normal University, for broadening my knowledge on Chemistry and Gas Chromatography implementations. It is very important to my research!

My thanks also go to my dear friend Dr. Yao Zhang, Dr. Nageshwar R. Bhaskar, Dr. Thomas D. Rockaway, Dr. Young Hoon Kim, and Mr. David Kessinger, for serving as the professional references of my PE license application.

I would like to thank my American house family, Mr. Jim Whitaker and Cindy Whitaker for always hosting and organizing interesting activities for international students like me. We learn a lot of great American culture, history, and spirit there. They make me feel like home even thousands of miles away from my hometown. May God bless them!

Special thanks to my iTalki English teacher Alexandra C. MacArthur from UC Berkley, for her enormous help to improve my language skills. It is beneficial to my research tasks, my teaching work, and my future career.

I also want to thank outstanding CEE students, Avery Bergdorf, Morgan Day, Grace Bank, Alexandra Wright, Diana Dunn, Eleanor Carrico, Briana Kozlowski, Emma Cecil, McKenna Jobe, Tom Jones, Matthew Groves, Cameron Gomes, Juan Aguero Martinez, etc.

Your questions, your efforts, and your energetic attitudes force me to be a better TA and civil engineer. There is no doubt that you would be the best engineers in the US tomorrow, and I look forward to having new collaborations with all you guys in my future career.

I thank my officemates and friends, Mr. Aofei Guo, Dr. Long Zheng, Dr. Brendan McLeod, Dr. Fengjuan Liu, Mr. Song Wang, Dr. Bashir Hasanzadeh, Mr. Mohammad Joshaghani, Dr. Sadra Javadi, Mr. Mahyar Ramezani, Ms. Jing Ma for their friendship and support.

I would like to thank the former faculty, Dr. Qian Zhao, for introducing the University of Louisville to me and serving as my master's thesis advisor.

I am grateful to my dear parents, Mr. Lin Shang and Ms. Lianhui Liu, for their never-ending support and encouragement to help me overcome the unexpected difficult time here. My parents sacrificed a lot of their personal lives to frequently visit me. We have a great time at Alaska, Arctic Ocean, Rocky Mountains, western and eastern coasts, and northern and southern states. I love my parents and I am so proud to be their son!

This work was also financially supported by the Civil and Environmental Department at J.B. Speed Engineering School, University of Louisville. I enjoy every day when studying here. It is a really great experience!

ABSTRACT

DEVELOP A MULTI-FUNCTIONAL GREEN PERVIOUS CONCRETE (MGPC) PAVEMENT WITH POLYCYCLIC AROMATIC HYDROCARBONS (PAHS) REMOVAL FUNCTION

Hong Shang

April 16, 2020

Stormwater runoff induced Polycyclic Aromatic Hydrocarbons (PAHs) contaminant increasingly imperils the groundwater quality and the sustainable development of human society due to the potential carcinogenic risks. Pavement can be considered as the first line of defense for contaminant removal of the stormwater runoff. New construction materials with stormwater runoff quantity and quality control are in urgent demand for updating the existing pavement system. An innovative material called Multi-functional Green Pervious Concrete (MGPC) was developed in the department of Civil and Environmental Engineering at University of Louisville. This material uses organoclay as the amendment to enhance the PAHs removal capacity of conventional pervious concrete. The objective of this study is to evaluate the potential implementation of MGPC as a pavement material with the groundwater contamination remediation functions.

The study was performed in five stages. First, The PAHs remediation function of MGPC was tested by introducing organoclay [bis (hydrogenated tallow alkyl) dimethyl ammonium modified montmorillonite] to the conventional pervious concrete. After test and verification, the mix proportion of MGPC was designed to meet the compressive strength and hydraulic conductivity requirements of pervious concrete. A small amount of organoclay addition was found not to adversely affect the compressive strength and hydraulic conductivity of MGPC.

The preliminary study of the PAHs removal functions of MGPC was conducted in stage two. The isothermal batch sorption test was conducted to quantify the sorption capacity of the organoclay modified cement paste, and the column test was performed to investigate the transport mechanism and retardation behavior of PAHs in MGPC. It was found that the developed MGPC with a small addition of organoclay could substantially remove PAHs contaminants and it also has much stronger adsorption and retardation capacity than the conventional pervious concrete.

In stage three, a series of comprehensive laboratory-scale tests were conducted to examine the effectiveness of stormwater induced PAHs removal by using the MGPC pavement. The results indicated that the initial concentrations of the PAHs and the flow rates would impact the removal efficiency of MGPC. The tests showed that the MGPC still maintained considerable sorption capacity after 50 PAHs sorption and desorption cycles.

An ideal site under steady-state groundwater conditions was generated to simulate the long-term performance of MGPC on PAHs removal by using the finite element method in stage four. The laboratory experiments were used to determine the physicochemical parameters of MGPC, and three sorption isothermal models (linear, Freundlich and Langmuir) were

fitted to the sorption test data. The computer simulation revealed that the MGPC had significant remediation efficiency on the PAHs contaminant. Other than the material properties of MGPC, the efficiency of contaminant remediation of MGPC was also found to be influenced by the permeability of the subbase and the initial concentration of PAHs. It was also found that the linear isotherm model would overestimate the removal efficiency of PAHs with higher concentration sources.

At last final fifth stage, a Pavement Environment and Performance Index (PEPI) was proposed to evaluate the environmental impacts of three different types of pavements (impervious concrete, conventional pervious concrete, and MGPC). The data from experiments and the Environmental Footprint Database was used to calculate the PEPI. Based on the Life Cycle Assessment (LCA) results, it was found that the MGPC pavement was much more environmentally friendly with relatively lower greenhouse gas emissions and energy consumption, and better environmental performance comparing with the other two types of pavements.

TABLE OF CONTENTS

LIST OF TABLES

LIST OF FIGURES

CHAPTER 1 INTRODUCTION

1.1 Problem statement and research significance

Groundwater quality is essential for drinking water supply, civil engineering practice, and sustainable development that influences our daily life. Due to metropolitan expansion and increases of impervious surfaces, the contaminants can be dissolved, carried and conveyed by the stormwater runoff and finally be discharged into the groundwater system (Göbel et al., 2007; Mikkelsen et al., 1997; Pitt et al., 1999; Pitt, 1996; Zobrist et al., 2000). Therefore, the stormwater runoff-induced contamination, primarily, from nonpoint source pollution, becomes one of the major contaminant sources to groundwater and increasingly imperils the quality and safety of groundwater supply (see **Fig. 1.1**).

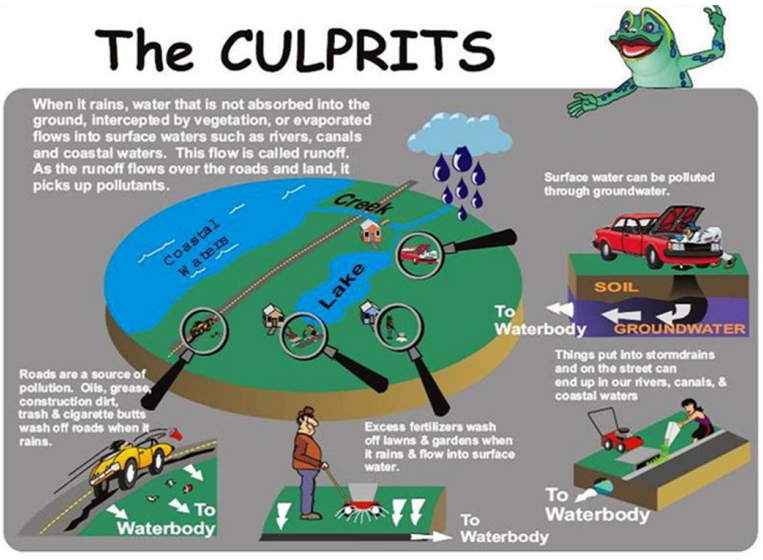

Fig. 1.1. Stormwater runoff induced nonpoint source contaminant (Palmetto Bay)

It is also found that stormwater runoff is a leading source of pollutants entering our waterways (Mikkelsen et al., 1994). According to previous studies, about 90 percent of surface pollutants are carried by the first flush (half to one inch) of the stormwater runoff (Chang et al., 1990; Froehlich, 2009; Ringler, 2007; Schueler, 1994). Stormwater drains do not typically channel this polluted runoff to treatment facilities, but instead, convey it directly into local water bodies. This can increase algae content and harm aquatic life, requiring expensive treatments to purify the water and eventually form a long-term contaminant source to water circle, especially to the groundwater system.

Among various stormwater induced runoff contaminants, Polycyclic Aromatic Hydrocarbons (PAHs) are ubiquitous and significantly cumulative cancerogenic components that threaten public health and the sustainability of ecosystem (see **Fig. 1.2**) (Benson et al., 2008; Chang et al., 2006; Gehle, 2009; Greish et al., 2018; Wilcke, 2007). Stormwater runoff induced PAHs are investigated mainly releasing from the vehicle emission, incomplete combustion of petroleum products, engine oil leakage, tire wear, asphalt deterioration, human sewage sludge, mining operation, industrial operation, landfill leachate, coal tar and roof tar erosion (Lowenthal et al., 1994; Marr et al., 1999; Miguel et al., 1998; Schuetzle, 1983; Wilcke, 2007; Zielinska et al., 2004). As non-polar substances with chemical stability, PAHs will eventually migrate into the groundwater system and degrade the water supply quality by a cumulative effect. It takes an extremely long time to finish the self-purification process only by the natural groundwater system itself due to cold environment, less bacterial breakdown, very slow water movement and precipitation of the rocks in the aquifer (Rothermich et al., 2002; Saba et al., 2012). PAHs could be cancerogenic after reaching certain concentrations. EPA has listed 16 PAHs as priority

pollutants due to their toxicity and potential for human exposure (Bojes and Pope, 2007; Chang et al., 2006; Yan et al., 2004). Therefore, mitigation PAHs contamination from stormwater runoff adjacent to transportation corridors needs significant attention.

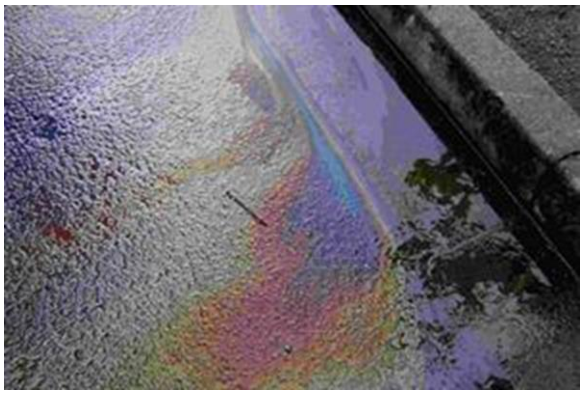

Fig. 1.2. Stormwater runoff induced PAHs contaminant (City of Lubbock)

The boundary between the natural environment and existing infrastructures need improvements on pollutions reduction without increasing infrastructure footprint. Additionally, the impervious pavement occupies a majority part of the ground surface in U.S. urban areas, such as the road systems, the parking lots, and the community ground surfaces. These pavement systems are aging, and the innovative construction materials are eagerly in demand to replace the deteriorated asphalt or concrete. The current pavement material needs to be redesigned to incorporate stormwater runoff quantity and quality control functions as it can play an important role in our efforts on stormwater management to integrate environmental protection and sustainability. To enhance the concrete performance by introducing additives through hydration process, such as clayey materials, nanocellulose plant fibers, and carbon nanotubes, has become a current hot topic (Guo et

al., 2019a; Guo et al., 2020a; Guo et al., 2020b; Guo et al., 2019b, 2020c; Ramezani et al., 2019). This research focuses on an innovative multi-functional green pervious concrete that is developed as paving material to reduce the flooding and stormwater runoff-induced PAHs contamination, and to create a more sustainable, resilient, and eco-friendly living environment.

1.2 Pervious Concrete (PC) Pavement

Urbanization not only promotes economic growth and well-being but also induces environmental issues. As discussed in the above section, the urbanization process can increasingly result in transferring natural soil and other initially permeable ground surfaces into impervious covers. It would bring high impacts on the urban watershed and lead to serious consequences such as rapid urban flood, increased runoff volume, soil erosion, nonpoint source pollutions, and higher local peak discharges (Damodaram et al., 2010; Dietz, 2007; Matos et al., 2019). If a Low Impact Development (LID) approach can be applied in the field design, by mimicking the natural flow regime associated with building centralized stormwater runoff management facilities, those issues could be avoided. Thus, a better-designed tactic of LID that can strategically and significantly reduce the environmental impacts is in urgent demand.

There are various reasons can result in urban watershed change and the impervious pavement can be considered as one of the main reasons (Arnold Jr and Gibbons, 1996). Although only about 1.3% of total US territory is paved, it still has a significant environmental impact in the urban area. Urban Heat Island (UHI) effect is one attribute to the impervious pavement application that impacts local climate, urban ecosystem, energy

consumption, and human health (Bornstein, 1968; Imhoff et al., 2010). In the US 94% of the impervious pavements are paved by asphalt and most of them are facing the deterioration issue. A good strategy of LID application can also solve the non-point source pollution issue and the UHI effect onsite.

The impervious surface basically consists of roads, parking lots and building roofs. And the non-point source pollution is mainly due to the increasingly severe traffic loads. The roads and parking lots play a vital role in protecting the water quality and the surrounding ecosystem and should be designed and maintained in such way to avoid and control the negative environmental impacts. The Best Management Practices (BMPs) have been in place for several decades which are the principles and engineering practices that protect the water quality in the field while maintaining the functions of the roads and parking lots (Damodaram et al., 2010; Field and Tafuri, 2006; Keller and Sherar, 2003; Kwiatkowski et al., 2007). If applied properly, BMPs can provide a practical, cost-effective, and environmentally friendly ground surface design. And it will also avoid the conflicts of land use that is especially important for some urban areas with limited land supply.

Permeable pavements could be a good solution that avoids changing the watersheds and functions of the roads. As one special solution of BMPs, permeable pavements can additionally save the land use with building the *in-situ* sewer and stormwater control and management infrastructures such as detention or retention ponds. There are different types of permeable pavements including gravel, tarmac (or pervious asphalt), rainwater harvesting, pervious concrete (or porous concrete), pervious blocks, wheel tracks, open concrete blocks or plastic blocks, etc. Among them, the pervious concrete attracts the public interests because it can be used as an alternative construction material for pavement

design (Chandrappa and Biligiri, 2016b; Debnath and Sarkar, 2018; Tennis et al., 2004; Zhong et al., 2018). Comparing with other permeable pavement materials, pervious concrete has more broad potential applications. It can supply adequately enough strength for most of the low volume pavements; it does not dramatically change the mix, installation and maintenance processes; and it still keeps considerable permeability for stormwater quantity control (ACI 522R-10, 2010; Obla, 2010). Pervious concrete is a unique type of concrete using a carefully controlled amount of cement paste to coat and bind the uniformly sized coarse aggregates and containing little or no fine aggregates to form a system of interconnected voids and high porosity that can drain water quickly (see **Fig. 1.3**) (ACI 522R-10, 2010; Ćosić et al., 2015; Obla, 2010; Tennis et al., 2004; Torres et al., 2015). When pervious concrete is used as a pavement material, the typical configuration is shown in **Fig. 1.4**. Due to the relatively lower compressive strength, pervious concrete is often used as a paving material for low traffic volume surfaces such as sidewalk, highway shoulders, parking lots, and residential roads (see **Fig. 1.5**).

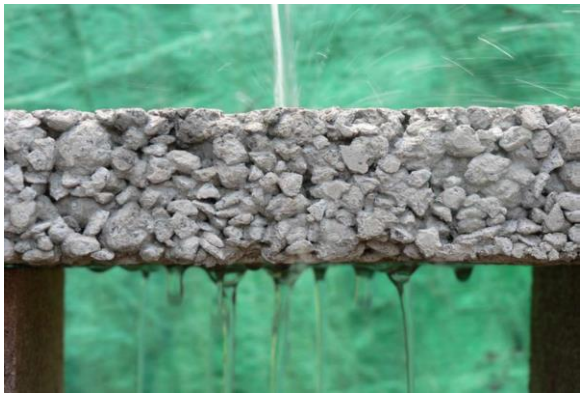

Fig. 1.3. Conventional pervious concrete (Ready Mixed Concrete Association)

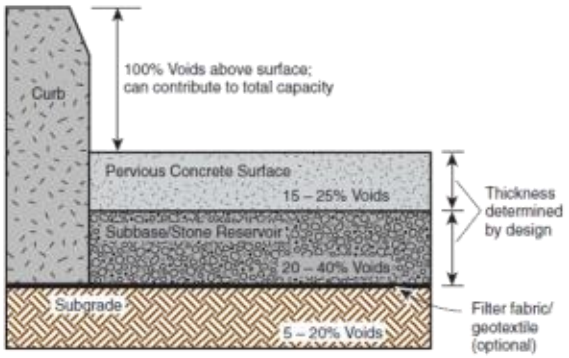

Fig. 1.4. Configuration of pervious concrete pavement (Adapted from Tennis et al. (2004))

(a) (b)

Fig. 1.5. Pervious concrete pavement used for (a) parking lot and (b) residential roads (Ready Mixed Concrete Association)

1.3 Modified Pervious Concrete Pavement

1.3.1 Short Review of the Studies for Modified Pervious Concrete

Pervious concrete pavement is basically a bi-functional strategy for using as both a low volume road and *in-situ* stormwater management. A pervious concrete pavement should be designed to provide sufficient compressive strength for the traffic loads as well as enough permeability for managing the stormwater runoff infiltration. As a plain

cementitious material, the conventional pervious concrete lacks the capability of adsorbing contaminants or purifying the stormwater onsite (Brattebo and Booth, 2003; Kasaraneni et al., 2014; Shang and Sun, 2019). The key idea of pervious concrete for water protection is to immobilize the stormwater in the very beginning as much as possible to avoid the runoff induced contaminants.

The watersheds are hardly predictable and are unable to totally control especially for the intensive rainfall events. Some relevant research has been done in order to enhance the pervious concrete pavement from a bi-functional structure to a multi-functional structure with self-purification functions. For example, Titanium Dioxide has been coated on pervious concrete pavement to reduce the nitrogen oxides and volatile organic compounds level by the photocatalytic reactions (Shen et al., 2012). Porous media such as natural zeolite, calcite, sand, iron, organo-bentonite, organo-zeolite or organo-kaolinite are found to improve the heavy metals or PAHs adsorption capacity from the liquid phase and can be used as the subbase or subgrade additives (Kasaraneni et al., 2014; Lee and Tiwari, 2012; Reddy et al., 2013, 2014b; Shang, 2015; Shang et al., 2017; Shu et al., 2010; Simpson and Bowman, 2009). Other filter materials like biochar have also been used as a filter media to remove selected contaminants including the PAHs (Reddy et al., 2014a; Xie et al., 2015a; Xie et al., 2015b).

1.3.2 Multi-functional Green Pervious Concrete (MGPC)

During the intensive rainfall events, the pervious concrete pavement will firstly capture and store the stormwater runoff into the interconnected voids of pervious concrete and subbase and then gradually finish the inflation back to groundwater through the subgrade.

If the pervious concrete itself has the water purification function, it would be highly efficient in stormwater quantity and quality control. **Fig. 1.6** presents a conceptual idea that introduces the organoclay particles into the conventional pervious concrete. Organoclay has been proved to be a reliable filter material for contaminants removal especially the organic contaminants like PAHs. This dissertation focuses on developing an organoclay amended pervious concrete that has a water purifying function. The developed Multi-functional Green Pervious Concrete (MGPC) is expected to adsorb the PAHs from the stormwater onsite in a short time window (see **Fig. 1.7**). The purified stormwater can be discharged back to the underlying groundwater as a safe recharge.

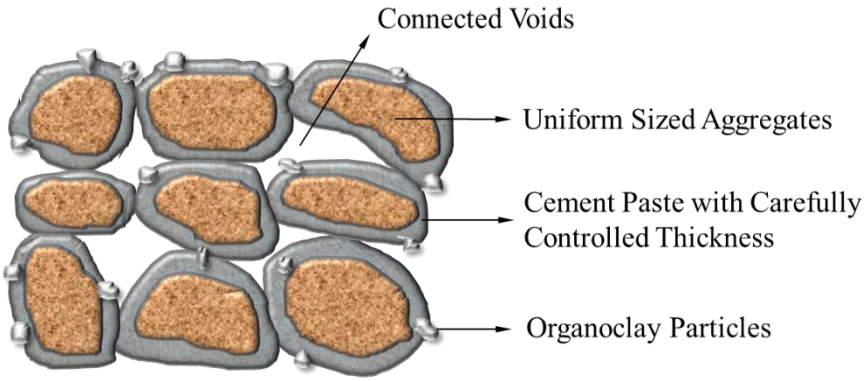

Fig. 1.6. Conceptual model of MGPC

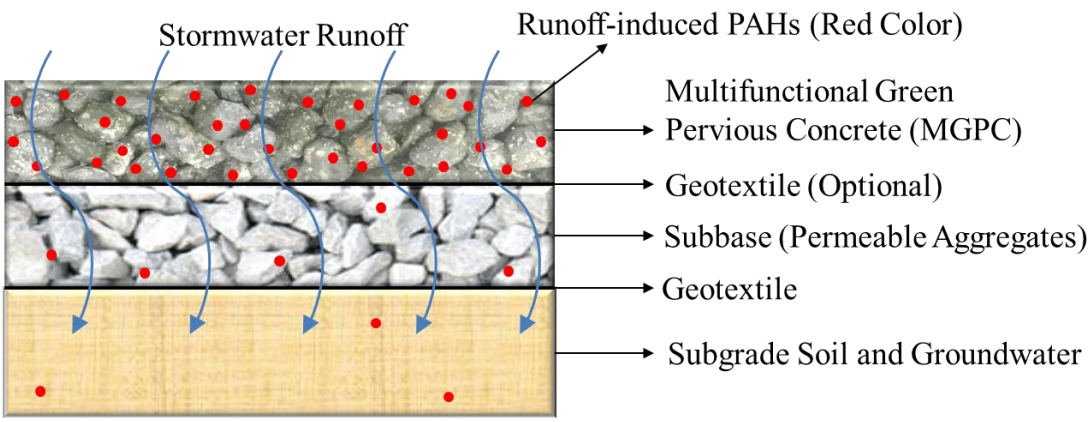

Fig. 1.7. Deliverables of MGPC Pavement System

1.4 Research Objectives

This dissertation aims to develop a multi-functional green pervious concrete (MGPC) as an alternative pavement material with the stormwater runoff-induced PAHs removal functions. Organo-bentonite is chosen as the absorbent in this study. To guarantee the water purifying function as well as the long-term serviceability of the proposed concrete, the research goal can be divided into several folds.

First, an appropriate filter material that can be used as the adsorbent in pervious concrete needs to be identified. Second, it is necessary to assure that the filter material additive would not lower or harm the inherent mechanical and hydraulic properties of the pervious concrete. Third, the effectiveness of PAH removal after incorporating this type of filter material in the developed MGPC needs to be evaluated. While functioning as a PAHs adsorbent, and the added organoclay must not interfere with cement hydration so that the strength development of the MGPC can be guaranteed. Fourth, key parameters related to field applications of the developed MGPC should be comprehensively tested. Finally, the

long-term performance of the MGPC pavement on purifying PAHs needs to be studied since the pavement is typically designed for several decades.

1.5 Structures of this Dissertation

The dissertation consists of three parts. Part one is a general introduction to the motivation and objectives of this research project (Chapter 1). A state-of-the-art literature review regarding the pervious concrete pavement research is also presented in Chapter 1. Chapter 2 introduces the raw materials for making the MGPC and the fundamental testing methods for investigating the compatibility between organoclay and cement paste after hydration. The experimental framework for developing a practicable MGPC is also discussed.

The second part mainly tests the short-term and long-term water purifying capacity of the developed MGPC, in which lab experiments have been systematically conducted and several empirical scenarios are simulated in order to verify that the innovative MGPC is appropriate construction material for field applications. The adsorption capacity, transport mechanism and retardation behavior of PAHs onto the MGPC are evaluated in Chapter 3. Additionally, the hydration age effect on the adsorption and retardation performance of MGPC are examined in this chapter. Chapter 4 elaborates on the extensive study of PAHs removal by the MGPC. Different laboratory experimental scenarios are carried out to mimic the real onsite conditions which would affect the MGPC performance. And the reusability and long-term performance of the MGPC is also investigated after being polluted by PAHs with multiple cycles. Following the lab experiments, the evaluation of the long-term performance of *in-situ* MGPC pavement under different pavement and field conditions is discussed in Chapter 5. A numerical model software, GeoStudio, is introduced

and used to simulate the transport mechanism and removal of PAHs by the MGPC pavement for 50 years. Critical analysis of MGPC using as a pavement material for *in-situ* stormwater runoff-induced PAHs purification is given.

The third part of this dissertation focuses on the Life Cycle Assessment (LCA) of the MGPC pavement. In Chapter 6, the LCA result of the MGPC pavement is compared with impervious concrete pavement and conventional pervious concrete pavement. The standard framework of LCA combined with PAHs purification function and permeability are applied to the LCA. Five phases of the whole life cycle of pavement including materials, construction, use, maintenance, and end-of-life are considered as the main factors in the LCA process. The primary data of the Life Cycle Inventory (LCI) analysis is obtained from lab experiments, and the secondary data is collected from OpenLCA software associated with the Environmental Footprint Database. A Pavement Environment and Performance Index (PEPI) using the normalization method is proposed to comprehensively give the assessment of the pavement environmental impacts.

CHAPTER 2 DEVELOPING A MULTI-FUNCTIONAL GREEN PERVIOUS CONCRETE (MGPC)

2.1 Introduction

The desired properties of pervious concrete such as hydraulic conductivity and strength are usually related to its porosity (Ibrahim et al., 2014). And an optimal porosity of MGPC could be obtained by controlling the level of aggregates to cement ratio, water to cement ratio, and initial compaction effort. The porosity which can affect the compressive strength is the overall porosity. In contrast, only the connected voids that is frequently called the effective porosity would determine the hydraulic performance of the pervious concrete (Montes et al., 2005).

Numerous studies have been reported in the literature about the mechanical and hydraulic behaviors of pervious concrete. In general, due to the open void structure, pervious concrete has relatively lower compressive strength from 3.5 MPa to 28 MPa compared to the conventional concrete (Deo and Neithalath, 2010; Obla, 2010; Tennis et al., 2004). The permeability (or hydraulic conductivity) of the pervious concrete is in the range from 0.076 cm/s to 3.5cm/s that highly depends on the effective porosity (Chandrappa and Biligiri, 2016a; Ibrahim et al., 2014; Li et al., 2013; López-Carrasquillo and Hwang, 2017; Neithalath et al., 2010). The water to cement ratio (targeted range is 0.27 to 0.36) should be controlled carefully to form an appropriate cement paste thickness just enough coating

on the aggregates because the excessive cement paste would significantly decrease the porosity and lower the permeability of the pervious concrete (Joshaghani et al., 2015; Nguyen et al., 2014; Torres et al., 2015).

Current research on pervious concrete mainly focuses on improving its compressive strength to extend its future applications such as highway or interstate highway pavements. High-performance pervious concrete (HPPC) with fibers, polymers, pozzolans (fly ash or silica fume), water reducer or superplasticizer amendment was found to have the compressive strength within the range from 10 MPa to 65.8 MPa without sacrificing the permeability performance (Aoki et al., 2012; Bhutta et al., 2012; Chindaprasirt et al., 2008; Huang et al., 2010; López-Carrasquillo and Hwang, 2017; Yang and Jiang, 2003; Zhong and Wille, 2015). Other studies tried to achieve a better understanding of the permeability characteristics of pervious concrete under turbulent flow when Darcy's law is invalid. Huang et al. (1999) developed a permeability testing apparatus to determine the hydraulic conductivity of the samples with large air voids under non-laminar flow. Chandrappa and Biligiri (2016a); Owabor et al. (2012) Chandrappa and Biligiri (2016a); Owabor et al. (2012) A nonlinear asymptotic relationship between the permeability and water head was observed and built up from the permeability test of pervious concrete. (Chandrappa and Biligiri, 2016a).

To achieve the goal of this research, organoclay is added to pervious concrete to achieve the water purifying function. This chapter evaluates the impacts of organoclay addition on the cement hydration, MGPC mechanical properties, and hydraulic performances of the MGPC. The hydration ages (1d, 7d, and 28d) and additive dosages of organoclay would be considered as the variables. The one-dimensional compressive test was used to investigate

the compressive strength of the MGPC. And a modified method with the self-built apparatus has been conducted to evaluate the hydraulic conductivity of the MGPC based on Darcy's law (Ibrahim et al., 2014; Li et al., 2013; Shang and Sun, 2019).

2.2 Materials and Methods

2.2.1 Cement

Type I/II LA Portland cement, sponsored by Cemex Kosmos Cement Plant, was used for this study (see **Fig. 2.1**). Different from the conventional concrete, cement mainly supplies the connection functions to the aggregates of the pervious concrete instead of strength contribution. The chemical oxide compositions and the mineral clinker compounds are shown in **Table 2.1 and Table 2.2**, respectively. The chemical oxide compositions were obtained from the manufacturer's daily production sample analysis data, and the mineral clinker compounds of this cement were identified based on the Bogue's equations (Bogue, 1955):

$$C_3 = 4.07(CaO) - 7.60(SiO_2) - 6.72(Al_2O_3) - 1.43(Fe_2O_3) - 2.85(SO_3) \quad (2-1)$$

$$C_2S = 2.87(SiO_2) - 0.75(C_3S) \quad (2-2)$$

$$C_3A = 2.65(Al_2O_3) - 1.69(Fe_2O_3) \quad (2-3)$$

$$C_4AF = 3.04(Fe_2O_3) \quad (2-4)$$

The Blaine surface area of this cement was 382.2 m^2/kg (ASTM C204-16), and the specific gravity was 3.15 (ASTM C188-16). 97.5% of the cement powder pass through the sieve

NO. 325 (45 μm) (ASTM C430-08(2015)). The initial setting time is 112 min and the final setting time is 240 min (ASTM C191-13).

Table 2.1 Chemical compositions of Type I/II LA Portland cement by the manufacturer's daily production sample analysis

Clinker Phases	Weight (%)
CaO	63.30
SiO_2	19.70
Al_2O_3	5.00
Fe_2O_3	3.47
MgO	3.59
SO_3	2.50
Na_2O	1.55
K_2O	0.45
Loss on Ignition	0.54

Table 2.2 The major compounds of Type I/II LA Portland cement by Bogue's equations

Compound	Chemical formula	Abbreviated Formula*	Weight (%)
Tricalcium Silicate	$3\ CaO{\cdot}SiO_2$	C_3S	60.37
Dicalcium Silicate	$2\ CaO{\cdot}SiO_2$	C_2S	15.12
Tricalcium Aluminate	$3\ CaO{\cdot}Al_2O_3$	C_3A	4.53
Tetracalcium Aluminoferrite	$4\ CaO{\cdot}Al_2O_3{\cdot}Fe_2O_3$	C4AF	12.40

*C = Calcium Oxide, S = Silicon Dioxide, A = Aluminum Oxide, and F = Iron Oxide.

Fig. 2.1. Type I/II LA Portland Cement

2.2.2 Aggregates

Gravels used for this study were sieved between 1/2 and 3/8 inch to maintain the size uniformity (see **Fig 2.2**) (ASTM C136/C136M-14). The uniform sizes of aggregates are important to maintain connected voids and large hydraulic conductivity for the pervious concrete (Ćosić et al., 2015; Schaefer et al., 2006; Tennis et al., 2004). The specific gravity of the aggregates is 2.74 (ASTM C128-15). The sieved aggregates were then oven-dried for 24h before casting pervious concrete samples.

Fig. 2.2. 0.9525 ~ 1.27 cm (3⁄8 ~ 1⁄2 in.) rounded aggregates

2.2.3 Modified Organoclay

For the filter material that can be used in concrete, clay is a good candidate. It is because clay is widely available on the market, and it is a common additive in the concrete mix. Among various types of clays (see **Fig. 2.3**), the sodium bentonite modified by an organic

surfactant has demonstrated to have one of the most efficient sorption capacities for the dissolved organic contaminants. It has been used as the pervious concrete amendment additive (Knox et al., 2007; Reible et al., 2008). To synthesize this organoclay, particle sodium bentonite needs to be treated by an organic surfactant amine, named bis (hydrogenated tallow alkyl) dimethyl ammonium chloride, based on the interlayer cation exchange modification (see **Fig. 2.4**). For this study, particle PM-199 (between mesh 14-40), a commercial organoclay (CETCO Co.) was chosen for conducting the experiments (see **Fig. 2.5**). The specific gravity of the particle PM-199 is 1.75 (ASTM D854-14) and the specific surface is 60.7 m^2/g determined by methylene blue (Fisher Scientific Co.) spot test (ASTM C837-14; Santamarina et al., 2002; Sivapullaiah et al., 2008):

$$S_S = \frac{1}{M_W}\frac{1}{V}(0.5N)A_v A_{MB}\frac{1}{M_S} \qquad (2-5)$$

where S_S (m^2/g) is the specific area of the tested organoclay, M_w (g/mol) is the molecular weight of the used methylene blue, V (mL) is the volume of deionized water used as a solvent for methylene blue, N is the number of methylene blue increments, A_v (6.02×10^{23} mol^{-1}) is the Avogadro number, A_{MB} (1.3 nm^2) is the area occupied by one methylene blue molecular, and M_S (g) is the total mass of soil in the soil solution.

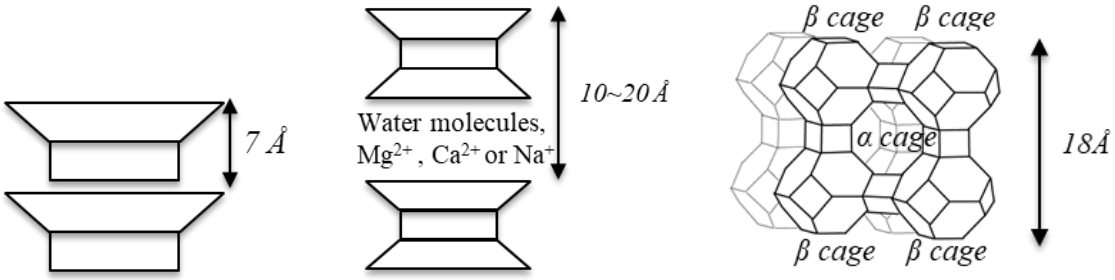

(a) (b) (c)

Fig. 2.3. Common clay minerals used for concrete mixing (a) Kaolinite (b) Montmorillonite (c) Zeolite

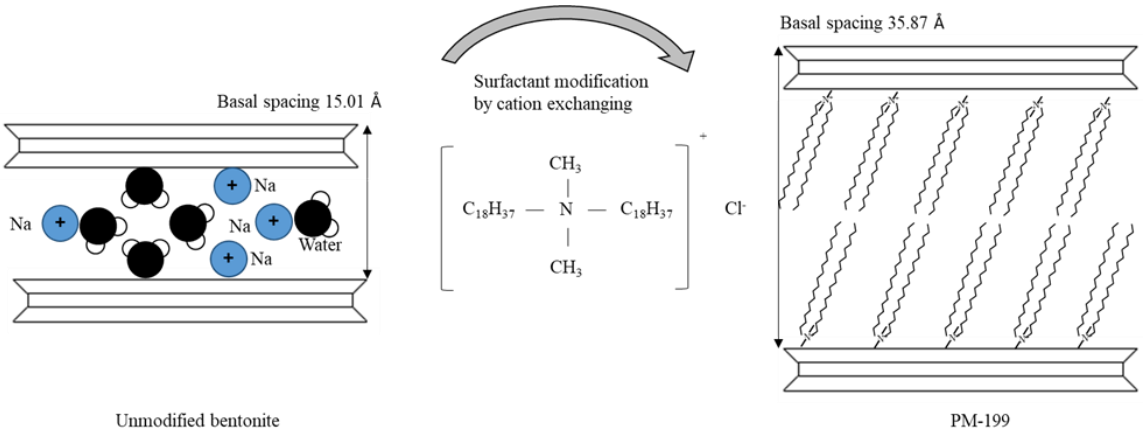

Fig. 2.4. The facile synthesis procedure of cationic surfactant modification (primary sorption) for organo-bentonite (PM-199)

Fig. 2.5. Organo-modified bentonite (mesh 40-14)

2.2.4 Naphthalene

Crystal naphthalene was used as the representative of PAHs contaminant in this study. It has organophilic property and also has a simple structure without any polar functional groups (shown in **Fig. 2.6**). Due to its low solubility in water (31.6 mg/L at 25 °C), the

naphthalene was dissolved in 30% methanol and 70% distilled water to formulate the designed concentrations of the organic contaminant solution for the tests.

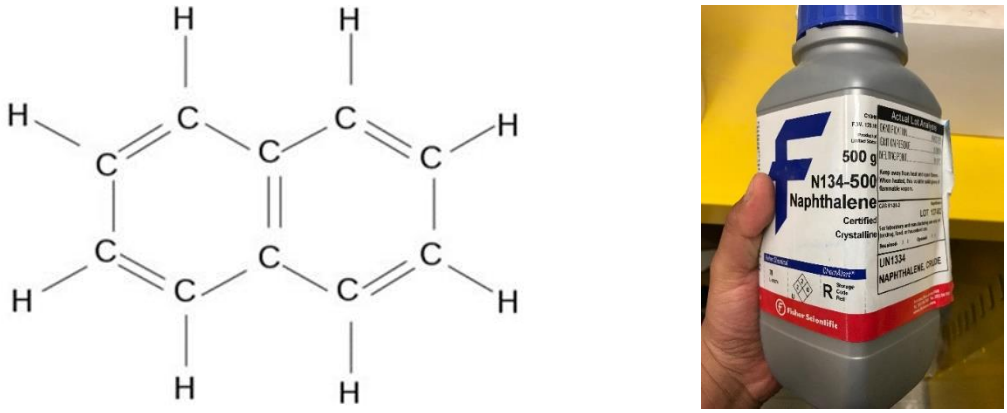

(a) (b)

Fig. 2.6. Naphthalene as a representative to make the PAHs solution (a) molecular structure (b) commercial product

2.2.5 Experimental Framework

The experimental framework for developing MGPC is shown in **Fig. 2.7**. The primary purpose here is to investigate the feasibility of using MGPC on liquid-phase organic contaminant remediation and to optimize an appropriate PM-199 replacement proportion of cement for the MGPC. The mix proportion of the MGPC should be adjusted to meet the strength and hydraulic conductivity requirements of pervious concrete. SEM was conducted to assure that the added PM-199 would not interfere with the hydration progress of cement in the long run. Finally, both the sorption and column tests were conducted to study the contaminant remediation function of the designed MGPC.

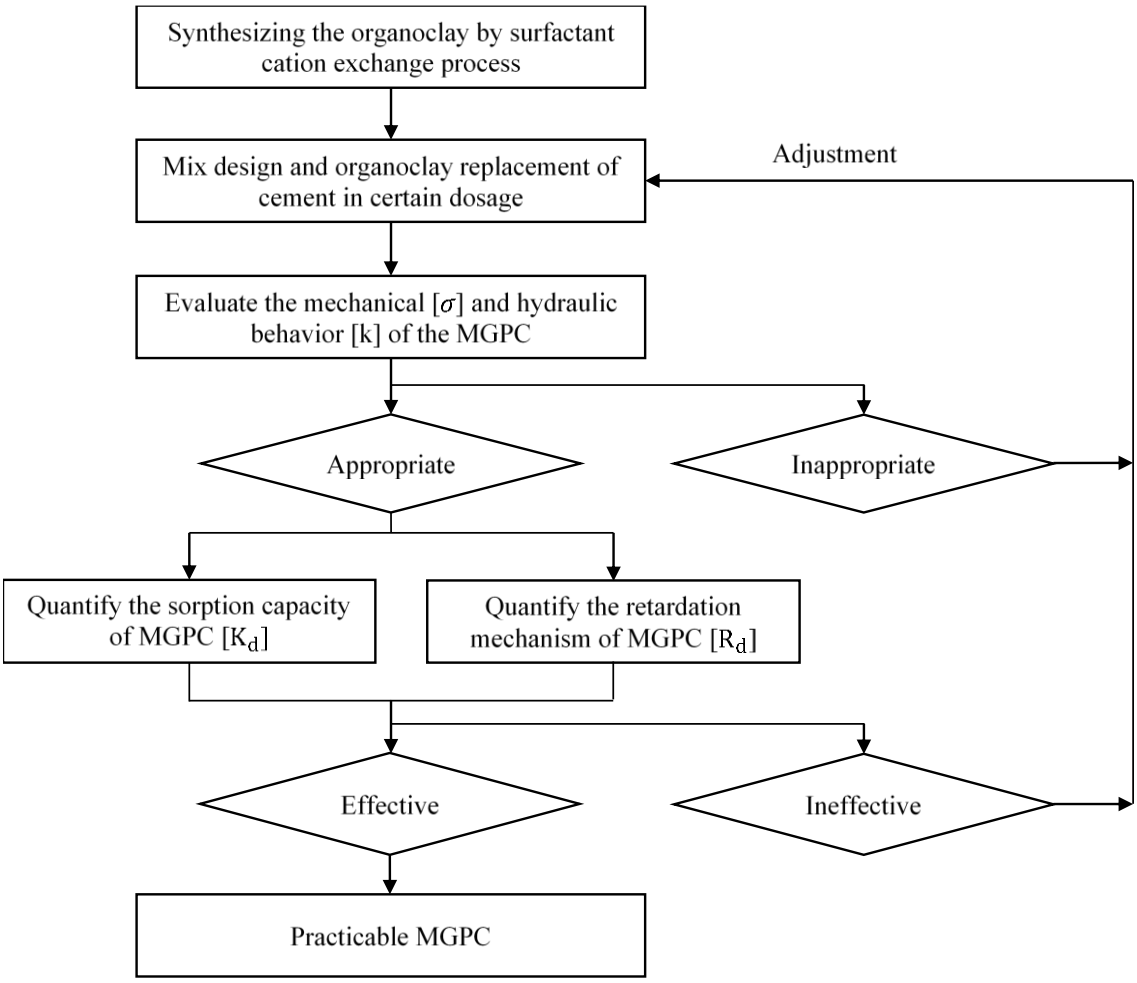

Fig. 2.7. The experimental framework for developing Multi-functional Green Pervious Concrete (MGPC)

2.2.6 X-ray Diffraction (XRD) for Organoclay

The x-ray diffraction (XRD) patterns of the unmodified bentonite and PM-199 were obtained in the range of 2° to 20° (2θ) by Bruker-AXS D8 DISCOVER Diffractometer

using Ni filtered Cu K radiation (with a wavelength λ= 1.5406 Å) at a scanning speed of 2° per min. The basal spacing was calculated by Bragg's law based on the tested 2θ:

$$2d\sin(\theta) = n\lambda \qquad (2-6)$$

where d (Å) is the distance between atomic layers in a crystal which is the basal spacing of the organic surfactant modified bentonite in this study, θ (°) is the diffraction angle, n (a positive integer) is the "order" of reflection, and λ (1.5406 Å) is the wavelength of the incident X-ray beam.

2.2.7 Total Organic Content for Organoclay

In order to study the efficiency of organic modification of bentonite thermogravimetric analysis (SDT Q600 by TA Instruments) was conducted on the PM-199 samples. About 10 mg PM-199 clay sample was measured and the temperature was increased from 25 ℃ to 1000 ℃ with a rate of 10 ℃/min. The weight loss was consistently measured and recorded during the test. Since the ignition points of organic surfactant and base clay are different the amount of the organic surfactant can be calculated by the final weight loss.

2.2.8 Optical Observation

To investigate the influence of the blending mechanical energy on the integrity of PM-199 particles, the surface of the PM-199 and cement paste after 28 d hydration was observed by using Olympus MX51 Optical Microscope (OM) (see **Fig. 2.8** (a) and (b)). Optical microscopy is a common method to analyze the surface microstructures of the sample. 1000× magnification was used in the tests.

(a) (b)

Fig. 2.8. (a) Olympus MX51 Optical Microscope (OM); (b) the cement paste sample with PM-199 additives

2.2.9 Scanning Electron Microscope (SEM)

This study chooses a commercially available organo-bentonite named PM-199 as a cement paste replacement of dry cement powder for the cement paste. The compatibility between PM-199 and cement paste was evaluated by the Scanning Electron Microscope (SEM) photos after 28 d hydration. The Scanning Electron Microscope (SEM) uses the electrons to form an image of the microstructural features of the paste sample. With a large depth of field and high resolution, the SEM inspection can present the degree of hydration of cement, formation, and distribution of hydration products, homogeneity of cement paste, and binding efficiency between PM-199 and cement paste. The total morphology of PM-199 particles embedded in the cement paste was observed by the VEGA3 TESCAN (**Fig. 2.9** (a)) with a working distance of 13.01mm. The boundary between 28d cement paste with PM-199 additives was observed by the FEI Nova NanoSEM 600 (**Fig. 2.9** (b)) with a working distance of 7.1 mm.

(a)

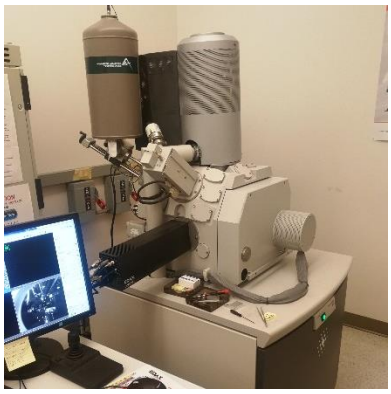

(b)

Fig. 2.9. (a) VEGA3 TESCAN and (b) FEI Nova NanoSEM 600

For the SEM tests, the paste sample was crushed and cut into small pieces, polished with 2000 grit silicon carbide sandpaper, and washed by using an ultrasonic bath. Due to relatively lower conductivity, the sample was coated by gold and attached with the sample holder by copper tape to enhance the conductivity before observation (see **Fig. 2.10**).

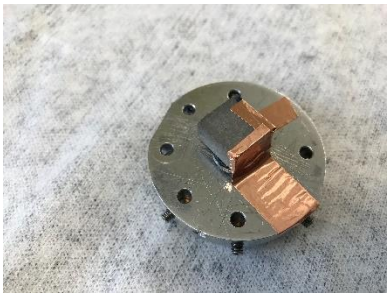

Fig. 2.10. Sample preparation of PM-199 and cement paste after 28 d hydration for SEM observation

2.2.10 Binder Drainage Test

With all the raw materials, a mix proportion for the pervious concrete to be tested is needed. The binder drainage test was conducted to develop an appropriate mix design. An appropriate amount of paste is expected to coat on the surface of the aggregates without dripping. The cylinders were drilled with bottom holes (see **Fig. 2.11** (a)), and different water to cement ratios (see **Fig. 2.11** (b) and (c)) have been tried to make the concrete to see whether there is cement paste drainage out of the bottom.

(a) (b) (c)

Fig. 2.11. Determining the mix proportion (a) making the testing mold (b) critical water to cement ratio (c) wet mix proportion

2.2.11 Compressive Strength Test

Compressive strength of cement pastes with particle organoclay replacements were tested using 5.08 cm × 5.08 cm × 5.08 cm cubes (ASTM C109 / C109M-16a, 2016) and the strength of concrete samples were tested on 1 day, 7 days, and 28 days by using 77.62 cm × 15.24 cm cylinders (ASTM C39 / C39M-17b, 2017). Three replicas were used for all

the tests (see **Fig. 2.12**). During the test, the loading rate of the universal machine was controlled so that the specimens were broken in between 1 to 2min (see **Fig. 2.13**).

Fig. 2.12. Sample preparations of pervious concrete with different sizes

Fig. 2.13. Universal compression testing machine with the load range to 400 kips

2.2.12 Hydraulic Conductivity Test

In order to make sure the developed concrete meet the specification of pervious concrete hydraulic conductivity test was also conducted. In this test, the hydraulic conductivity (k) can be measured using the constant head permeameter (see **Fig. 2.14**) and calculated by the following equation:

$$k = \frac{VL}{Ath} \qquad (2-7)$$

where k (cm/s) is the hydraulic conductivity of the tested concrete; V (mL) is the quantity of flow; L (cm) is the length of the concrete specimen along the path of flow; A (cm^2) is the cross-sectional area of the specimen; t (s) is the interval of time for collecting a certain amount of permeated flow, and h (cm) is the difference in hydraulic head across the specimen.

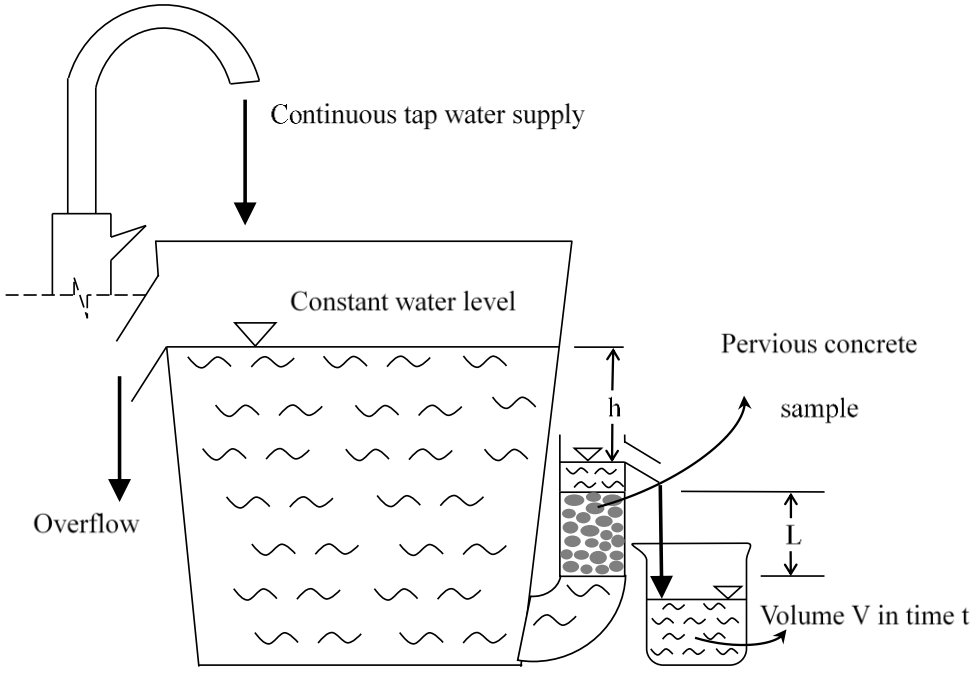

Fig. 2.14. Experimental procedures of the hydraulic conductivity test

2.3 Results and Discussions

2.3.1 Evaluate the Organoclay after Surfactant Modification

Total Organic Content (TOC) of the Organoclay can be determined by the thermo-gravimetric weight loss. **Fig. 2.15** shows that the weight losses from 0 ℃ to 200 ℃ is about 2% (moisture content) and from 200 ℃ to 1000 ℃ is about 35% (organic surfactant) which indicates the surfactant modification is effective by using the following equation to calculate:

$$f = \frac{M_{cation}}{CEC \cdot M_{clay} \cdot GMW_{cation} \cdot X} \qquad (2-8)$$

where f (%) is the desired percentage of *CEC* that will be satisfied by organic cation, M_{cation} (g) is the mass of the organic cation that is needed to achieve the designed *CEC*, *CEC* (meq/mol) is the cation exchange capacity of the base bentonite, M_{clay} (g) is the mass of the bentonite that will be used to modify, GMW_{cation} (g/mol) is the molecular weight of the bis (hydrogenated tallow alkyl) dimethyl ammonium, and X is the number of charge moles per each equivalent.

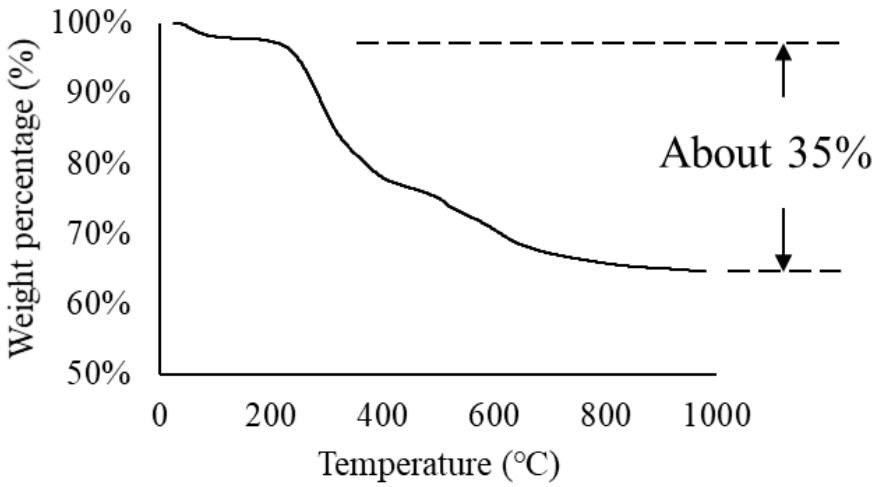

Fig. 2.15. Thermogravimetric analysis of organic surfactant modified bentonite

The XRD results of untreated bentonite and PM-199 is shown in **Fig. 2.16**. The basal spacing of untreated bentonite and PM-199 are 15.01 Å and 35.87 Å, respectively. The significant increase of the basal spacing is caused by the intercalated cation surfactant (Knox et al., 2007; Lagaly, 1986; Lee and Tiwari, 2012; Vaia et al., 1994). This is also due to the dramatically increased the total organic carbon content of PM-199 by the double long hydrocarbon chains of the bis (hydrogenated tallow alkyl) dimethyl ammonium. Compared with untreated bentonite, the hydrophilicity of the PM-199 surfaces was changed to lipophilicity after the treatment. The paraffin bilayers conformation of PM-199 provided more space for the PAHs molecular to pass by and be adsorbed by the surfactant. As the basal spacing is an important indication of the emplacement of the surfactant cation intercalation, this increase of basal spacing hints a much higher capacity of accommodating the organic surfactant and secondary sorption.

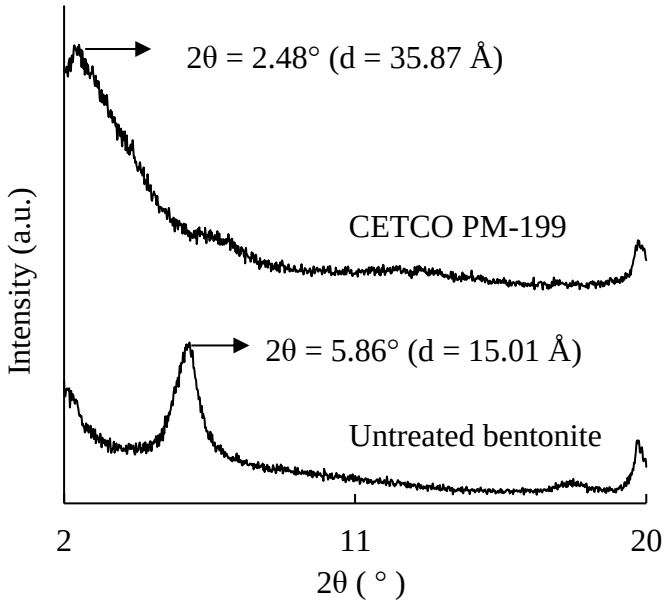

Fig. 2.16. X-ray diffraction patterns of untreated bentonite and PM-199

2.3.2 Evaluate the Cement Paste with Organoclay Addition after Curing

The optical micrograph of P035PM10 using Olympus MX51 OM is shown in **Fig. 2.17**. It can be seen that the PM-199 particles are bonded very well with the cement paste. The PM-199 particles maintain the integrities and original distribution sizes (mesh 40-14) which are important for being embedded in/or being exposed from the cement paste. The blending energy of the cement paste would not break down the organoclay particles.

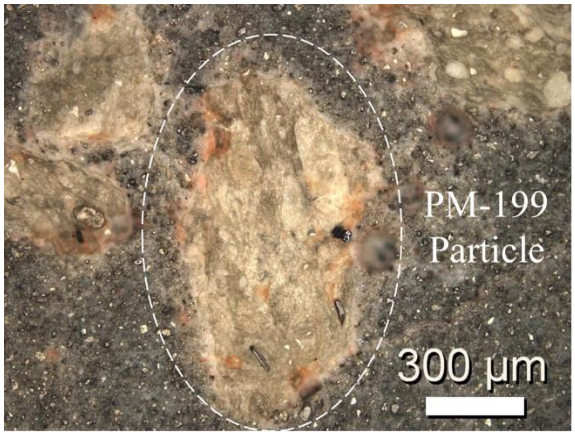

Fig. 2.17. Optical micrograph of P035PM10

The SEM images of 28 days hydrated P035PM10 are shown in **Fig. 2.18** (a) and (b). **Fig. 2.18** (a) shows a PM-199 particle macroscopically embedded in the cement paste, and these two materials were well bonded. The boundary between the cement paste and PM-199 can be seen clearly in **Fig. 2.18** (b) (dash line). The PM-199 is revealed as less foliated structures with some rough edges, and the cement paste visibly had some hexagonal or polygonal platy structures which are the typical hydration product of cement paste (Liu and Sun, 2016). No secondary product was identified in the presence of PM-199/cement paste mixture by observation, indicating no interference of the hydration process by PM-199 addition.

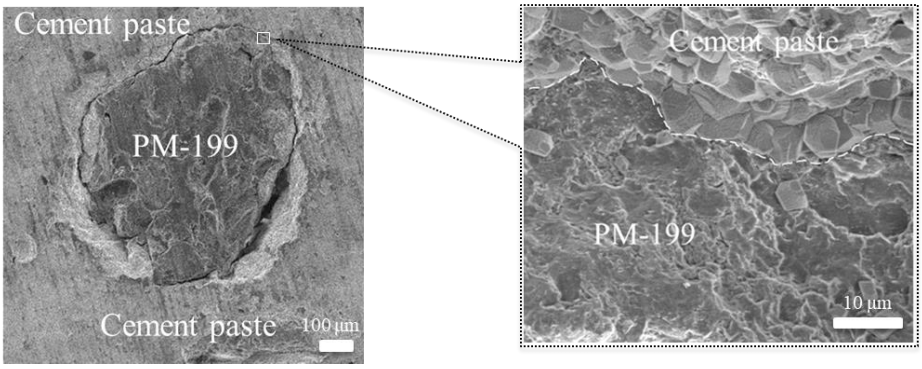

(a) (b)

Fig. 2.18. SEM images of P035PM10 at the age of 28days (a) Organoclay particle (PM-199) in cement paste (b) Zoom in the boundary between the organoclay and cement paste

2.3.3 Mix Design of MGPC

Table 2.3 shows the threshold of water to cement ratio is 0.38 which indicates that there is no extra paste dripping down when the water to cement ratio smaller than this value. Based on the binder drainage test 0.35 is chosen as the water to cement ratio in the following research. This value is a typical water to cement ratio that is used on job sites for concrete construction.

Table 2.3 Quantities of raw material for the pervious concrete binder drainage test

w/c	Aggregates (g)	Cement (g)	Water (g)	Porosity
0.28	2500	500	140	0.26
0.30	2500	500	150	0.26
0.32	2500	500	160	0.25
0.34	2500	500	170	0.25
0.36	2500	500	180	0.24
0.38	**2500**	**500**	**190**	**0.23**
0.40	2500	500	200	0.23

Comparing to the conventional concrete, the pervious concrete is relatively a new construction material used as the pavement building material. Although numerous studies and research have been done in this area, there is still no mix design standards or specifications pervious concrete that can be followed. It is because the characteristics of the pervious material compositions are quite different, and in general the results from different studies are hardly comparable. The aggregate-to-cement ratio (a/c) can significantly affect the mechanical and hydraulic behavior of pervious concrete (Nguyen et al., 2014; Sonebi and Bassuoni, 2013; Tennis et al., 2004; Yahia and Kabagire, 2014). For this study, a/c ratio of 5 was used based on the literature review. A w/c ration of 0.35 was used for all the samples listed in **Table 2.4**. For the comparison purpose, 5% and 10% replacement of organoclay were used. For example, in P035PM10, 10% (by mass) of the cement powders were replaced by PM-199, while all other proportions were kept the same.

Table 2.4 Mixing proportions of paste and pervious concrete specimens

Specimen name		w/b (or w/c)	a/b (or a/c)	Cement (g)	PM-199 (g)	Water (g)	Aggregates (g)
Paste 5.08 × 5.08 cm cubic	P035*	0.35	5	195.2	0.0	68.3	0.0
	P035PM05*	0.35	5	183.0	9.6	67.4	0.0
	P035PM10*	0.35	5	171.0	19.0	66.5	0.0
Concrete 7.62 × 15.24 cm cylinder	C035*	0.35	5	206.0	0.0	72.1	1030.0
	C035PM05*	0.35	5	195.7	10.3	72.1	1030.0
	C035PM10*	0.35	5	185.4	20.6	72.1	1030.0
Concrete 5.08 × 10.16 cm cylinder	C035*	0.35	5	58.5	0.0	20.5	292.5
	C035PM05*	0.35	5	55.575	2.925	20.5	292.5
	C035PM10*	0.35	5	52.65	5.85	20.5	292.5

P035: pure cement paste under w/c 0.35;

P035PM05 (or P035PM10): cement paste with 5% (or 10%) PM-199 replacement of cement under w/c 0.35;

C035: pure pervious concrete under w/c 0.35;

C035PM05 (or C035PM10): MGPC with 5% (or 10%) PM-199 replacement of cement under w/c 0.35.

2.3.4 Mechanical Properties of Cement Paste and MGPC Samples

The measured compressive strength of the cement paste and concrete samples are summarized in **Table 2.5**. For the paste samples, the compressive strength decreases with an increased amount of PM-199 (see **Fig. 2.19**). It is because as an organic material, PM-199 does not participate in the hydration process, and the clay particles act as some small fillers inside the cement paste which would reduce the ultimate compressive strength. For the pervious concrete samples, the difference in strength gains among the three mixes is very minimum (see **Fig. 2.20**). This is because the strength of pervious concrete is mainly

provided by the interlocking effects of the aggregates, therefore, the negative impact of PM-199 on concrete strength does not exist.

Table 2.5 Compressive test and hydraulic conductivity test results of pervious concrete with different organoclay replacement dosages

Specimen name		Bulk density (g/cm^3)	1d [σ] (MPa)	7d [σ] (MPa)	28d [σ] (MPa)	Hydraulic conductivity (cm/s)	Porosity (%)
7.62 × 15.24 cm cylinder sample	C035	1.88	3.01	4.75	**5.64**	**2.05**	26.10
	C035PM05	1.88	4.36	5.21	**5.45**	**1.72**	25.72
	C035PM10	1.88	3.45	5.07	**5.61**	**1.59**	25.35

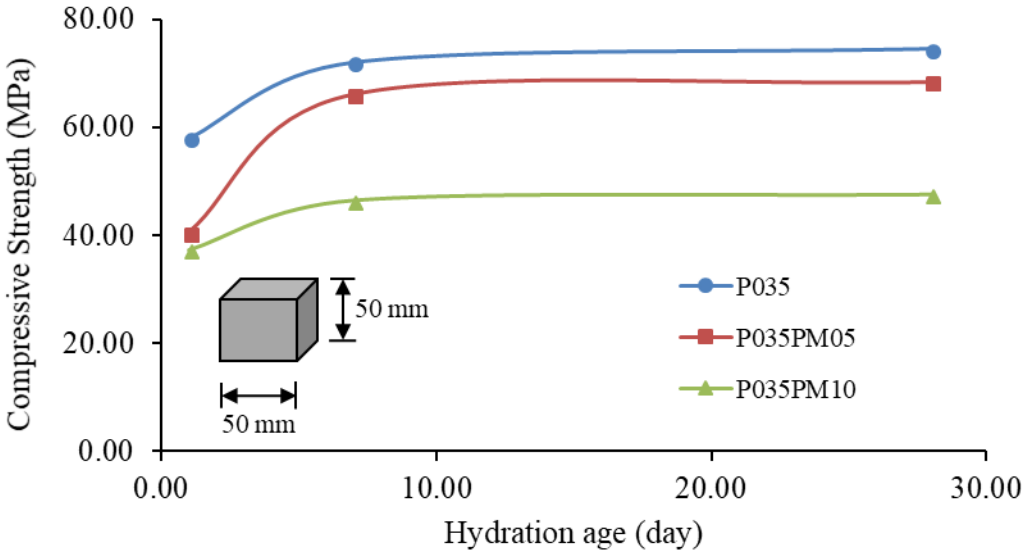

Fig. 2.19. Compressive strength for cement paste with different organoclay replacement dosages and hydration ages

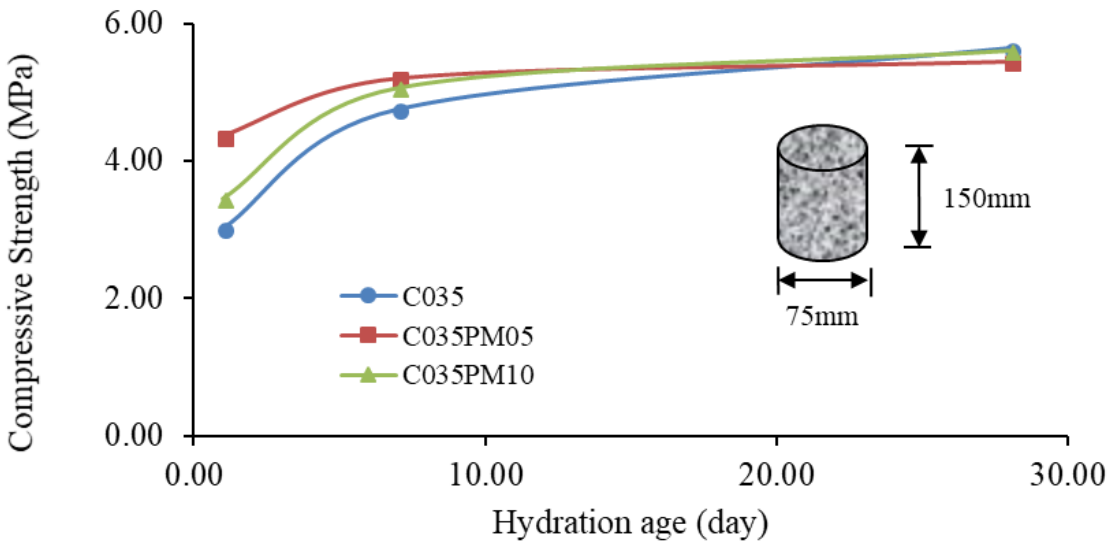

Fig. 2.20. Compressive strength for pervious concrete with different organoclay replacement dosages and hydration ages

2.3.5 Hydraulic Properties of MGPC Sample

The hydraulic conductivities of C035, C035PM05, and C035PM10 are also presented in **Table 2.5**. It can be seen that the porosity slightly decreases by PM-199 addition, and the hydraulic conductivity of pervious concrete decreases with the increased amount of PM-199. This attributes to the fact that the PM-199 particles may occupy more interconnected void space. Huang at el. indicated that high porosity and the interconnected voids of the pervious concrete might lead the permeated flow to be the turbulent flow instead of laminar flow (Huang et al., 2010). And Darcy's law for laminar flow might not be applicable. By checking the Reynold Number, the permeated flow through the pervious concrete samples of this study can still approximately be considered as the laminar flow. Since the main

purpose of this study is to evaluate the feasibility of the contaminant removal function of MGPC, and the initial hydraulic gradient effect on permeability could be neglected.

2.4 Summaries and Conclusions

In this chapter, the influence of organoclay additive on the cement hydration was evaluated. The mechanical and hydraulic performances of MGPC were also investigated. Based on the experimental results, the following conclusions can be drawn:

1. The organoclay is relatively isolated in the cement paste and would not affect the cement hydration. And the blending energy would not affect the integrity of the organoclay particle;
2. 5% and 10% organoclay replacement of cement had little impact on the mechanical and hydraulic properties of MGPC. Compared to the conventional pervious concrete, the compressive strength of MGPC slightly increased, and the hydraulic conductivity of MGPC moderately decreased.

CHAPTER 3 PRELIMINARY STUDY OF PAHS REMOVAL BY USING MGPC

3.1 Introduction

This chapter focuses on testing the PAHs removal capacity of the MGPC by conducting the isotherm batch sorption test. To assure the PAHs removal capability of the developed MGPC, this part of the study has been divided into two steps. First, isotherm batch tests have been conducted on the paste samples to examine the influence of adding PM-199 on the adsorption capacity of the paste matrix. This preliminary step is critical because as the binder and coating of aggregates, paste layer in pervious concrete is the main contact with the contaminants, and good adsorption capacity of the paste is the initial step of good adsorption of contaminants of the concrete composite. As a further step, the transport mechanism and retardation behavior of PAHs in MGPC were investigated by using a breakthrough column test. The hydration age effect on the MGPC performance on PAHs removal was also evaluated.

3.2 Material and Methods

3.2.1 Sample Preparation for Batch Sorption and Column Test

The aggregate-to-cement ratio (a/c) can significantly affect the mechanical and hydraulic behavior of pervious concrete (Nguyen et al., 2014; Sonebi and Bassuoni, 2013; Tennis et al., 2004; Yahia and Kabagire, 2014). For this study, a/c ratio of 5 was used based on the literature review. A w/c ration of 0.35 was used for all the samples listed in **Table 2.4** in chapter 2. For the comparison purpose, 5% and 10% replacement of organoclay were used. For example, in P035PM10, 10% (by mass) of the cement powders were replaced by PM-199, while all other proportions were kept the same.

When mixing the paste, the cement powder and organoclay (for P035PM05 and P035PM10) were dry mixed for 1 minute at a low speed of 136 rpm and the mixing water was then slowly poured into the mixed powders then the paste was mixed for 2 additional minutes. After 2 minutes of rest, the paste was then mixed for 3 more minutes at a higher speed of 195 rpm (ASTM C305 - 14, 2014). After mixing the paste was cast in the 5.08 × 5.08 cm cubic mold.

When mixing the concrete, the cement and water were mixed following the same procedure of mixing the paste. And then the aggregates were added to the paste and mixed with the steel rod until the aggregate surface was uniformly coated by cement paste. The organoclay was added at last and was additionally mixed to embed onto the paste coating (see **Fig. 3.1**). The concrete cylinders were prepared according to ASTM C31/C31M-18a (ASTM C31 / C31M - 18a, 2018). It should be pointed out that the concrete mix proportions were determined based on no excessive paste to clog the connected voids (see section 2.3.3) and

two replacement levels of organoclay are considered herein. All the paste and concrete specimens were cured under 25 ℃ with a sealed condition (see **Fig. 3.2**).

Fig. 3.1. Process for making the MGPC with organoclay embedded in the cement paste coating

(a)

(b)

Fig. 3.2. MGPC sample preparation (5.08 cm × 10.16 cm or 2×4 in.) for column test

3.2.2 Calibration of the Gas Chromatography

It is necessary to do calibration before analyzing the concentrations of PAHs samples for both the batch test and column test with Gas chromatography. For this study, the retention time of naphthalene was identified firstly. It is about 6.5 min. And a calibration curve was obtained to relate the areas of the peaks on chromatograms of naphthalene to the predesigned concentrations of the naphthalene solutions. The slope of the linear regression is the converting factor that can be used to test the unknown concentration of naphthalene solution.

3.2.3 Kinetic Study

In order to know how fast that the adsorption process can reach the equilibrium state, the kinetic study was conducted. For the kinetic study, the same sorbent and contaminant solution to do sorption under different durations. The data is the concentration of the solution versus the sorption time.

3.2.4 Batch Sorption Tests

Series of batch sorption tests were conducted to quantify the naphthalene sorption under equilibrium condition onto pure PM-199, P035PM10, P035PM05, and P035 (**Fig. 3.3**). The sorbents P035PM10, P035PM05, and P035 were cured for 28 days, crushed and sieved between sieve No. 20 to No. 30. Crystal naphthalene was dissolved into 30% methanol and 70% distilled water solvent to make the representative organic contaminant solution with predesigned concentrations (1, 2, 3, 5, 10, 15, 20, 40 mg/L). 10 mL of naphthalene

contaminant solutions with different concertation were respectively placed in conical centrifuge tubes with PTFE cap before 0.2 g (± 0.001 g) of each sorbent was added. The sorption kinetic study revealed that the naphthalene sorption reached the equilibrium state between 24 hours to 48 hours. As a result, all the sample tubes were agitated for 48 hours and centrifuged for 1 hour. The supernatant was filtered by a 2μm syringe filter and extracted with hexane at a volume ratio of 10:1 (v/v) in the separatory funnel. A few drops of Methylene blue solution were added to the supernatant/hexane mixture to illustrate the lipid-liquid boundary. And another few drops of saturated NaCl solution were mixed to help the naphthalene solute separate out from the liquid phase solvent. The extracted naphthalene/hexane samples were analyzed by gas chromatography equipped with a flame ionization detector (GC-FID) (Clarus 480, PerkinElmer, Inc., Waltham, MA). The GC parameters for this study were set up according to the searchable Chromatogram Library's database. The injecting and detecting temperatures were 280 °C. The initial oven temperature was 100 °C, and after holding 1min, the oven temperature increased as the rate of 20 °C/min till 240 °C. The concentration of absorbed naphthalene by solid can be defined as Equation:

$$S = \frac{V_m(C_0 - C_e)}{M_s} \qquad (3-1)$$

where S (mg/kg) is defined as the mass of the sorbate (naphthalene) sorbed by a unit mass of the sorbent, C_0 (mg/L) and C_e (mg/L) are the initial and equilibrium aqueous-phase concentrations of naphthalene, respectively, V_m (mL) is the volume of the contaminant

solution added in the batch reactor, and M_s (g) is the mass of the sorbent added in the batch reactor.

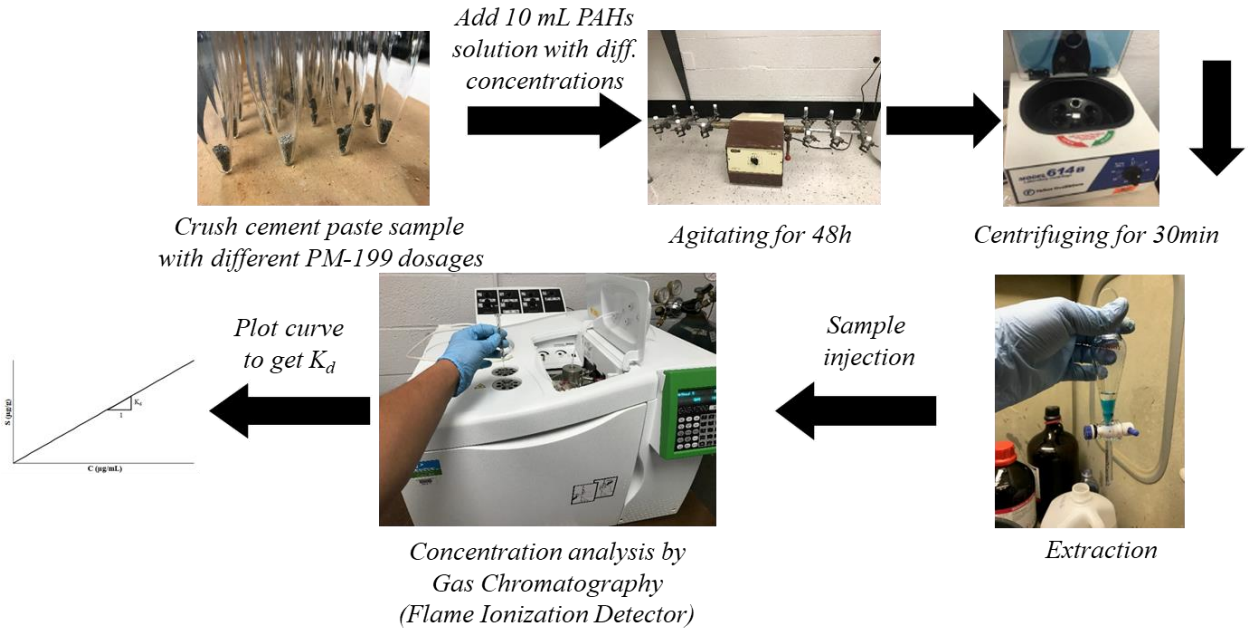

Fig. 3.3. The procedure of the batch sorption test

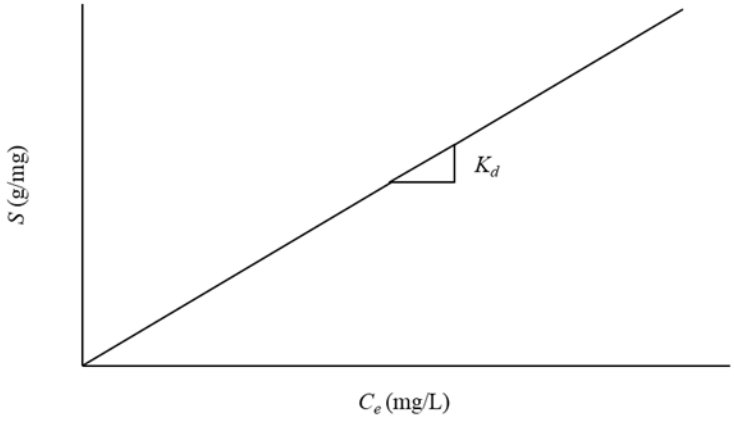

Fig. 3.4. The linear sorption isotherm

For the most common cases, the linear sorption isotherm (see **Fig. 3.4**) model is used to describe the adsorption mechanism of the organic contaminant by organic surfactant modified soil at relatively low concentration (Shang et al., 2017; Shu et al., 2010). The linear isotherm is defined mathematically by Equation $(3-3)$:

$$S = K_d C_e \qquad (3-2)$$

where the sorption isotherm was obtained by plotting the sorbed concentration of naphthalene by sorbents S (mg/kg) versus the equilibrium concentration of naphthalene in aqueous solution C_e (mg/L), and the slope of isotherm is defined as partitioning coefficient K_d (L/kg).

3.2.5 Column Tests

The schematic of the experimental apparatus of pervious concrete column test is shown in **Fig. 3.5**. Laboratory column tests were conducted to determine the retardation factor (R_d) of naphthalene transport in concrete with a fast flow rate (0.5 mL/s) under non-equilibrium conditions (see **Fig. 3.6**). Naphthalene was dissolved in 30% methanol and 70% distilled water solvent to make a solution with the concentration of 100 mg/L. The column specimens were cast with C035, C035PM05, and C035PM10 for 28 days. The Teflon tape and PTFE paste were used to separate the pervious concrete sample from the column to avoid naphthalene adsorption by the inner wall. The columns have a height of 10.16 cm and an inner diameter of 5.08 cm. The column specimens were first flushed with 2 pore volumes (approximately 120 mL) of deionized water. The prepared naphthalene solution was then injected from a glass syringe pump. A pulse-type contaminant flow injection was

conducted for one pore volume (60 mL). After naphthalene injection, the columns were switched back again to the deionized water until the effluent concentration was below the detection limit. The breakthrough curve of naphthalene was obtained by measuring the effluent concentration, following the sample extraction and the analyzing method of batch sorption test.

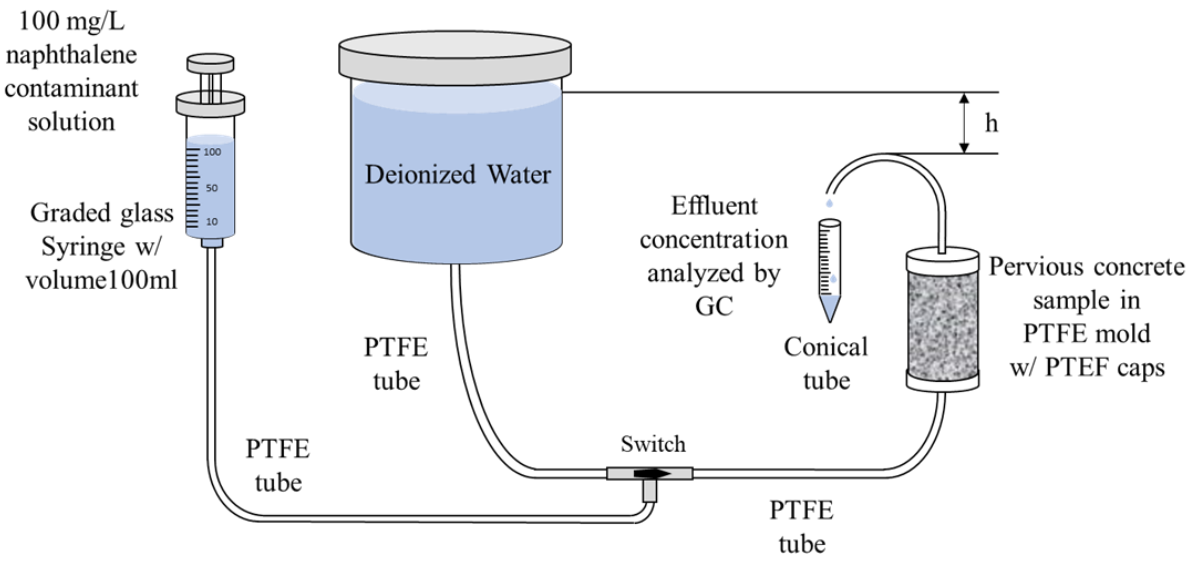

Fig. 3.5. Schematic of experimental apparatus of pervious concrete column test

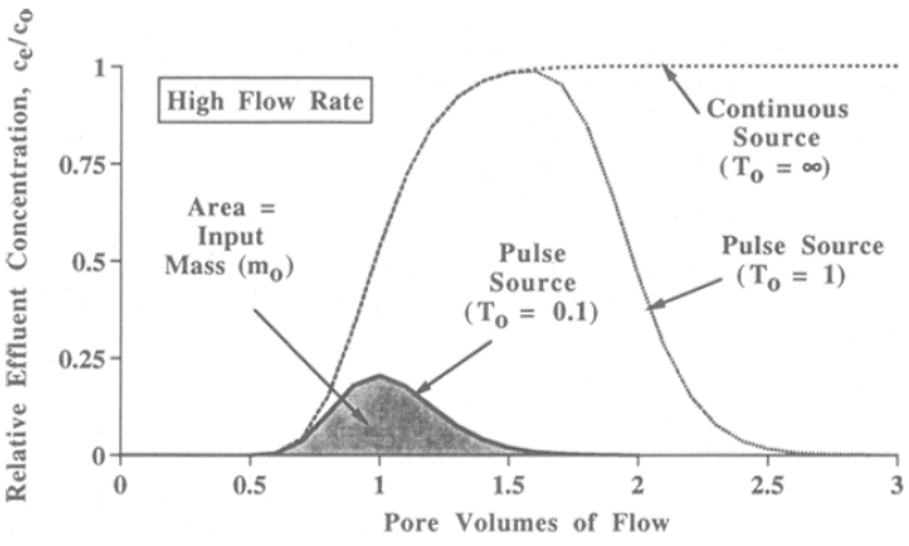

Fig. 3.6. High flow rate breakthrough curve for different types of contaminant injection (Shackelford, 1994)

3.3 Results and Discussions

3.3.1 Gas Chromatography Calibration for Analyzing the PAHs Concentration

It is necessary to do calibration prior to analyzing the concentrations of PAHs samples for batch test and column test with Gas chromatography. For this study, the retention time of naphthalene was identified first. And a calibration curve was obtained to correlate the areas below the peaks on chromatograms of naphthalene to the known concentrations.

For instance, a representative result of the gas chromatogram for the standard solution of naphthalene dissolved in the hexane solvent is presented in **Fig. 3.7**. A large peak appeared around 2min during the run indicating the lighter molecules of hexane came out from the GC column that reached the detector earlier. Later another clear peak was observed around 6.5min and this peak represented the naphthalene molecule reaching the detector. All the

naphthalene extracts samples by hexane in this study had a similar peak occurrence time. The higher the naphthalene concentration, the larger the average area of the response peak (around 6.5min). Septum flow was used to prevent the naphthalene vapor residue attach to the upper septum of the injector. The septum flow rate should be strictly constant for all series of samples since the concentrations of the naphthalene extract samples in this study were relatively low, and the response peak shape was sensitive to the flow rate change.

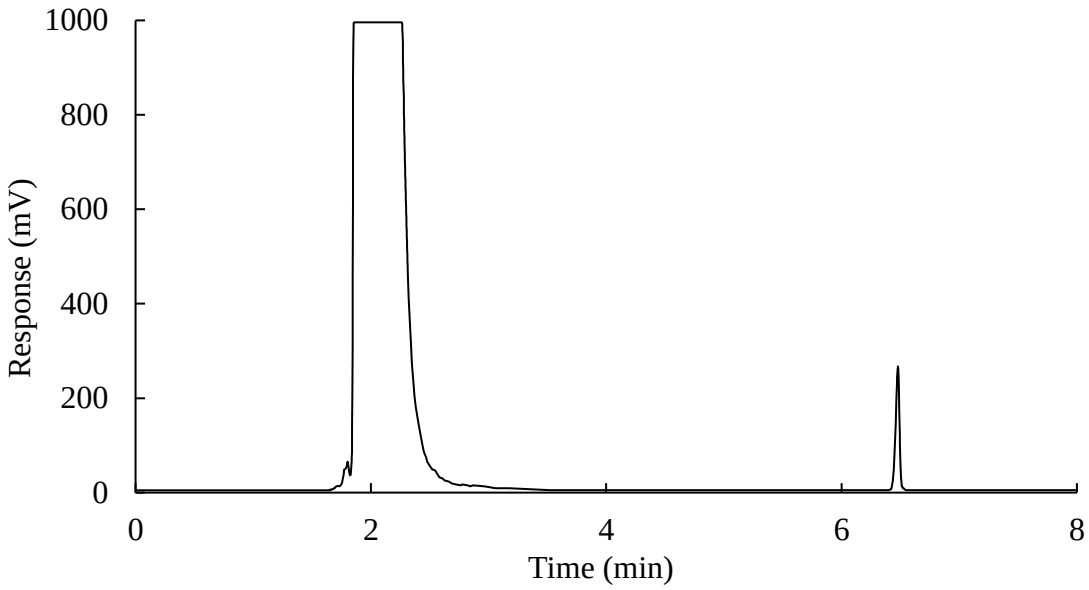

Fig. 3.7. Gas Chromatogram of naphthalene solute dissolved in hexane solvent with the concentration of 2000 mg/L

There was a linear relationship between the naphthalene concentration of the extracts and the average area of the response peak (shown in **Fig. 3.8**). The linear regression line was forced to pass through the origin, and the slope was 2427.2 μv·s·L/mg which could be used as the conversion factor to determine the unknown concentration of naphthalene extracts in this study.

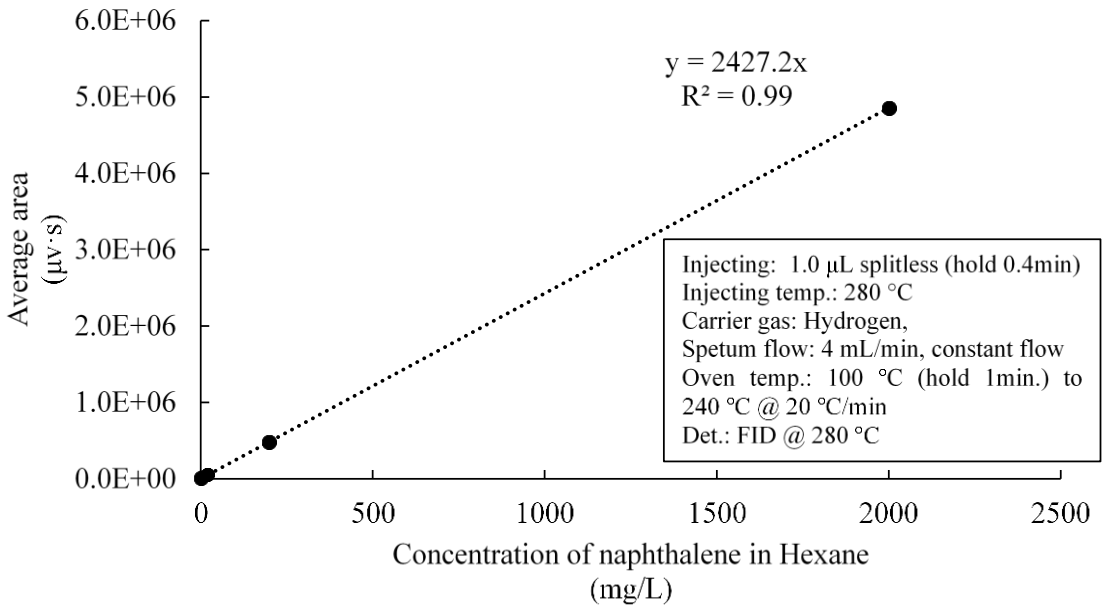

Fig. 3.8. Calibration curve for naphthalene standard solution with different concentrations

3.3.2 Sorption Kinetics Study of Organoclay in Paste

The sorption kinetics of naphthalene on the 28 days P035PM10 is shown in **Fig. 3.9**. After 12min the sorption kinetics tended to be slow and finally reached an equilibrium between 24 hours to 48 hours, which was consistent with previous studies (Kasaraneni, 2015; Kaya et al., 2013; Reible et al., 2008). The data obtained from the kinetic sorption test was analyzed and fitted with a first-order one-site mass transfer model (OSMTM) to estimate the kinetic parameters (Nzengung et al., 1997):

$$C_t = C_e + [C_0 - C_e] exp\left[-\left(\frac{\varepsilon}{\psi}\right) t\right] \qquad (3-3)$$

where C_t is the solution concentration at time t (min) (mg/L); C_e is the solution concentration at equilibrium (mg/L); C_0 is the solution initial concentration (mg/L); ε is the mass transfer coefficient (1/min) which is the only unknown parameter for OSMTM, and ψ is the ratio of C_e over C_0.

The mass transfer coefficient $\varepsilon\ (1/\text{min})$ was optimized as 0.25 ± 0.01 and the fitting curve of the OSMTM model matched the experimental data. It is also worthy to note that the sorption process of the naphthalene on P035PM10 did not happen as quickly as some previous study in the initial 12min (Javadi et al., 2017; Nzengung et al., 1997). It was believed that the particles allowed more time to let the naphthalene solute penetrate and saturate.

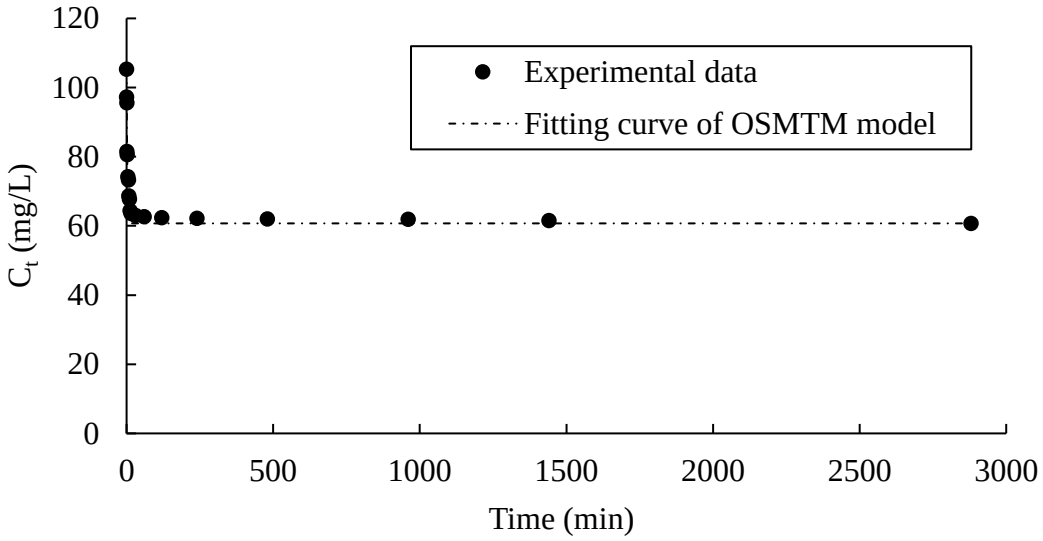

Fig. 3.9. Sorption kinetics of naphthalene on 28 days P035PM10

If 48 hours sorption is considered as the equilibrium state of the sorption, then the accomplishment rate to the certain time of the sorption process can be calculated and plotted in **Fig. 3.10**. It can be found that the sorption process built up rapidly in the initial 12min and almost 92% of the equilibrium accomplished. The time window for the contaminant solution contacting with the sorbent is important for designing the discharging rate of the subbase or subgrade beneath the MGPC pavement. It is expected that the MGPC pavement system not only has enough discharging rate for reducing the stormwater runoff shortly but also has effective contact time with the contaminant solution.

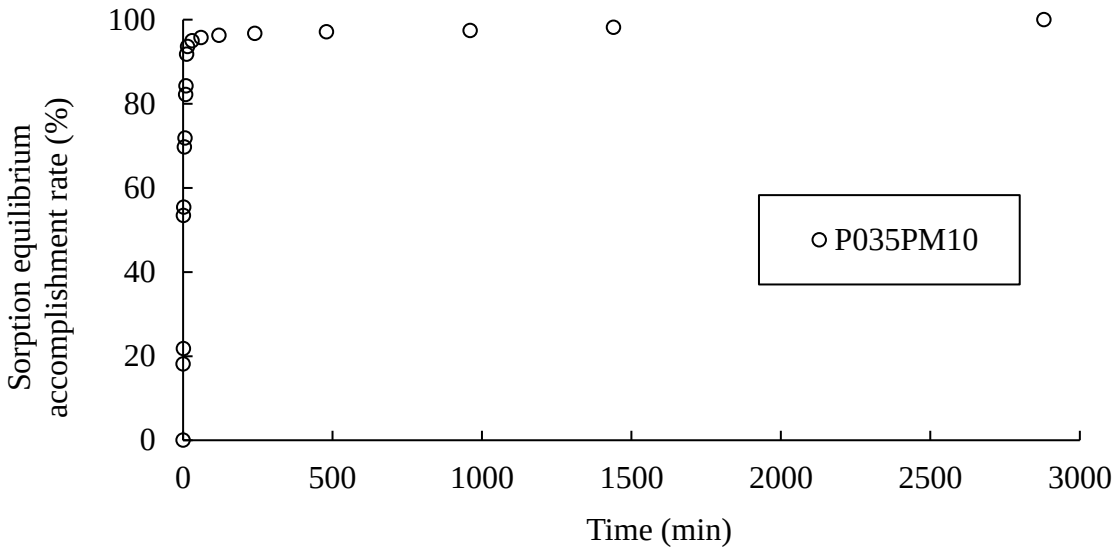

Fig. 3.10. The naphthalene sorption equilibrium accomplishment rate on 28 days P035PM10

3.3.3 Sorption Isotherms of Paste Samples with Different Organoclay Dosages

A series of equilibrium batch isotherms for aqueous naphthalene passing through organoclay and cement paste with different dosages PM-199 replacement are presented in **Fig. 3.11**. All cement paste samples were crushed and sieved between sieve No.20 to No.30 as discussed in section 3.2.1. Linear regressions passing the original point were fitted for all the sorbents under the range of naphthalene concentration (1 mg/L to 40 mg/L). The slope was determined as the partitioning coefficient, K_d, an important indication of adsorption capacity. The partitioning coefficient of PM-199, P035PM10, P035PM5 and P035 were 2370.54 L/kg, 161.47 L/kg, 70.18 L/kg, and 14.91 L/kg, respectively. As the organoclay replacement percentage increased the partitioning coefficient of the paste, this indicates the enhanced adsorption capacity of the paste matrix when PM-199 is added. Although the pure cement past also had a certain amount of sorption capacity of naphthalene, adding only 5% or 10% PM-199 can significantly improve the K_d value. This is because the intercalated organic cation surfactant sufficiently increased the lipophilicity of the clay and then enhanced the adsorption capacity of organic contaminants.

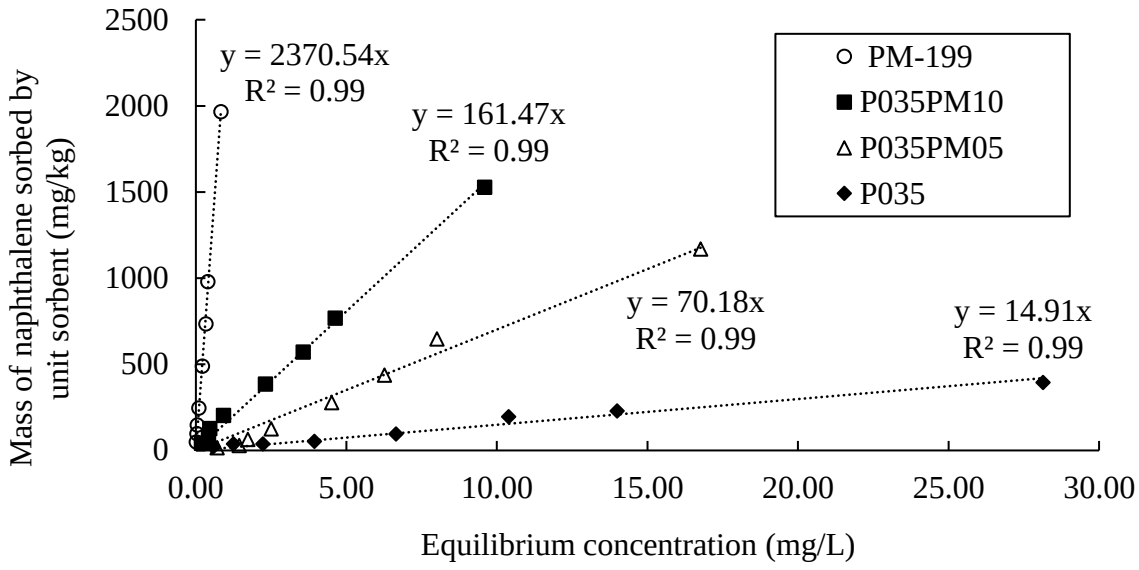

Fig. 3.11. The linear sorption isotherms for the sorption of naphthalene on paste samples of different organoclay replacement dosages

3.3.4 Organoclay Dosage Effect on Naphthalene Transport and Retardation in MGPC

The transport mechanisms of naphthalene through all the column samples under a high flow rate (0.5 mL/s) are governed by the one-dimensional advection-dispersion-retardation equation in the homogenous saturated porous media due to adsorption (Freeze and Cherry, 1979) shown as follows (equation $(4-3)$):

$$\frac{\partial C}{\partial t} = D_L \frac{\partial^2 C}{\partial x^2} - v_x \frac{\partial C}{\partial x} + \frac{\rho_b}{n}\frac{\partial S}{\partial t} \qquad (3-4)$$

Where C (mg/L) is the concentration of PAHs, is D_L (cm^2/min) is the longitudinal coefficient of hydrodynamic dispersion, v_x (cm/s) is the seepage velocity along the flowline, t (s) is the time, x (cm) is the distance along the direction of transport, ρ_b (g/cm^3) is the bulk density of the pervious concrete samples, n (%) is the porosity, and S (mg/kg) is the mass of PAHs adsorbed on a unit mass of the pervious concrete samples.

The retardation factor was defined as the ratio of the average flow velocity of the solvent to the average migration rate of the PAHs mass center (Shackelford, 1994). Therefore, the migration rate of naphthalene can be evaluated based on the flow rate and the retardation factor. A pulse-type injection with one pore volume (30 mL) 100 ppm naphthalene solution applied to the samples and the deionized water was switched. After about 20 pore volumes being flushed with deionized water, the concentrations of the effluent solution were close or under the detecting limitation of GC. But part of the introduced naphthalene was still not flushed out from all the samples. Therefore, the concentration of effluent after 20 pore volumes was assumed to be the same value as that of the concentration of the 20^{th} pore volume for all the samples until the area under the breakthrough curve equals the total mass of naphthalene initially introduced into the influent solution. The naphthalene breakthrough curves for 28 days C035, 28 days C035PM05, and 28 days C035PM10 are plotted in **Fig. 3.12**. The 28 days C035 sample has a little retarded effect on the permeated contaminant flow. The peaks of breakthrough curves tend to shift to the right-bottom side and the curves shape become flatter that indicates the column samples have stronger retardation capacity to the contaminant flow. The peak concentration of the 28 days C035PM05 and 28 days C035PM10 breakthrough curves are less than 0.5 of the initial concentration of the injecting naphthalene solution. The smaller peak values indicate that with the organoclay modification, it enhances the retardation capacity of PAHs. This is due to the high sorption capacity of organoclay which was demonstrated in the batch sorption test.

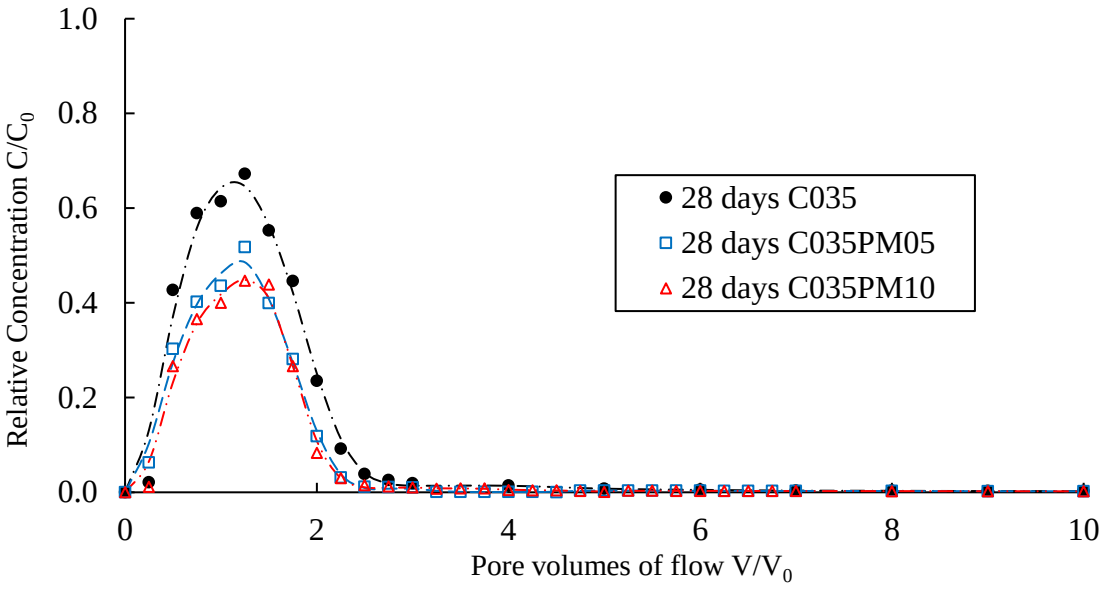

Fig. 3.12. The breakthrough curve of naphthalene solution in 28 days pervious concrete samples

For reversible adsorption of naphthalene with linear isotherm under low concentration, the equation $(3-2)$ can be substituted into equation $(4-3)$ to get:

$$\frac{\partial C}{\partial t} = D_L \frac{\partial^2 C}{\partial x^2} - v_x \frac{\partial C}{\partial x} - \frac{\rho_b}{n} \frac{\partial (K_d C)}{\partial t} \qquad (3-5)$$

$$\left(1 + \frac{\rho_b}{n} K_d\right) \frac{\partial C}{\partial t} = D_L \frac{\partial^2 C}{\partial x^2} - v_x \frac{\partial C}{\partial x} \qquad (3-6)$$

And the retardation factor R_d can also be derived from the partitioning coefficient K_d as (Freeze and Cherry, 1979):

$$R_d = 1 + \frac{\rho_b}{n} K_d \qquad (3-7)$$

As a pulse-type contaminant injection, the retardation factors of naphthalene in pervious concrete columns were determined by the first moment equation (Valocchi, 1985):

$$R_d = \frac{\sum(C_e/C_0)PV\Delta PV}{\sum(C_e/C_0)\Delta PV} - 0.5PV_0 \qquad (3-8)$$

where R_d (unitless) is the dimensionless retardation factor, C_0 (mg/L) and C_e (mg/L) are the initial and equilibrium concentrations of PAHs in an aqueous phase, respectively, PV (mL) is the corresponding pore volume to each measured concentration, ΔPV (mL) is the differential pore volume between each sampling step, and PV_0 (mL) is the initially injected pore volume of the solution to the pervious concrete column.

And the retardation factor R_d can also be derived from the partitioning coefficient K_d as (Freeze and Cherry, 1979):

$$R_d = 1 + \frac{\rho_b}{n}K_d \qquad (3-9)$$

Take the 28 days C035PM10 sample as an example, the retardation factor R_d can be calculated by equation (4 - 8):

$$R_d = 1 + \frac{\rho_b}{n}K_d = 1 + \frac{1.88}{0.2535} \times \left(\frac{0.1}{6.35} \times 2370.54 + \frac{0.9}{6.35} \times 14.91\right) = 293.53 \qquad (3-10)$$

Comparing to the retardation factor R_d (summarized in **Table 3.1**) from the first-moment equation $(3-8)$, the R_d value calculated by equation $(3-7)$ was relatively larger. The reason is that the partitioning coefficient K_d in equation $(3-7)$ was derived from the equilibrium sorption condition. However, the column test was conducted by a fast flow rate (0.5 mL/s) and the naphthalene solute took only about 2min to flush through the column sample. So, the sorption in the column test was in non-equilibrium (or kinetic) condition and the first-moment equation is more appropriate. Moreover, the particle

organoclay was embedded in the cement paste and partially exposed in the interconnected voids (white dots in **Fig. 3.13**). The exposed parts of the organoclay performed the contaminant remediation function, the embedded part of the organoclay hardly participated in partitioning mechanism under the fast flow.

Fig. 3.13. MGPC sample with PM-199 replacement of cement

Table 3.1 The retardation factors and naphthalene mass balance of pervious concrete column samples

Sample name	Age (d)	Flow rate (mL/s)	Dispersion (cm^2/min)	Retardation factor R_d	The total mass of contaminant injection (mg)	The total mass of contaminant ejection (mg)	Sorbed rate after 20 pore volumes ejection
C035	28	0.50	6.05	1.61	6.21	6.10	1.74%
C035PM05	28	0.50	6.06	66.95	6.81	4.59	32.64%
C035PM10	28	0.50	6.06	81.83	6.81	4.24	37.77%
C035PM05	3	0.50	6.06	60.01	6.68	4.63	30.68%
C035PM10	3	0.50	6.06	76.32	6.68	4.26	36.22%

3.3.5 Hydration age effect on Naphthalene Transport and Retardation in MGPC

The column tests were conducted to concrete samples at the ages of 3 days and 28 days. The retardation factors were calculated by the first moment equation $(3-8)$ and summarized in **Table 3.1** too. By checking the mass balance, more than 30% of the naphthalene was still held by the small segment of organoclay in MGPC. The mass flux of naphthalene was substantially reduced by the MGPC and efficiency could be additionally improved by increasing the organoclay fraction or controlling the permeated contaminant flow rate.

The effects of hydration age on the adsorption behavior of the developed pervious concretes are evaluated and illustrated in **Fig. 3.14** and **Fig. 3.15**. It is shown that the 28 days hydration samples have measurably larger retardation factors than the 3 days hydration samples. It is believed that the PH value evolution during the hydration influenced the retardation of naphthalene onto MGPC. Adams and Ideker (2015) indicated that the PH value of the concrete tended to change from neutral to 10.5 as the hydration developed. And Owabor et al. (2012) demonstrated that alkaline modification of the soil sorbents improved the adsorption capacity of naphthalene. Although only the natural clay was conducted by Owabor's tests, the results suggested that the organoclay had a similar trend. Cement hydration product, calcium hydroxide (CH), induces alkalinity that can enhance the adsorption capacity and retardation behavior of the MGPC, which is beneficial for the long-term service. This hints a long-term effectiveness of the proposed MGPC on contaminant remediation.

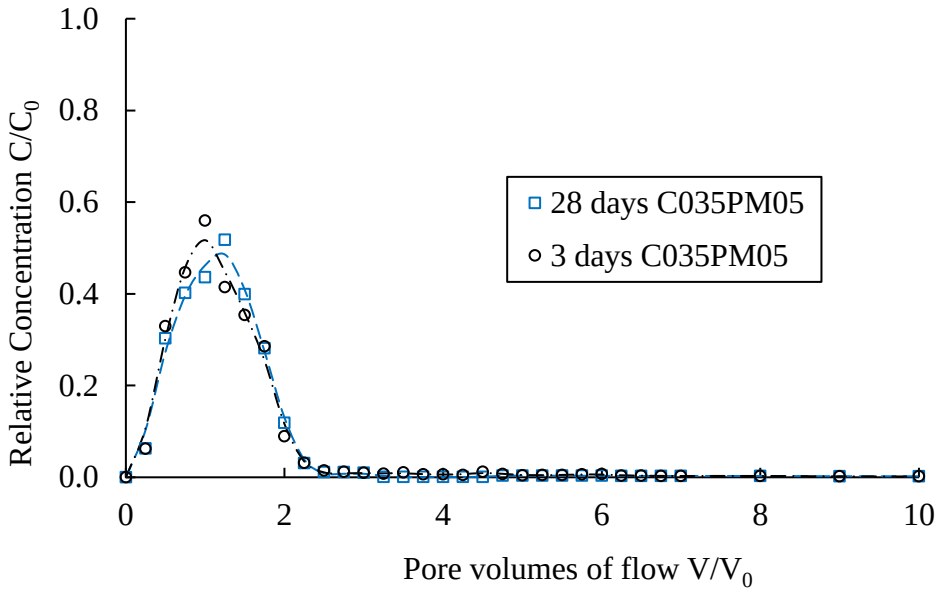

Fig. 3.14. The breakthrough curve of naphthalene solution in 28 days C035PM05 and 3 days C035PM05

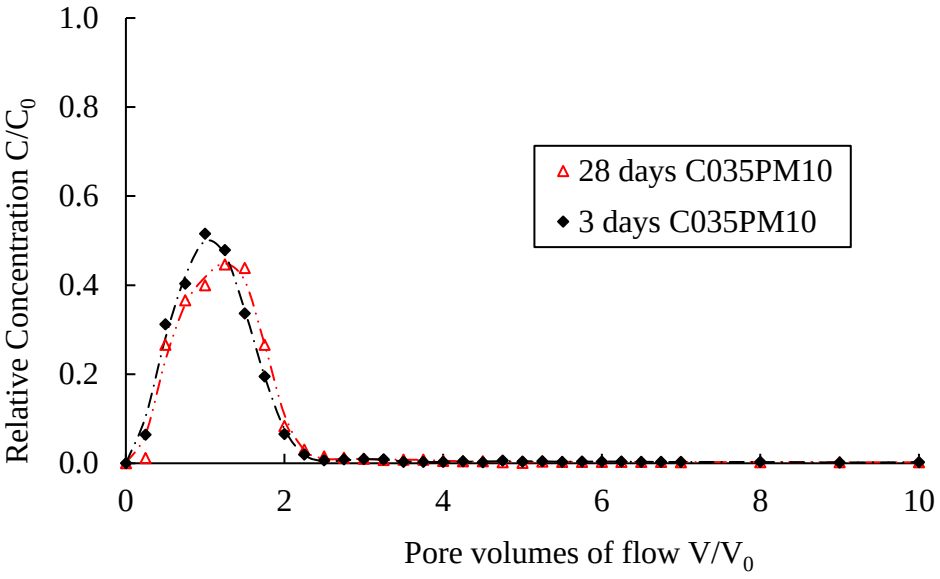

Fig. 3.15. The breakthrough curve of naphthalene solution in 28 days C035PM10 and 3 days C035PM10

3.4 Summaries and Conclusions

In this chapter, the water purifying function of the developed MGPC was realized by partially replacing cement powder with organoclay. Tests on both micro and macro levels have been conducted. Based on the experimental results, the following conclusions can be drawn:

1. The isothermal batch test revealed that with a small amount of organoclay amendment, the cement paste adsorption capacity of PAHs contaminants has been substantially improved;
2. The column test indicated that under a fast flow rate, the retardation factors of the two MGPCs has been dramatically increased compared to that of the conventional pervious concrete;
3. Cement hydration induced alkalinity can additionally improve the adsorption capacity and retardation behavior of the developed concrete, which indicate long-term stability of the material on contaminant remediation;
4. The overall results suggested that the MGPC has the great potential to be implied as an innovative multi-functional construction material.

CHAPTER 4 APPLICABILITY AND REUSABILITY OF MGPC PAVEMENT ON PAHS REMOVAL BY MIMICKING THE REAL ONSITE CONDITIONS

4.1 Introduction

The proposed MGPC has been proven to be a potential construction material for pavement implementation with the stormwater purification function as demonstrated in Chapters 2 and 3. The organoclay amendment can substantially enhance the PAHs removal efficiency of the MGPC pavement and the cement hydration induced alkalinity can additionally improve the PAHs sorption capacity of the material. To continue studying the field applicability of the proposed MGPC, extensive experiments have been further conducted by considering multiple variables that represent different scenarios, such as rainfall intensity, traffic flow, and traffic loads, etc. (Shang and Sun, 2021).

The initial concentrations of PAHs dissolved in stormwater by the various levels of emission can easily be influenced by the traffic load. In the urban area, the concentration of PAHs contaminants can range from several μg/L to more than 1mg/L (Bojes and Pope, 2007). Since the sorption efficiency of PAHs of organoclay is concentration-dependent, the performance of MGPC pavement under various initial PAHs concentration needs to be further investigated (Braida et al., 2001; DiVincenzo and Sparks, 1997; Giannakopoulou et al., 2012).

Similarly, rainfall intensity can cause different flow rates and leachability through the permeable pavement (Hernández-Crespo et al., 2019). Heavy rainfall can increase the hydraulic gradient rapidly which would result in a fast infiltration rate. Sorption kinetics study shows that under a faster flow rate sorption process is nonequilibrium and the leachable rate is relatively higher (Kaya et al., 2013; Owabor et al., 2012; Reible et al., 2008). Therefore, it is necessary to understand the mechanism of the rainfall intensities and/or flow rates that affect the PAHs sorption behavior of MGPC pavement.

The lifespan of pavement for service is typically ranging from two to five decades (ACI 522R-10, 2010; Association, 2009; Obla, 2010; Tennis et al., 2004). The concerns about the long-term efficiency of the PAHs removal function of MGPC pavement are raised. Theoretically, organoclay can adsorb a considerable amount of organic contaminant including PAHs by up to 50% of its self-weight (Alkaram et al., 2009; Nourmoradi et al., 2012). With the daily traffic flow and precipitations, the ultimate sorption performance of MGPC pavement on PAHs removal needs to evaluate by considering multiple cycles of contamination.

In this chapter, laboratory-scale evaluations are performed to examine the effectiveness of stormwater runoff induced PAHs removal by using the MGPC pavement. A series of column tests are conducted by varying (1) the initial concentrations of PAHs contaminants; (2) flow rates; and (3) contamination cycles. Results from this study suggest that MGPC pavement is a feasible stormwater management solution for controlling runoff-induced PAHs contamination.

4.2 Materials and Methods

4.2.1 Raw Materials

Ordinary Type I/II LA Portland cement provided by Cemex Kosmos Cement Plant was used for all experiments. The chemical compositions and major compounds were listed in **Table 2.1** and **Table 2.1**. Other physical properties can also be found in section 2.2.1. Gravels sieved between 1/2 and 3/8 inches and PM-199 provided by CETCO Co. were used when casting MGPC. The adsorption capacity of the aggregates was 1.5%.

4.2.2 Sample Preparation

C035PM10 is used to be MGPC for all the tests in this chapter. The sample preparation method is described in section 3.2.1 and the mix design is listed in **table 2.4**.

4.2.3 Test Matrix

100mg/L and 40 mg/L PAHs solutions are chosen to study the impact of the initial concentrations on the MGPC adsorption efficiency. According to the kinetic study in chapter 3, the MGPC sample needs at least 12 min to reach the equilibrium state of PAHs sorption. Therefore, three different flow rates are simulated by making the percolating time of PAHs solution of 2 min, 6 min and 12 min (correspond to 1/12mL/s, 1/6 mL/s and 1/2 mL/s) in order to investigate the impacts of the PAHs flow rates on the MGPC pavement adsorption efficiency. And contamination cycles of 1 and 50 are adopted to study the long-term performance of the proposed MGPC. Each sorption/desorption cycle includes one pore volume PAHs injection and 19 pore volume distilled water injection since the

concentration of PAHs would smaller than 1 mg/L after a cycle. All the testing conditions used in this chapter are summarized in **Table 4.1**.

Table 4.1 Different test scenarios to mimic the real onsite situations

Column test names	100 mg/L PAHs	40 mg/L PAHs	1/2 mL/s pore water flow rate	1/6 mL/s pore water flow rate	1/12 mL/s pore water flow rate	1 cycle treatment	50 cycles treatment
C40-F1/2-T1*	–	Yes	Yes	–	–	Yes	–
C100-F1/2-T1	Yes	–	Yes	–	–	Yes	–
C100-F1/6-T1	Yes	–	–	Yes	–	Yes	–
C100-F1/12-T1	Yes	–	–	–	Yes	Yes	–
C100-F1/2-T50	Yes	–	Yes	–	–	–	Yes

*C40-F1/2-T1: Column test of C035PM10 on PAHs solution under 40mg/L concentration (C40) and 1/2 mL/s flow rate (F1/2) with one cycle treatment (T1);

C100-F1/2-T1: Column test of C035PM10 on PAHs solution under 100mg/L concentration (C100) and 1/2 mL/s flow rate (F1/2) with one cycle treatment (T1);

C100-F1/6-T1: Column test of C035PM10 on PAHs solution under 100mg/L concentration (C100) and 1/6 mL/s flow rate (F1/6) with one cycle treatment (T1);

C100-F1/12-T1: Column test of C035PM10 on PAHs solution under 100mg/L concentration (C100) and 1/12 mL/s flow rate (F1/12) with one cycle treatment (T1);

C100-F1/2-T50: Column test of C035PM10 on PAHs solution under 100mg/L concentration (C100) and 1/2 mL/s flow rate (F1/2) with fifty cycles treatments (T50).

4.2.4 Test Methods

Column tests are conducted to determine the retardation factor R_d which indicates the adsorption capacity and retardation behavior of the MGPC on PAHs. The testing apparatus is shown in **Fig. 4.1**. The naphthalene is dissolved as the description in section 2.2.4 to make the PAHs solution with predesigned concentrations for the following tests. The testing procedures are described in section 3.2.5. During the test, one pore volume PAHs

solution is introduced to the MGPC sample first and then the injection is switched to distilled water until the effluent concentration is below the detecting limit of Gas Chromatography (GC). The first-moment equation $(3-8)$ is used to calculate the retardation factor R_d for all the tests.

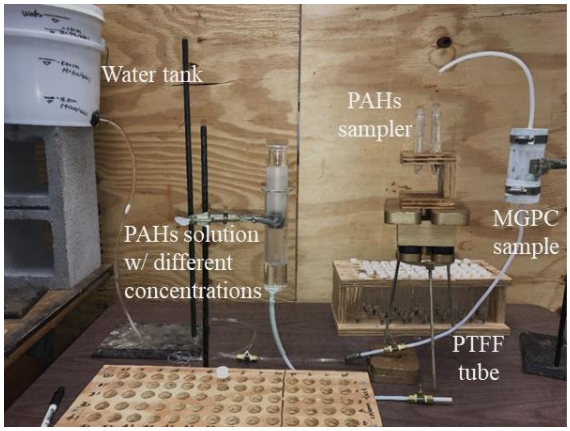

Fig. 4.1. Testing apparatus for column test

In order to further study the PAHs adsorption on the organoclay particle in MGPC under multiple cycles of pollution, a part of the MGPC sample is taken after the column test for scanning electron microscope (SEM) analysis. Fourier transform infrared spectroscopy (FT-IR) is also applied to get spectra of naphthalene, pure PM-199, and the PM-199 with adsorbed naphthalene after 50 cycles in the range of 650 ~ 4000 cm^{-1} with the resolution of 1 cm^{-1} by using a PerkinElmer Spectrum 100 and FT-IR Spectrometer (see **Fig. 4.2**). During the test, 0.975 g PM-199 organoclay is placed in a glass conical centrifuge tube. One cycle means that a 10 mL naphthalene solution with a concentration of 100 mg/L is added to the tube and shaken until reaching the equilibrium adsorption state. After 50

cycles, approximately 0.1 g of the PM-199 sample is placed in the center of the IR machine, and then being compressed to generate an even thickness. The scanning speed is 0.76 scan/s and the spectra are normalized and smoothed by the OMNIC software.

Fig. 4.2. PerkinElmer Spectrum 100 and FT-IR Spectrometer

4.3 Results and Discussions

4.3.1 Impact of Initial Concentrations on PAHs Removal Efficiency by MGPC

The initial concentrations of PAHs are highly relevant to the traffic flow and auto emission levels (Bojes and Pope, 2007; Gehle, 2009). The breakthrough curves of PAHs with different initial concentrations adsorbed by the MGPC sample (C035PM10) are shown in **Fig. 4.3** (a) and (b). Compared to the 100 mg/L initial concentration test, the curve shape of the 40 mg/L test is relatively flatter, and the curve enveloped area is smaller, which indicates better performance in PAHs adsorption This can also be proven by the retardation

factors that are calculated by the first moment equation $(3-4)$ and summarized in **Table 4.2**. It can be seen that the retardation factor R_d increases as the initial concentration of PAHs decreases. A higher percentage of the injecting contaminant is adsorbed by MGPC with the lower initial concentration by checking the PAHs mass balance before and after the breakthrough test. The GC detecting limitation is about 1 mg/L and the PAHs concentration of the effluent is generally less than this value after being washed by 20 pore volumes water. It is reported that the initial concentration of the contaminant can influence the adsorption efficiency of the adsorbent under liquid-phase (Altin et al., 1999; Braida et al., 2001; DiVincenzo and Sparks, 1997; Kah et al., 2011). This experiment results herein are consistent with the results reported by other researchers, which indicates that the sorption efficiency of MGPC pavement is dependent on the concentration of PAHs source. The rainfall intensity and traffic emission can affect the initial PAHs concentration of stormwater runoff which is needed to be considered before a proper design of the MGPC pavement. It should be noted that the PAHs concentration in stormwater runoff close to traffic corridors is normally lower than the concentration used in this lab test. This indicates that the PAHs sorbed rate of MGPC will be higher in a real-life case.

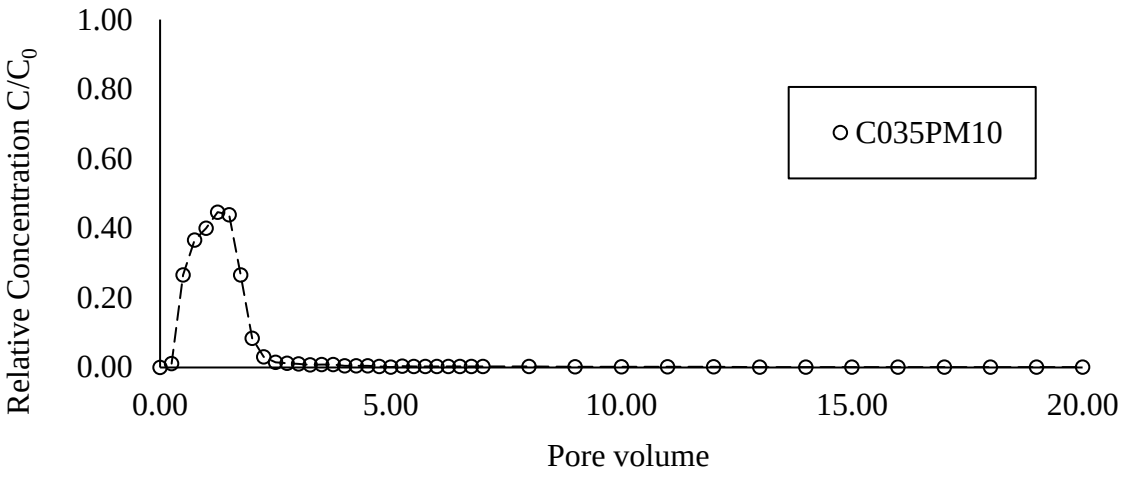

(a)

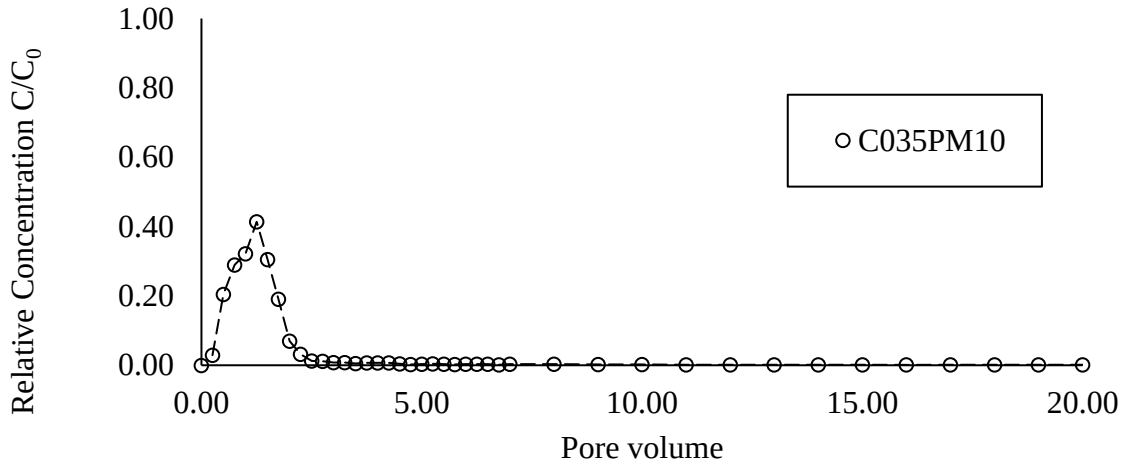

(b)

Fig. 4.3. Breakthrough curves of PAHs in MGPC with different initial concentrations (a) 100 mg/L (b) 40 mg/L

Table. 4.2 The Retardation Factors and the Contaminant Mass Balance of column tests with different initial concentrations of PAHs by MGPC

Sample	The initial concentration of PAHs (mg/L)	Flow rate (mL/s)	Retardation factor R_d	The total mass of PAHs injection (mg)	The total mass of PAHs ejection after 20 pore volumes (mg)	Sorbed rate after 20 pore volumes ejection
C035PM10	100	1/2	**81.83**	6.81	4.24	**37.77%**
C035PM10	40	1/2	**119.00**	2.31	1.18	**48.92%**

4.3.2 Impact of Flow Rate on PAHs Removal Efficiency of MGPC

The flow rate is an important parameter that influences the MGPC pavement performance on PAHs removal. There are several factors that can affect the flow rate, which is the permeability of the pavement layer, subbase and subgrade, and the rainfall intensity. Permeability is the material properties while the rainfall intensity is highly dependent on season, weather and topography (Tennis et al., 2004). Since permeability is usually predesigned before the pavement installation, the rainfall intensity induced variabilities of flow rate needs to be considered when designing a pervious pavement material. In this study, the basic idea is to find a balance point that can simultaneously maintain a substantial infiltration rate while still allow enough time for MGPC to adsorb the PAHs from the stormwater runoff.

PAHs breakthrough curves for the MGPC sample (C035PM10) under different flow rates (1/2 mL/s, 1/6 mL/s and 1/12 mL/s) are shown in **Fig. 4.4** (a), (b) and (c). Clearly, the shape of the curve tends to be flatter and the peak point of the curve shifts to the right-

when the flow rate decreases, and the enveloped area is getting smaller. This means that the duration of the contacting time between PAHs and MGPC can significantly influence the adsorption performance. The retardation factors R_d and the sorbed fraction are listed in **Table. 4.3**. It can be seen clearly that when the flow rate is decreased, the retardation factor improves significantly even being applied very high initial concentration of PAHs (100mg/L). It is because the used organoclay is relatively coarse and it is believed that the advection and dispersion of PAHs solute need much more time to penetrate through the surface of organoclay. Although there is a negligible impact of particle size effect on the adsorption capacity of the sorbent, the particle size is believed to affect the adsorption kinetics (Tsai et al., 2003). Even with the applied high PAHs concentration, if the flow rate is controlled appropriately, the adsorption capacity of MGPC is still considerably high when checking the adsorbed fraction.

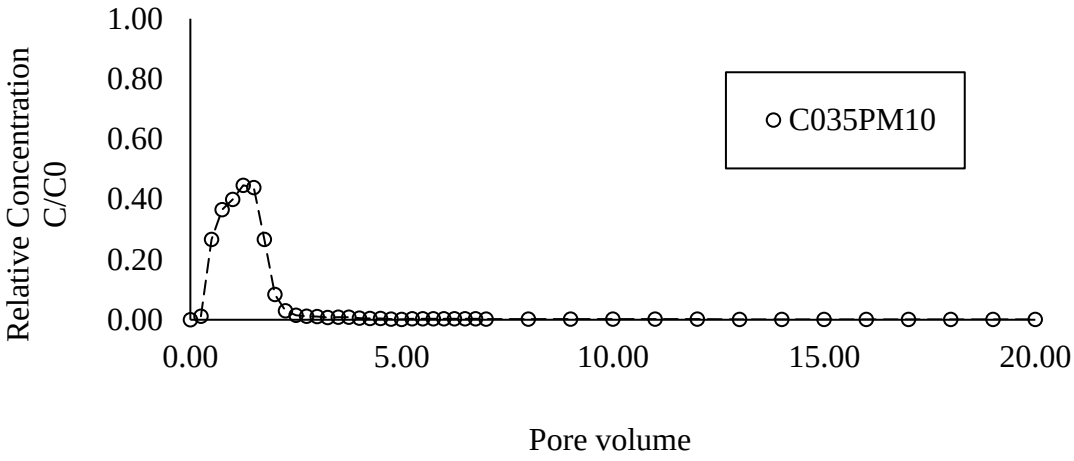

(a)

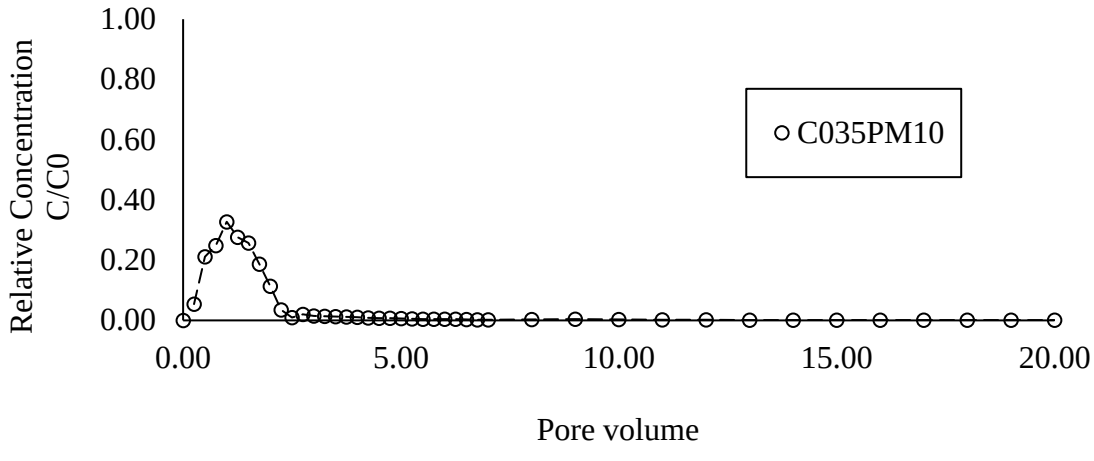

(b)

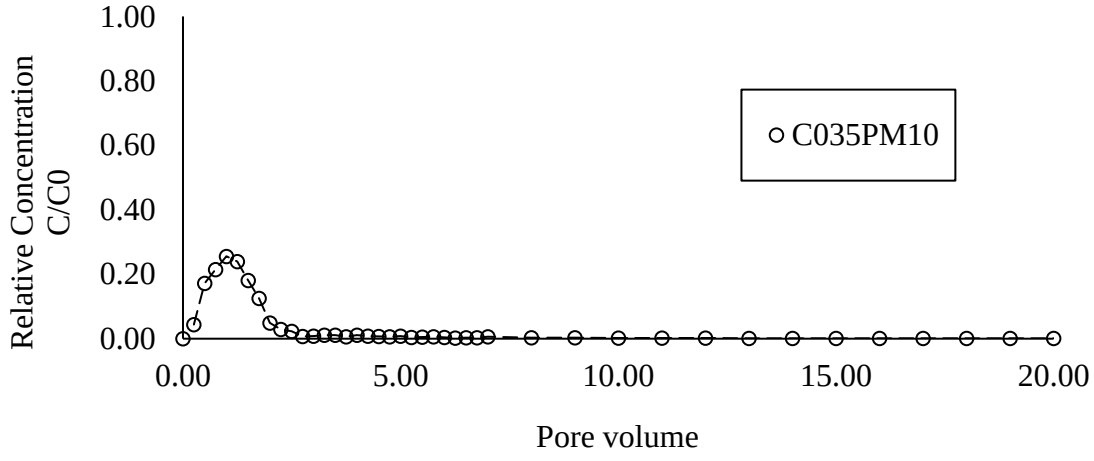

(c)

Fig. 4.4. Breakthrough curves of PAHs removal by MGPC under different flow rates (a) 1/2 mL/s (b) 1/6 mL/s (c) 1/12 mL/s

Table. 4.3 The Retardation Factors and the Contaminant Mass Balance of column tests with different flow rates by MGPC

Sample name	The initial concentration of the contaminated source (mg/L)	Flow rate (mL/s)	Retardation factor R_d	The total mass of PAHs injection (mg)	The total mass of PAHs ejection after 20 pore volumes (mg)	Sorbed rate after 20 pore volumes ejection
C035PM10	100	1/2	**81.83**	6.81	4.24	**37.77%**
C035PM10	100	1/6	**140.80**	5.35	2.61	**51.21%**
C035PM10	100	1/12	**187.68**	6.12	2.35	**61.60%**

4.3.3 Long-term Efficiency of MGPC on PAHs Removal after Multiple Sorption/desorption Cycles

In order to correlate the materials microstructure and its macro performance, SEM and FT-IR are both applied. Secondary electron images of the uncontaminanted C035PM10 and the same sample contaminated by the PAHs solution after 50 sorption/desorption cycles are shown in **Fig. 4.5** and **Fig. 4.6**, respectively. In **Fig. 4.5** the organoclay (PM-199) from the uncontaminated sample originally has a relatively flat and clean surface by observation. **Fig. 4.6** shows an organoclay embedded in MGPC being treated by PAHs solution after 50 sorption and desorption cycles. Comparing the organoclay (PM-199) part in **Fig. 4.5** the surface texture of the PM-199 after 50 cycles of contamination is changed to a cotton-like structure. This morphology change is believed to be attributed to the PAHs accumulation that is not washed out during the desorption process, which is in agreement with studies by other researchers (Altare et al., 2007).

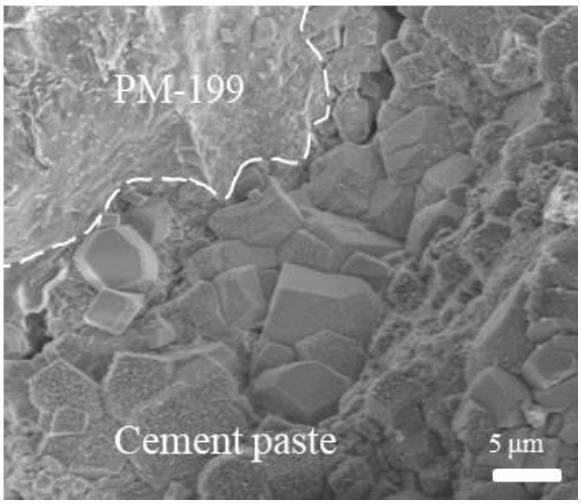

Fig. 4.5. SEM image of uncontaminated C035PM10 after 28 days age

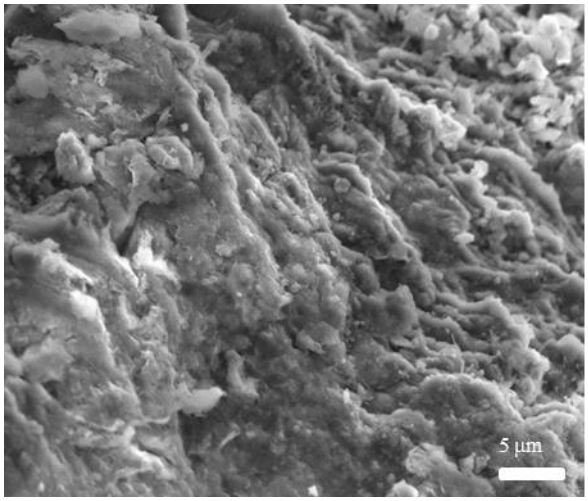

Fig. 4.6. SEM image of C035PM10 being contaminated by PAHs solution after 50 sorption/desorption cycles

FT-IR spectrum test is further used as a supplement to prove the PAHs surface adsorption onto the MGPC. The spectra of naphthalene, uncontaminated PM-199, and contaminated PM-199 after 50 cycles of sorption are illustrated in **Fig. 4.7** (a). To compare all three

spectra, the spectrum of naphthalene is shifted up for a better view. According to the previous study it is known that for the uncontaminated PM-199 and contaminated PM-199 certain molecular groups can be identified by their related wavenumbers and their absorbances such as O–H stretching bands (3000~3700 cm^{-1}), C−H asymmetric stretching vibrations (with the peak at 2922 cm^{-1}) and symmetric stretching vibrations (with the peak at 2852 cm^{-1}), interlayer water deformation vibrations (1600 cm^{-1} ~1700 cm^{-1}), asymmetric C–H bending vibrations of both CH_3 and CH_2 groups (1400 cm^{-1} ~1500 cm^{-1}), and Si–O stretching bands (with the peak at 1008 cm^{-1}) (Anbalagan et al., 2010; Arroyo et al., 2003; Hrachová et al., 2007).

From the figure, it is obvious that after 50 cycles of PAHs sorption, the intensities of the molecular groups increase due to the adsorption. The increased O–H stretching bands are attributed to the water adsorption by the organoclay surface while the enhanced H–O–H bends are due to the sorbed water in the organoclay interlayer (Arroyo et al., 2003; Hrachová et al., 2007). The increased intensities of the C−H asymmetric and asymmetric stretching vibrations (3000~3200 cm^{-1}) suggest that the PAHs adsorption leads to a higher organic carbon content of the organoclay surface. It is a supplementary evidence for the PAHs sorbed by the organic surfactant part. The Si–O stretching bands also increase apparently because of the interaction between the hydrocarbons and the siloxane surface.

The C−H group is selected to illustrate in **Fig. 4.7** (b) to compare the pure PM-199 and contaminated PM-199 by 50 cycles. The C−H group is the main component of the surfactant hydrocarbon chain. After PAHs sorption, the frequencies of two peaks are both shifted to the higher values. It indicates that the PAHs molecules are adsorbed on the C−H group which leads to an increased bending and torsion of the surfactant hydrocarbon chains.

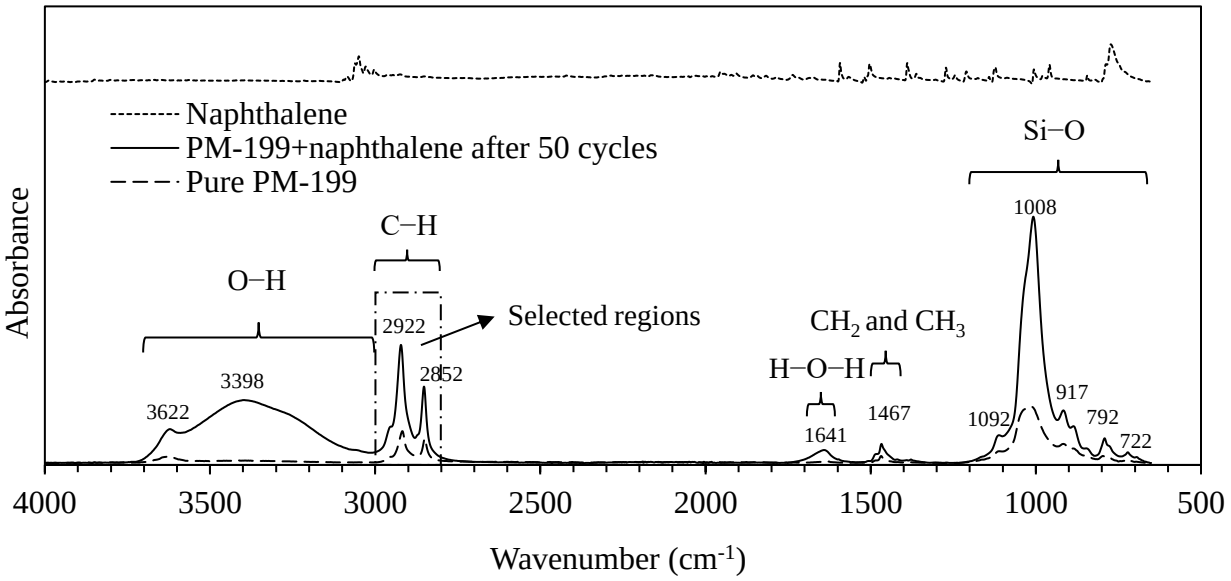

(a)

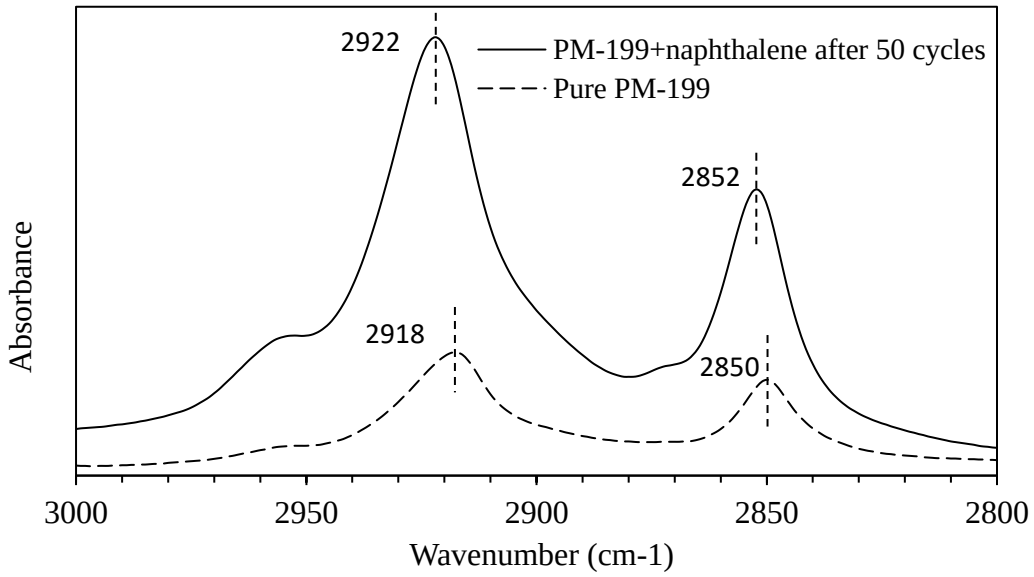

(b)

Fig. 4.7. FT-IR spectra of (a) naphthalene, pure PM-199, and PM-199 adsorbed by naphthalene after 50 cycles; (b) selected regions of pure PM-199 and PM-199 with adsorbed naphthalene after 50 cycles

The breakthrough curves for the MGPC sample (C035PM10) after 1st, 2nd, 3rd, 4th, 5th, 10th, 20th, 30th, 40th, and 50th sorption/desorption cycle are shown in **Fig. 4.8** (a) and (b), respectively. All the tests are conducted under a fast flow rate 1/2 mL/s which means that the PAHs solution takes about 2 min to percolate the MGPC sample. From the figure, it can be seen that the shapes of the breakthrough curves for various cycles are similar to each other. Peak values slightly fluctuated up and down and increases with the increased number of cycles of sorption/desorption. **Fig. 4.8** (a) and (b) also show that the curve enveloped areas tend to become larger especially after 20 cycles. This may be due to the desorption from the cumulative PAHs precipitation (from previous cycles) on MGPC.

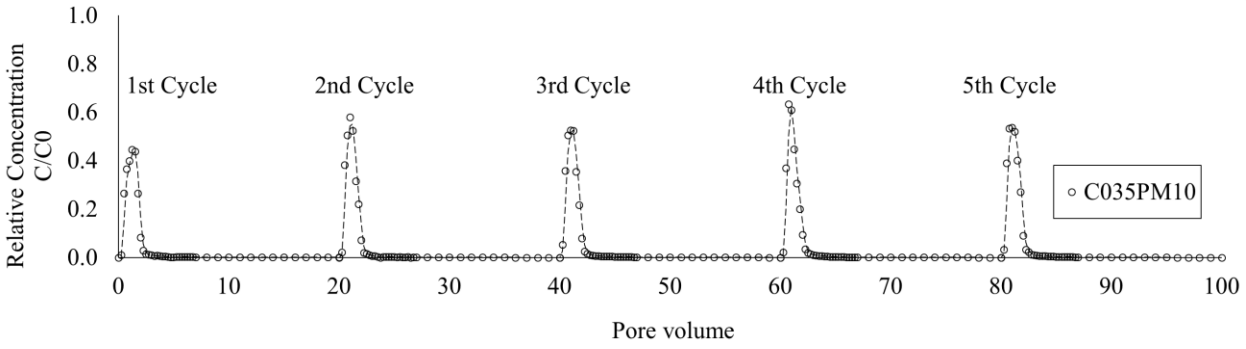

(a)

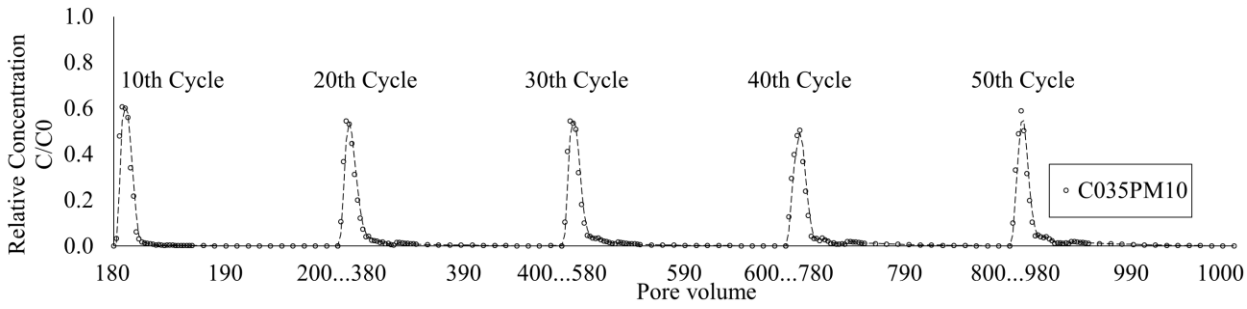

(b)

Fig. 4.8. (a) and (b) Breakthrough curves of PAHs removal by MGPC under 1/2 mL/s flow rate for 50 cycles

The retardation factors R_d for each observed sorption/desorption cycle are summarized in **Table. 4.4**. As shown, the values of R_d become smaller gradually as the cycles increase which either indicates losing of the sorption capacity and retardation ability of MGPC subsided after multiple cycles or can be due to some wash out of the adsorbed PAHs from previous cycles since the fastest flow rate is used in this section. With the on-going contamination cycles, it would take more time for the subsequent contaminant to penetrate the surface and be immobilized by the deeper part of the organoclay. Similarly, the cumulative sorbed fraction calculated from the tests decreased from 37.7% for 1 cycle to 25.01% for 50 cycles. However, one should notice that the decreasing rate is not as significant after 20 cycles of contamination (see **Fig. 4.9**). This means the PAHs contaminants increasingly being adsorbed on the organoclay particle of MGPC after multiple cycles. Considering that the testing flow rate is much faster, and the initial concentration of PAHs is significantly higher than the real situation, the MGPC still maintains considerably adsorption capacity after 50 cycles especially comparing to the conventional pervious concrete. By the observation during the 50 cycles adsorptions, the hydraulic conductivity of the MGPC maintains a stable value and there are few deteriorations of organoclay from the effluent. Particle organoclay cast together with pervious concrete is suggested to be durable enough for preventing the water erosion under the long-term service.

Table. 4.4 The Retardation Factors and the PAHs Mass Balance of column tests by MGPC (C035PM10) after 50 cycles

No. of cycles	Flow rate (mL/s)	Retardation factor R_d	Total mass of PAHs injection every sorption/desorption cycle (mg)	Total mass of PAHs ejection every sorption/desorption cycle (mg)	Cumulative sorbed rate after certain sorption/desorption cycles(%)
1st	1/2	**81.83**	6.81	4.24	**37.77%**
2nd	1/2	**72.73**	5.82	4.04	**34.44%**
3rd	1/2	**66.73**	5.82	4.09	**32.95%**
4th	1/2	**63.74**	5.69	4.10	**31.77%**
5th	1/2	**61.98**	5.69	4.25	**30.54%**
10th	1/2	**58.79**	6.01	4.63	**29.27%**
20th	1/2	**53.93**	6.77	5.34	**27.97%**
30th	1/2	**51.12**	6.99	5.61	**26.81%**
40th	1/2	**47.75**	7.46	5.87	**26.10%**
50th	1/2	**42.20**	7.83	6.49	**25.01%**

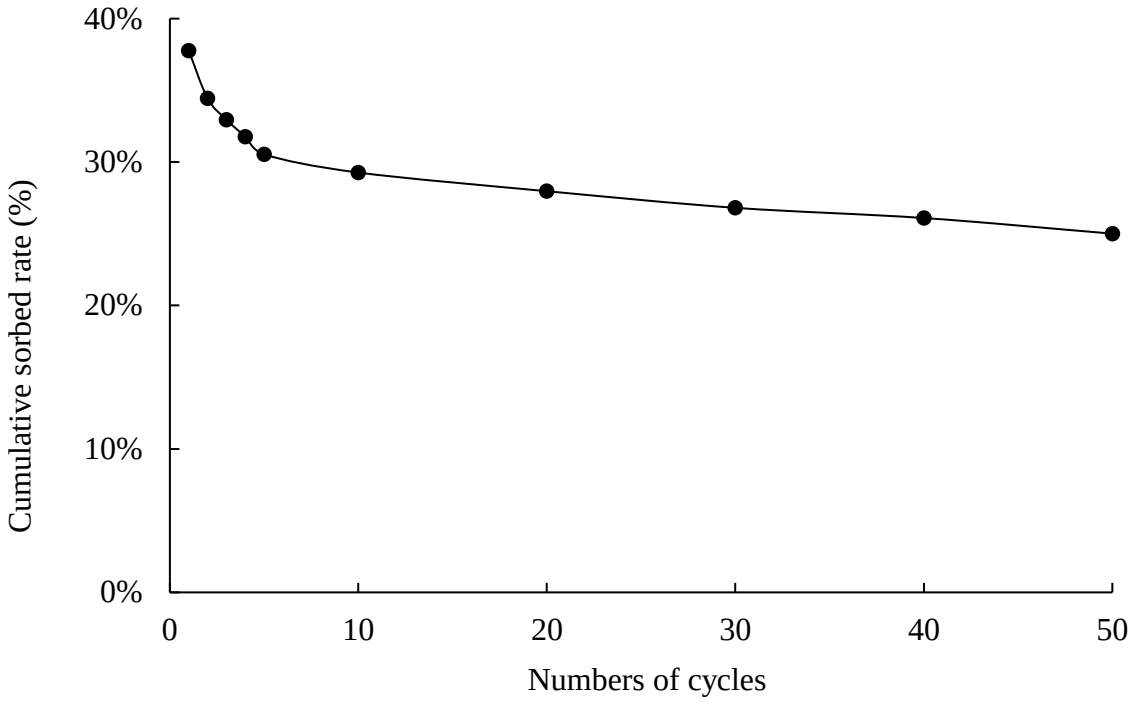

Fig. 4.9. Cumulative sorbed rate of PAHs on MGPC versus the numbers of cycles of MPGC adsorption

4.4 Summaries and Conclusions

In this chapter, the applicability and reusability of MGPC pavement under different onsite conditions including traffic flow, rainfall intensity, multiple rainfall cycles, etc., are mimicked by varying experimental controlled parameters. In particular, the following conclusions can be drawn:

1. The adsorption efficiency of MGPC pavement increases when the initial concentration of the synthetic PAHs solution decreases;

2. The sorption effect of MGPC pavement substantially improves as the flow rate of the penetration liquid tends to be slow. And the increasing retardation factor R_d also indicates

that the MGPC pavement performs better on PAHs removal under the slower stormwater flow rate;

3. FT-IR spectra provide additional evidence that the PAHs molecules are sorbed by the surfactant hydrocarbon chains of the organoclay and lead to an increased bending and torsion;

4. Long-term repeated breakthrough column tests (50 adsorption cycles; 1000 pore volumes synthetic contaminant liquid and water) demonstrate that MGPC pavement can still maintain the capacity of PAHs removal comparing to the conventional pervious concrete.

CHAPTER 5 SIMULATION OF THE LONG-TERM PERFORMANCE OF MGPC PAVEMENT

5.1 Introduction

This chapter provides a whole process of numerical simulation of the long-term performance of MGPC pavement implemented in field-scale (Shang et al., 2020). The process basically includes testing the key physicochemical parameters of MGPC in the lab, gaining the characteristic parameters of the *in-situ* soil stratum, building up the groundwater conditions of the modeling field, and simulating PAHs removal by MGPC pavement under long-term.

Contaminant fate and transport modeling have been studied for several decades. There are several books that cover various theories and practices and one outstanding example is the book edited by Zheng and Bennett (2002), which mainly focuses on the theory of contaminant transport in the groundwater system and simulations of some case studies. And there are also numerous technical papers published during the past decades related to this topic. Some numerical models have interdisciplinary knowledge from other fields, such as chemical engineering, material science, and mechanics. Numerical simulation is an efficient method to evaluate the long-term performance of MGPC on PAHs removal.

Previous laboratory tests in this study demonstrate an effective short-term performance (28 d) of MGPC for PAHs remediation. However, a lab study of its long-term performance (up to 50 years) for field application is not feasible. With the help of numerical simulation and lab tested physicochemical parameters, the long-term in-situ performance of MGPC pavement can be predicted and optimized prior to the real application.

In this chapter, results from the evaluation of the long-term performance of MGPC as a pavement material for stormwater runoff-induced PAHs remediation are presented. Using a numerical model and the governing equations, PAHs remediation and transport in the subsurface soil stratum is investigated. The transport of PAHs in the pavement system was simulated by building up a two-dimensional (2D) site. The physicochemical parameters of MGPC are obtained from lab experiments. Three isotherm models of adsorption, i.e. the linear, Freundlich, and Langmuir models, were separately fitted to MGPC. Besides the comparison of the in-situ long-term performances between the MGPC and the conventional pervious concrete, the impacts of subbase permeability and the initial concentrations of PAHs source on the whole system's purifying efficiency are also examined. Additionally, the applicability of the three isotherms to the long-term simulation of the PAHs removal by MGPC pavement is analyzed.

5.1.1 Theoretical Background and Governing Equations

The PAHs transport and remediation in groundwater are governed by Darcy's law and the law of conservation of mass (Todd and Mays, 2004; Zheng and Bennett, 2002). In this study, the seepage to the soil stratum beneath the proposed pavement materials is

established and simplified as a saturated groundwater flow under steady-state conditions as governed by the following 2D Darcy's law.

$$\frac{\partial}{\partial x}\left(k_x \frac{\partial H}{\partial x}\right) + \frac{\partial}{\partial y}\left(k_y \frac{\partial H}{\partial y}\right) + Q = 0 \qquad (5-1)$$

where k_x (m/s) is the horizontal hydraulic conductivity, k_y (m/s) is the vertical hydraulic conductivity, H (m) is water head, and Q (m^3/s) is the applied boundary flux.

The passing of PAHs through the pervious concrete pavement and its transport in the underside soil stratum are identified as a problem equivalent to solute transport in a reactive saturated porous media and are governed by the 2D advection-dispersion-retardation equation (Freeze and Cherry, 1979; Shackelford, 1994; Zheng and Bennett, 2002):

$$R_d \frac{\partial C}{\partial t} = (D_x \frac{\partial^2 C}{\partial x^2} + D_y \frac{\partial^2 C}{\partial y^2}) - \left(\bar{v}_x \frac{\partial C}{\partial x} + \bar{v}_y \frac{\partial C}{\partial y}\right) + \frac{\rho_b}{n}\frac{\partial S}{\partial t} \qquad (5-2)$$

where R_d (dimensionless) is the retardation factor, C (mg/L) is the contaminant concentration, D_x and D_y (m^2/s) are the longitudinal and transverse coefficients of the hydrodynamic dispersion coefficient, $\bar{v}_x$ and $\bar{v}_y$ (m/s) are the longitudinal and transverse average linear velocities, ρ_b (g/m^3) is the bulk density of the pervious concrete samples, n (%) is the porosity of the pervious concrete samples, and S (mg/g) is the mass of PAHs adsorbed on a unit mass of MGPC or pervious concrete.

The longitudinal and transverse hydrodynamic dispersion coefficients D_x and D_y (m^2/s are related to the longitudinal and transverse dispersivity α_L or α_T (m), average longitudinal and transverse average linear velocity $\bar{v}_x$ or $\bar{v}_y$ (m/s), and diffusion coefficient D^* (m^2/s) by the following equations respectively:

$$D_x = \alpha_L \bar{v}_x + D^* \qquad (5-3)$$

$$D_y = \alpha_T \bar{v}_y + D^* \qquad (5-4)$$

The longitudinal dispersivity α_L (m) and transverse dispersivity α_T (m) were determined using the flow path L (m) of the soil stratum in conjunction with Equation $(6-3)$ and $(6-4)$ below (Todd and Mays, 2004; Xu and Eckstein, 1995):

$$\alpha_L = 0.83(logL)^{2.414} \qquad (5-5)$$

$$\alpha_T = 0.1\alpha_L \qquad (5-6)$$

The diffusion coefficient D* of the PAHs in MGPC and the adsorption function of the PAHs onto the MGPC were determined by the experimental tests. The analytical solution of the equation $(6-7)$ is as follows (van Genuchten et al., 2013):

$$C(x,t) = \frac{1}{2} erfc\left[\frac{R_d x - vt}{\sqrt{4D^* R_d t}}\right] + \sqrt{\frac{v^2 t}{\pi D^* R_d}} exp\left[\frac{(R_d x - vt)^2}{4D^* R_d t}\right] - \frac{1}{2}\left(1 + \frac{vx}{D^*} + \frac{v^2 t}{D^* R_d}\right) exp\left(\frac{vx}{D^*}\right) erfc\left[\frac{R_d x + vt}{\sqrt{4D^* R_d t}}\right] \quad (5-7)$$

where C (μg/mL) is the concentration of the naphthalene in an aqueous phase, R_d is the dimensionless retardation factor, v (m/s) is the seepage velocity along the flowline, t (s) is the time, x (m) is the distance along the direction of transport, and D^* (m^2/s) is the diffusion coefficient.

The diffusion coefficient D^* required in the analytical solution of the PAHs in MGPC and pervious concrete are determined by fitting the curve of the analytical solution to the experimentally measured data.

5.1.2 Background of the GeoStudio

GeoStudio is an integrated powerful software that uses the finite element method to model the complicated geotechnical problems. For this study, the SEEP/W is chosen for modeling

the saturated steady-state flow in porous media, while the CTRAN/W is preferred to simulate the advection-dispersion-retardation mechanism of PAHs solute in the MGPC and the underlying stratum with first-order reactions.

5.2 Materials and Experiments

The testing samples are all cast in 5.08 cm × 10.16 cm cylinders. The mix proportions can be found in **Table 2.4** in section 2.3.3.

5.2.1 Sample preparation

Type I/II LA Portland cement, pre-sieved uniformly graded rounded aggregates, and particle organoclay PM-199 were used to prepare the cement paste and pervious concrete samples for lab testing. The cement paste samples were used for testing the sorption function of PAHs while the concrete samples were used to determine the diffusion coefficient D^* of the stormwater induced PAHs.

The sample preparation method was adapted from Shang and Sun (2019). For preparing the cement paste samples, the cement powder and PM-199 (if needed) were dry mixed by blender with a lower speed of 136 rpm for 1 min and then water was slowly added into the mixture to make the paste. The paste was blended for 2 additional min with the same blender speed and then rested for another 2 min. After rest, the paste was blended for 3 more min with a higher speed of 195 rpm and cast in the 5.08 × 5.08 cm cubic mold (ASTM C305 - 14, 2014). After hardening, the paste sample was crushed and sieved between sieve No. 20 and No. 30 for the batch test.

For preparing the pervious concrete samples, the cement paste was mixed following the same procedure of making paste samples. And then the aggregates were added and mixed uniformly with the cement paste by using the steel rod. The water-to-cement ratio (w/c) was kept in a relatively lower range (0.35 for this study) to maintain the viscosity required to avoid the sagging of extra cement paste (Chandrappa and Biligiri 2016a; Schaefer et al. 2006). The amount of the cement used in pervious concrete was strictly calculated using the theoretical surface area of the aggregates to ensure that the coating thickness was thinner than the mean particle size of the organoclay (Shang and Sun, 2019; Torres et al., 2015). And then the pervious concrete sample was cast in the 5.08 cm × 10.16 cm Teflon coated cylinder mold for column test.

The mix design of pure cement paste with 0.35 water-to-cement ratio (C035), cement paste with 0.35 water-to-binder ratio and 10% of cement replacement by organoclay by mass ratio (C035PM10), conventional pervious concrete with 0.35 water-to-cement ratio (PC035), and MGPC with 0.35 water-to-binder ratio and 10% of cement replacement by organoclay by mass ratio (MGPC035PM10) are listed in **Table 2.4**.

5.2.2 Batch sorption test for adsorption capacity

Batch sorption tests were conducted to test the PAHs sorption capacity of C035PM10 and C035. The details of the testing procedure were described in a previous study (Shang and Sun, 2019). Naphthalene solutions with a volume of 10 mL and predesigned concentrations (1, 2, 3, 5, 10, 15, 20, 40, 50, 100, 150, 200 mg/L) were added into conical centrifuge tubes with PTFE caps respectively. And 0.2 g (±0.001 g) C035PM10 (or C025) were added to each tube. All tubes were agitated for 48 h and centrifuged for 1 h. The supernatant was

filtered by a sterile PTEF syringe filter and extracted by hexane for analyzing the concentration by using gas chromatography equipped with a flame ionization detector (GC-FID). The lab test data of the concentration of adsorbed PAHs by the prepared cement paste samples are fitted to the linear (see **Fig. 5.1**), Freundlich (see **Fig. 5.2**) and Langmuir (see **Fig. 5.3**) isotherms, as defined by Equation $(5-8)$, $(5-9)$ and $(5-10)$, respectively:

$$S = K_d C_e \qquad (5-8)$$

$$S = K_F {C_e}^{1/n} \qquad (5-9)$$

$$S = \frac{q_m K_a C_e}{1 + K_a C_e} \qquad (5-10)$$

where S (mg/g) is the adsorbed concentration of naphthalene by prepared cement paste sample, C_e (mg/L) is the equilibrium concentration of naphthalene in aqueous solution, K_d (L/g) is the partitioning coefficient which is the slope of the linear isotherm, K_F (mg/g) is the Freundlich constants, n (%) is the adsorption intensity, q_m (mg/g) is the adsorption capacity of the system, which is a measure of the total number of binding sites available per gram of sorbent, and K_a (L/mg) is the empirical constant with units of the inverse of concentration C_e.

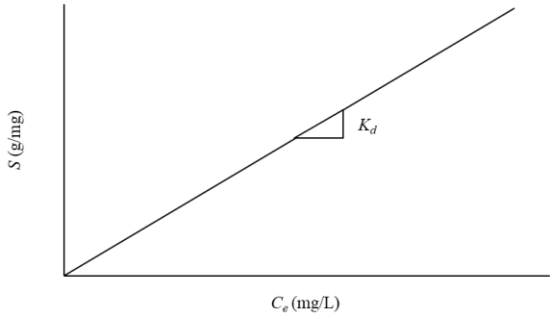

Fig. 5.1. The linear sorption isotherm

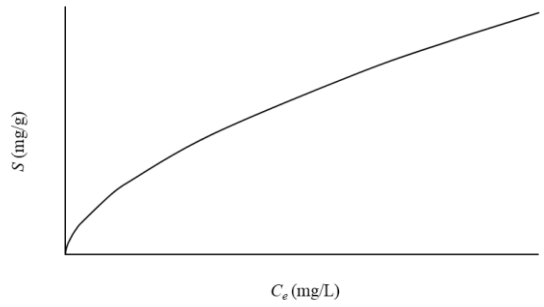

Fig. 5.2. The Freundlich sorption isotherm

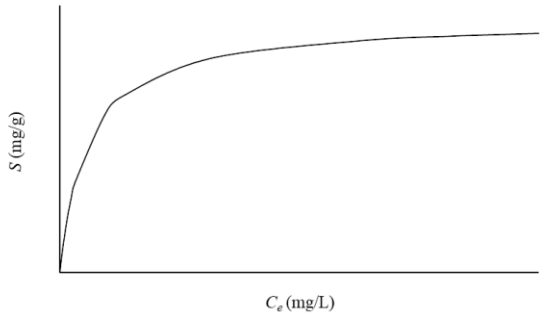

Fig. 5.3. The Freundlich sorption isotherm

5.2.3 Column Tests for Diffusion Coefficient

Laboratory column tests were conducted to determine the diffusion coefficients of the PAHs in PC035 and MGPC035PM10. The detailed testing procedures were presented in a preliminary study by Shang and Sun (2019). The column samples of pervious concrete were sterilized first and flashed with 2 pore volumes (about 120 mL) of deionized water till being saturated. After that, one pore volume (about 60 mL) of naphthalene solution with 100 mg/L concentration was introduced to the column sample by using a glass syringe pump connected with the Teflon tube. And then the inflow was switched to deionized water again. The effluent solution was consistently collected and analyzed by GC-FID until the

concentration was below the detection limit. A pulse-type stormwater runoff-induced PAHs flow passing through the pervious concrete sample can be simplified as a one-dimensional advection-dispersion-retardation problem which is governed by:

$$R_d \frac{\partial C}{\partial t} = D_L \left(\frac{\partial^2 C}{\partial x^2}\right) - v \left(\frac{\partial C}{\partial x}\right) + \frac{\rho_b}{n} \frac{\partial S}{\partial t} \qquad (5-11)$$

where D_L = the longitudinal coefficient of hydrodynamic dispersion (m^2/s); v = the seepage velocity along the flowline (m/s); t = the time (s); C = the concentration of naphthalene in the aqueous phase (mg/L); S = the mass of naphthalene adsorbed on a unit mass of the pervious concrete samples (mg/g) ; ρ_b = the bulk density of the pervious concrete samples (g/m^3); and n = the porosity of the pervious concrete samples (%).

The retardation factor, which is the ratio of the average flow velocity of the simulated stormwater flow to the average migration rate of the PAHs mass center, was determined by the first moment equation (Valocchi, 1985):

$$R_d = \frac{\sum(C_e/C_0)PV\Delta PV}{\sum(C_e/C_0)\Delta PV} - 0.5PV_0 \qquad (5-12)$$

where R_d = the dimensionless retardation factor; C_0 and C_e = the initial and equilibrium concentrations of naphthalene in the aqueous phase (μg/mL), respectively; PV = the corresponding pore volume to each measured concentration (mL); ΔPV= the differential pore volume between each sampling step (mL); and PV_0 (mL) = the initially injected pore volume of the solution to the pervious concrete column.

The analytical solution of the equation $(6-13)$ is as follows (van Genuchten et al., 2013):

$$C(x,t) = \frac{1}{2} erfc\left[\frac{R_d x - vt}{\sqrt{4D^* R_d t}}\right] + \sqrt{\frac{v^2 t}{\pi D^* R_d}} exp\left[\frac{(R_d x - vt)^2}{4D^* R_d t}\right] - \frac{1}{2}\left(1 + \frac{vx}{D^*} + \frac{v^2 t}{D^* R_d}\right) exp\left(\frac{vx}{D^*}\right) erfc\left[\frac{R_d x + vt}{\sqrt{4D^* R_d t}}\right] \quad (5-13)$$

where C = the concentration of the naphthalene in aqueous phase (μg/mL); R_d = the dimensionless retardation factor; v = the seepage velocity along the flowline (m/s); t = the time (s); x = the distance along the direction of transport (m); and D^* = the diffusion coefficient (m^2/s).

The diffusion coefficient D^* required in the analytical solution (equation $(5-13)$) of the PAHs in MGPC and pervious concrete are determined by fitting the curve of the analytical solution to the experimentally measured data.

5.3 Numerical Model Development

To study the long-term performance of MGPC on PAHs remediation, FEM through GeoStudio software was used to simulate the PAHs adsorption and transport in soil stratum. This study chose two sub-software SEEP/W and CTRAN/W from GeoStudio to model the movement of dissolved PAHs in the pore-water (Krahn, 2004a, b). This simulation was a complex process involving advection, dispersion, diffusion, and adsorption. In order to study the influence of PAHs concentration and the various conditions of the subbase on the long-term performance of MGPC, several simulation scenarios are proposed and listed in **Table 5.1**. The parameters needed to be obtained from the lab experiment and literature for simulation are summarized in **Table 5.2**.

Table 5.1 Simulation matrix of MGPC pavement optimization

Impact of onsite condition	Pavement materials		PAHs concentration		Hydraulic conductivity of subbase			Three isotherm models		
	Pervious concrete	MGPC	100 mg/L	20 mg/L	Small	Moderate	Large	Linear	Freundlich	Langmuir
1. MGPC	Yes	–	Yes	–	–	Yes	–	Yes	–	–
	–	Yes	Yes	–	–	Yes	–	Yes	–	–
2. Subbase permeability	–	Yes	Yes	–	Yes	–	–	Yes	–	–
	–	Yes	Yes	–	–	Yes	–	Yes	–	–
	–	Yes	Yes	–	–	–	Yes	Yes	–	–
3. PAHs concentration	–	Yes	Yes	–	–	Yes	–	Yes	–	–
	–	Yes	–	Yes	–	Yes	–	Yes	–	–
4. Isotherm model	–	Yes	Yes	–	–	Yes	–	Yes	–	–
	–	Yes	Yes	–	–	Yes	–	–	Yes	–
	–	Yes	Yes	–	–	Yes	–	–	–	Yes
	–	Yes	–	Yes	–	Yes	–	Yes	–	–
	–	Yes	–	Yes	–	Yes	–	–	Yes	–
	–	Yes	–	Yes	–	Yes	–	–	–	Yes

Table 5.2 Parameters needed for Simulation

Parameters	Alphabet	Testing method	Reference
Bulk Density	ρ_b	Density test for hardened PC	ASTM C175 M-12
Porosity	n	Void content test for hardened PC	ASTM C175 M-12
Hydraulic conductivity	k	Hydraulic conductivity test	Modified apparatus
Longitudinal dispersity	α_L	Xu and Eckstein equation	(Xu and Eckstein 1995)
Transverse dispersity	α_T	Xu and Eckstein equation	(Xu and Eckstein 1995)
Coefficient of volume compressibility	M_V	Literature review	(Lee et al. 1992)
Sorption functions	$K_d, n, K_F, q_{m,K}$	Batch sorption test	Linear isotherm Freundlich isotherm Langmuir isotherm
Diffusion coefficient	D^*	Column test	Mass conservation law

5.3.1 Site Build-up and Simulation Scenarios

In order to simulate the transport of PAHs, a site consisting of 5 layers including pavement, subbase, miscellaneous fill, silt, and clay (see **Fig. 5.4**) is built up. Physicochemical parameters of the pervious concrete pavement are obtained from the lab test while the soil stratum distributions and thicknesses beneath the MGPC are chosen based on the previous studies and represented the typical soil stratum distributions commonly found in urban areas (see **Table 5.3**) (ASTM C1754M-12, 2012; Miller and White, 1998; Terzaghi et al., 1996).

Steady-state conditions are assumed for the simulation. A hydraulic gradient of 1%, commonly encountered in natural groundwater systems (Todd and Mays, 2004), is used for the simulation. Boundary conditions of groundwater are constant depths of 0 m on the left and -2 m on right separately for the adopted site in this study. The steady-state seepage analysis of the water table in all the layers is conducted by the SEEP/W program (Krahn, 2004a), which is a primary fluid transport model and is used to define the initial groundwater conditions for the contaminant transport analysis (**Fig. 5.5**). The depths of groundwater are distributed equally. The flow paths (green lines) are paralleled with the ground surface. And the steady groundwater table is shown as the dashed line (**Fig. 5.5**).

Table 5.3 Parameters needed for the Steady-state Seepage Analysis

Layer Name	Length (m)	Depth (m)	Saturated Horizontal Hydraulic Conductivity k_x (m/s)	Horizontal/ Vertical Hydraulic Conductivities k_y/k_x	Rotation (°)	Saturated Volumetric Water Content (m^3/m^3)	Coefficient of Volume Compressibility M_v (kPa^{-1})
Pavement (MGPC or Pervious concrete)	200	0.4	3×10^{-7}~10^{-5}	1	0	0.29	1×10^{-7}
Subbase	200	0.4	3×10^{-7}~10^{-5}	1	0	0.3	1×10^{-6}
Miscellaneous Fill	200	1.2	3×10^{-4}	1	0	0.3	5×10^{-6}
Silt	200	13	5×10^{-6}	1	0	0.4	1×10^{-5}
Clay	200	3	5×10^{-9}	0.25	0	0.4	5×10^{-5}

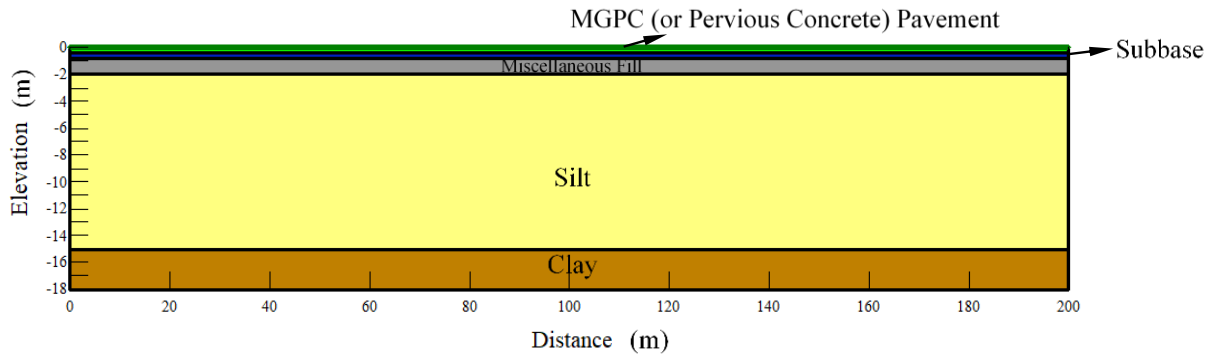

Fig. 5.4. Ideal site for the simulation of PAHs transport

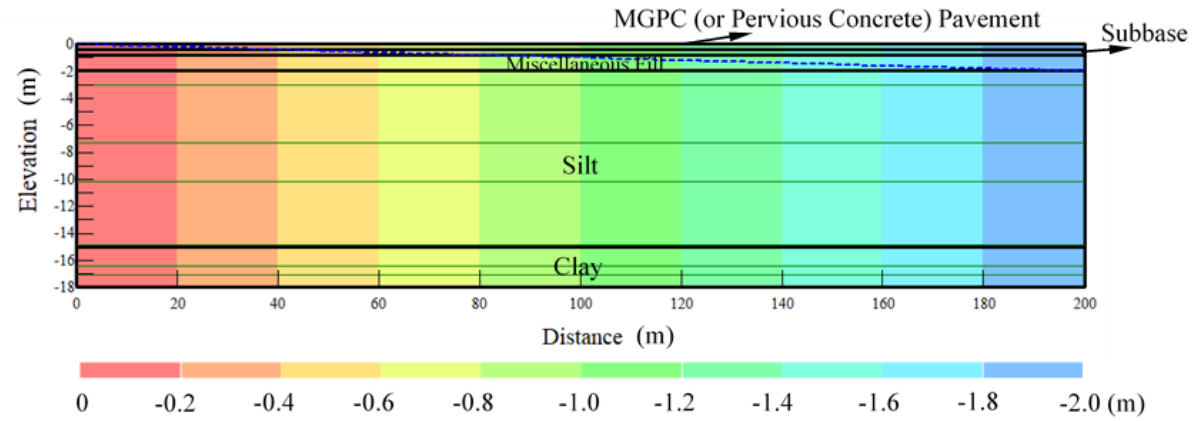

Fig. 5.5. Results for steady-state seepage analysis

5.3.2 PAHs Transport and Remediation Analysis

The CTRAN/W program (Krahn, 2004c) is used to analyze both the stormwater runoff-induced PAHs removal by pavement and PAHs transport in the underneath soil stratum under different scenarios. The FEM mesh size used is 0.5 m including 14837 nodes and 14400 elements, and the mesh type of all the elements was rectangular due to the fact that the pavement and soil stratum are completely parallel (see **Fig. 5.6**). **Fig. 5.6** illustrates the

boundary conditions for PAHs transport analysis. Stormwater runoff-induced PAHs concentration (red line) is assumed to be a constant line boundary condition (100 mg/L or 20 mg/L) that can be approximately considered as a continuous flood. Free drain exit boundaries (blue lines) are applied to both sides. And the zero-concentration boundary (green line) is assigned to the bottom of the clay layer in order to consider the bottom layer to be an impermeable bedrock. The physicochemical parameters of each layer of the site for the PAHs removal and transport analysis are summarized in **Table 5.4**. The diffusion coefficient (D^*) values for the soil stratum are determined by empirical values which is a proportional function of the volumetric water content proposed by Kemper and Van Schaik (1966). Long-term pavement performance over a 50-year period is simulated. Based on this, the 1, 10, 25, 50-year results are presented in the following section.

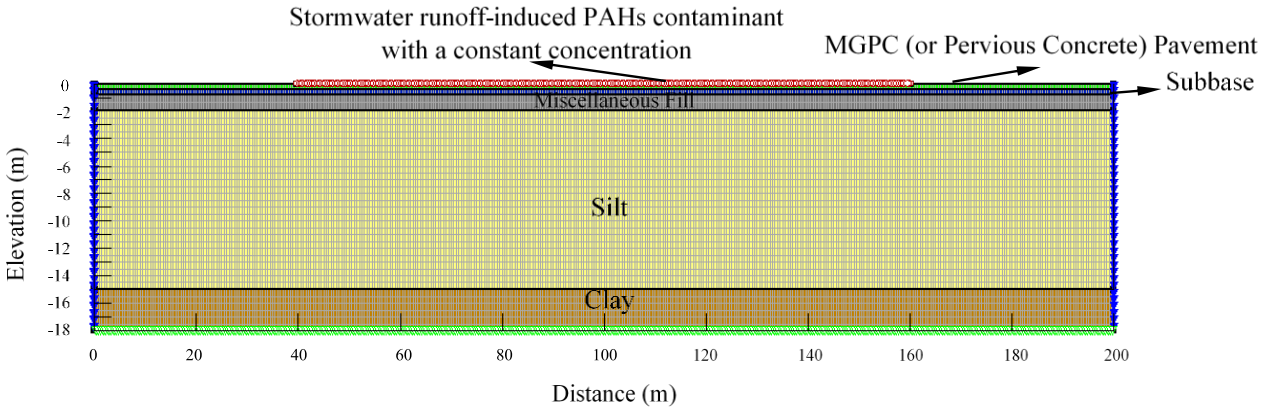

Fig. 5.6. Mesh and boundary conditions for the PAHs transport analysis

Table 5.4 The physicochemical parameters for the PAHs transport analysis of different simulation scenarios

Layer Name		Length (m)	Depth (m)	Diffusion Coefficient D^* (m^2/s)	Longitudinal Dispersivity α_L (m)	Transverse Dispersivity α_T (m)	Bulk Density ρ_b (g/m^3)	Adsorption Functions (m^3/g)
Pavement Materials	Pervious Concrete	200	0.4	4×10^{-10}	4.42	0.44	1.35×10^{6}	Linear Isotherm
	MGPC	200	0.4	3×10^{-10}	4.42	0.44	1.40×10^{6}	Three Isotherms
Soil Stratum under the Pavement	Subbase	200	0.4	4×10^{-10}	4.42	0.44	1.7×10^{6}	2×10^{-13}
	Miscellaneous Fill	200	1.2	4×10^{-10}	4.42	0.44	1.6×10^{6}	2×10^{-13}
	Silt	200	13	4×10^{-10}	4.42	0.44	1.49×10^{6}	2×10^{-13}
	Clay	200	3	3×10^{-10}	4.42	0.44	1.50×10^{6}	2×10^{-11}

5.4 Results and Discussions

5.4.1 PAHs Remediation and Transport with Conventional Pervious Concrete or MGPC Pavement

The PAHs sorption of CP035 and CP035PM10 are analyzed by the linear isotherm model and results are plotted in **Fig. 5.7**. From this figure, it can be seen that the cement paste amended by organoclay has significantly higher PAHs sorption capacity than conventional cement paste. Linear isotherms were fitted using the linear part of the results for both cement paste samples. Equation $(6-14)$ below is fitted for CP035PM10, and equation $(6-15)$ is for CP035, respectively.

$$S = 0.1615C_e \qquad (5-14)$$

$$S = 0.0026C_e \qquad (5-15)$$

where S is the adsorbed concentration of naphthalene by prepared cement paste sample (mg/g); C_e is the equilibrium concentration of naphthalene in aqueous solution (mg/L).

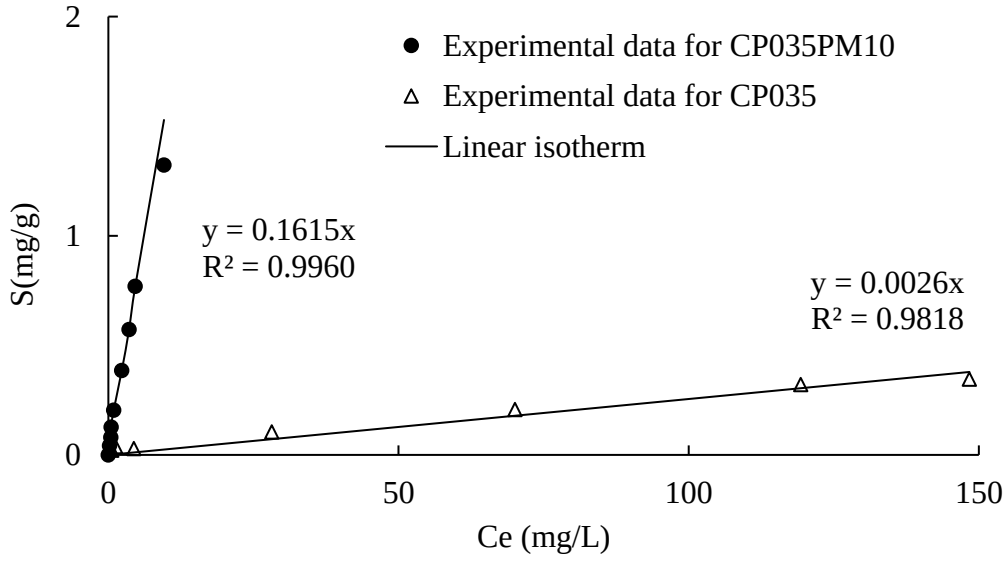

Fig. 5.7. Linear isotherm sorption for the PAH on CP035 and CP035PM10

It can be seen that the cement paste amended by organoclay with partitioning coefficient 0.1615 L/g has significantly higher PAHs sorption capacity than conventional cement paste with partitioning coefficient 0.0026 L/g. Ten-year simulation results of stormwater runoff-induced PAHs transport on the site were chosen to show the MGPC impact on the remediation performance. The onsite advection-dispersion-retardation analysis results of PAHs with the conventional pervious concrete pavement are shown in **Fig. 5.8** (a). The gradient rainbow contours represent the PAHs concentration distributions after 10 years of simulation. Moderate permeability (3×10^{-6} m/s) of subbase and linear isotherm sorption function for pavement material were chosen. A line boundary of the PAHs source with 100 mg/L constant concentration was applied from (40 m, 0 m) to (140 m, 0 m).

Another scenario by using the MGPC pavement under the same conditions was conducted and the effects of MGPC on PAHs 10-year remediation are illustrated in **Fig. 5.8** (b). It can be noted that the shape of the PAHs plume in the MGPC scenario is smaller than the conventional pervious concrete site after 10 years. As shown in the experimental section, the pervious concrete had some sorption capacity of PAHs, but it was negligible when compared to MGPC after a 10-year service. Based on this it can be concluded that the MGPC pavement had an anticipated and remarkable PAHs remediation capacity under the long-term onsite service. It is also worth mentioning that the PAHs plume has penetrated the subbase to affect the groundwater which is reserved in the miscellaneous fill layer. Because the contaminant source is assumed to be constant and continuous, once the PAHs amount exceeding the MGPC sorption capacity the plume would spread and disperse in the next soil layer.

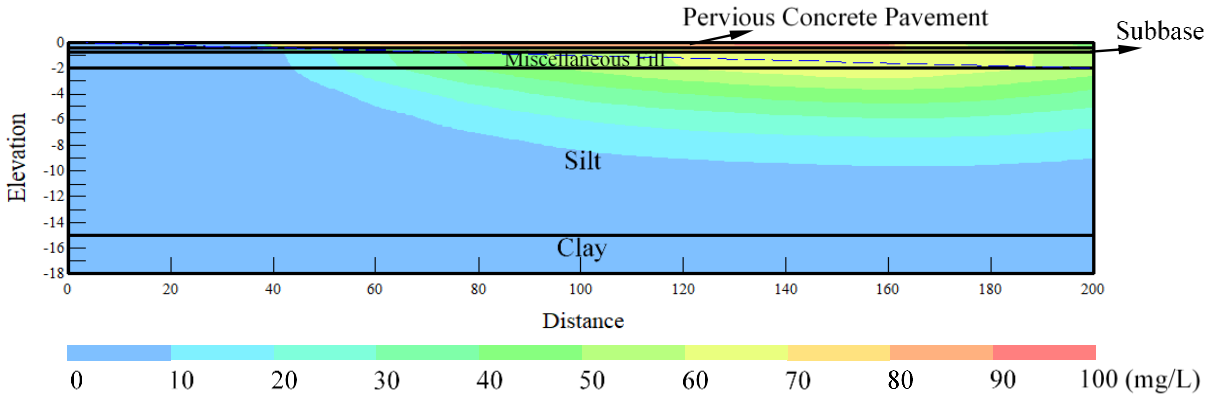

(a)

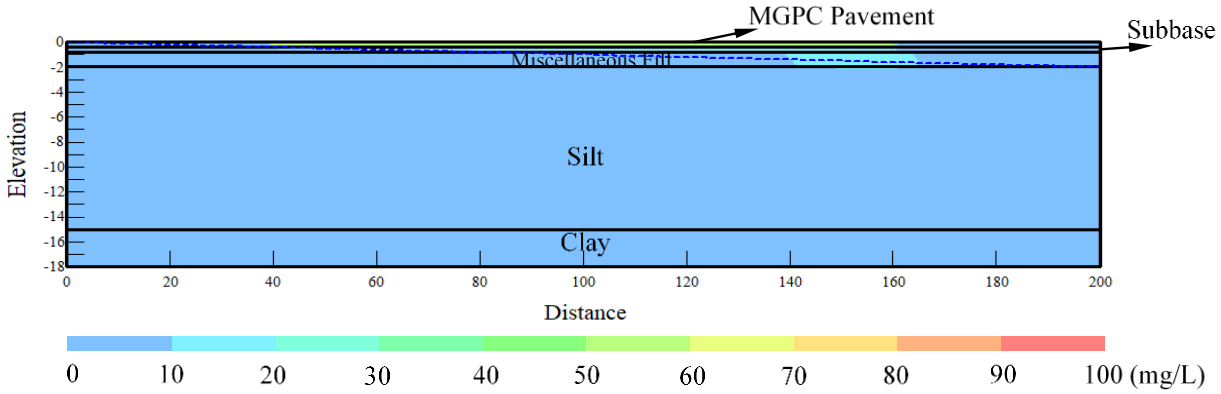

(b)

Fig. 5.8. PAHs transport analysis by (a) using the conventional pervious concrete pavement vs. (b) using the MGPC pavement with linear isotherm after 10 years

5.4.2 Impact of Subbase's Permeability on the PAHs Removal

Permeability and the porosity of the MGPC pavement are key factors for design. The surface permeability and porosity of the pavement should be appropriate to capture a 2-year storm runoff to avoid the ponding issue (Tennis et al., 2004). Meanwhile, the bottom

permeability of the pavement, which is controlled by the critical cross-section area between the pavement and subbase, is critical for the recharge rate of the stored runoff. The bottom permeability of the pavement equals the permeability of the subbase which in turn depends on the degree of consolidation of the subbase before the MGPC pavement installation. Moreover, the recharge rate is also essential to PAHs removal. Previous studies of the kinetic sorption tests showed that an adequate duration for the sorbent and sorbate contacting, ranging from few seconds to more than 10 min, was necessary to let the sorption/remediation processes to be mostly completed (Kaya et al., 2013; Owabor et al., 2012; Reible et al., 2008; Shang and Sun, 2019). Therefore, the permeability of the subbase should be carefully designed and the impact on the PAHs removal must be evaluated in advance.

Fig. 5.9 illustrates the impact of the subbase permeability on the MGPC pavement's long-term performance of PAHs removal. All the scenarios used the same boundary conditions and physicochemical properties for MGPC pavement and soil stratum, except that the only varying parameter was the permeability of the subbase. According to another work (Tennis et al., 2004), the infiltration rate with the value of 3.52×10^{-6} m/s was suitable for the subbase under the proposed pervious pavement. In this study, 3×10^{-7} m/s, 3×10^{-6} m/s, and 3×10^{-5} m/s were selected as low, moderate, and high permeability values of the subbase, respectively. It should be noted that from the left column of the simulation results in **Fig. 5.9** there is no occurrence of PAHs plume even after 50 years of simulation. Due to the relatively smaller permeability of the subbase the recharge rate of the stored stormwater in MGPC pavement was lower. The MGPC had enough time to contact and remediate the PAHs from the stormwater and then release the purified water to the subsurface layers. In

the moderate permeability scenario (shown in the middle column), the PAHs plume started to break through the pavement and spread in 10 years. While the spreading rate was still low, a small PAHs plume with relatively low concentration was built up after 25 years and the plume became a little larger when the simulation stopped at 50 years. In contrast, the simulation results in the right column are different. The PAHs plume passed through the pavement from 1 year and transported rapidly in the subsurface layers. The size and concentration of PAHs plume in the third scenario (permeable subbase) are visibly larger than the other two. As the permeability of the subbase was comparatively higher, the MGPC didn't have sufficient time to complete the adsorption process and the untreated contaminated runoff went downward into the groundwater system. Shang and Sun (2019) demonstrated that 12 min was the critical time scale for PAHs adsorption by the proposed MGPC to mostly reach the equilibrium state (more than 90%). For design purposes of the subbase permeability, the recharging time should be as low as possible and simultaneously guarantees the critical adsorption period.

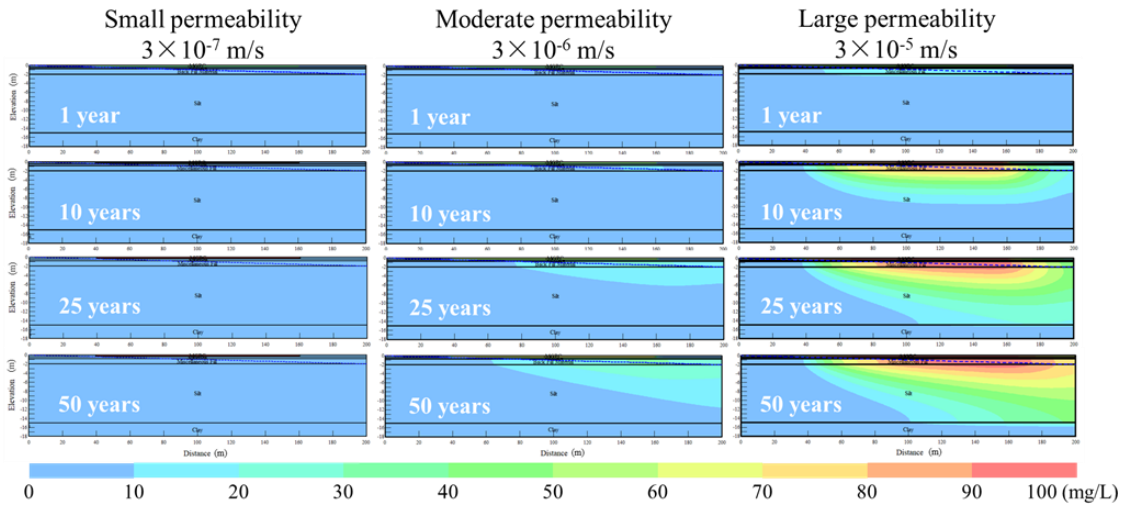

Fig. 5.9. Results for PAHs remediation and transport analysis with 100 gm/L PAHs and linear isotherms MGPC pavement under different permeability of subbase

5.4.3 PAHs Sorption Function of MGPC

The sorption isotherm model is generally used to describe the sorption behavior of certain sorbent for a specific sorbate at chemical equilibrium and evaluate the potential capability of sorption under long-term service. For the MGPC pavement, an appropriate isotherm model is important for accurate assessment of PAHs removal and the economic efficiency of construction design. The particle organoclay embedded in the MGPC plays a key role in PAHs adsorption. The adsorption of PAHs by organoclay is mainly fitted by the linear, Freundlich or Langmuir isotherm (Bartelt-Hunt et al., 2003; Benson et al., 2008; Lee et al., 2011; Shang and Sun, 2019).

The experimental data are plotted in a log-log scale (see **Fig. 5.10**) in order to obtain the Freundlich isotherm parameters. The Freundlich isotherm sorption function can be written as:

$$S = 0.1958{C_e}^{0.597} \qquad (5-16)$$

Meanwhile, the Langmuir isotherm parameters can be also determined by plotting $1/C_e$ vs. 1/S (see **Fig. 5.11**). And the Langmuir isotherm sorption function is written as:

$$S = \frac{0.2778C_e}{1 + 0.1175C_e} \qquad (5-17)$$

The linear, Freundlich and Langmuir isotherms are plotted together with the PAHs sorption experimental data by the C035PM10 in **Fig. 5.12**. As seen, an increasing concentration of PAHs sources from 1 mg/L to 40 mg/L does not result in a visible change of the slope of the sorption curve. However, the slope tends to be zero as the initial PAHs concentrations increased from 50 mg/L to 200 mg/L suggesting that the Langmuir isotherm best fitted this part of experimental data. This finding indicates that when PAHs concentration is high (e.g. for a heavy traffic load), the Langmuir isotherm model tends to better present the sorption process.

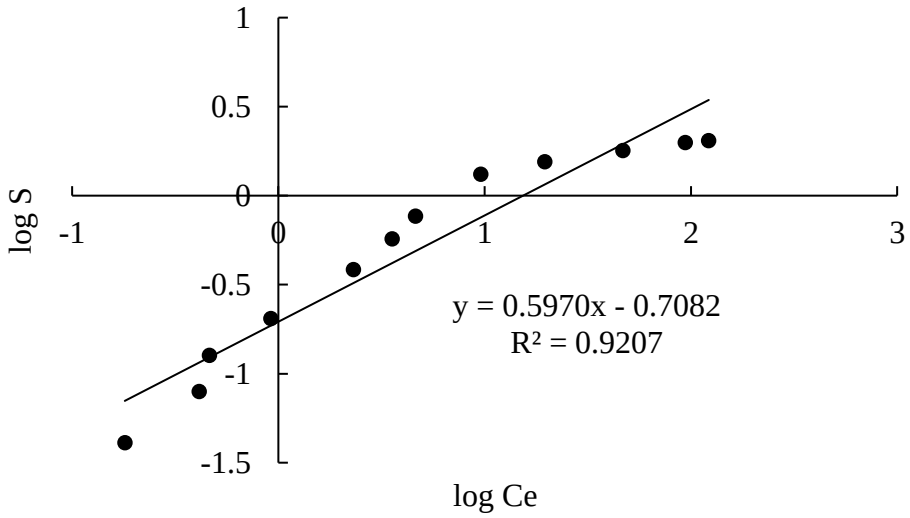

Fig. 5.10. Fit the data with Freundlich isotherm

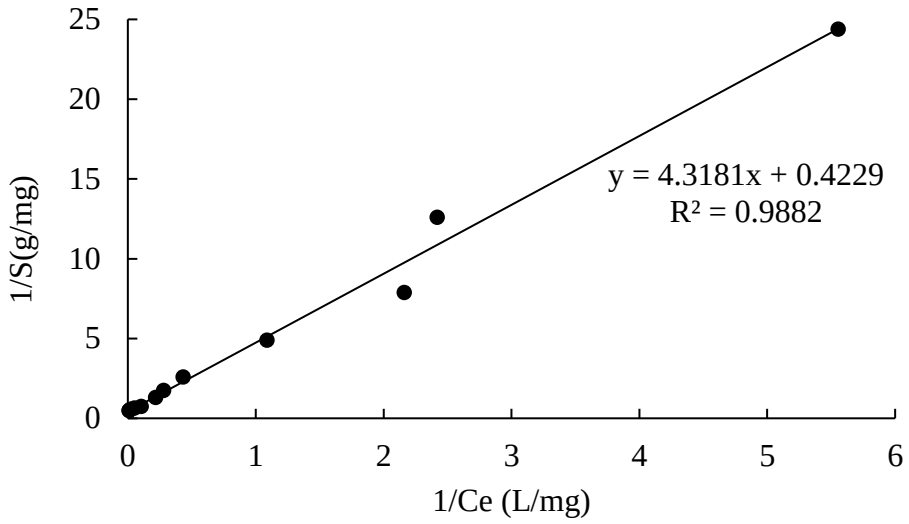

Fig. 5.11. Fit the data with Langmuir isotherm

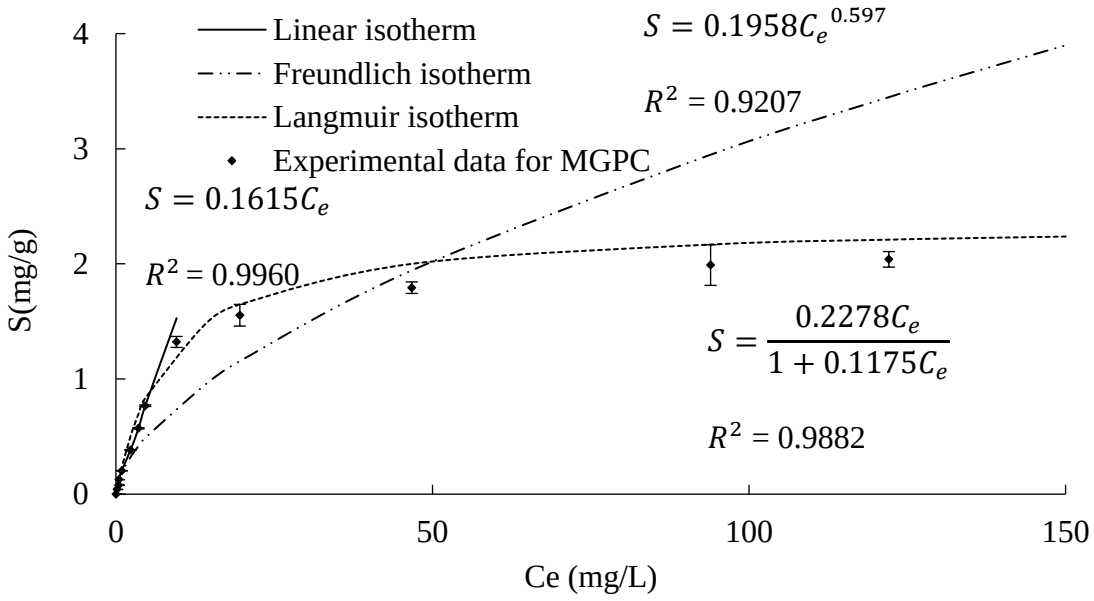

Fig. 5.12. Linear, Freundlich and Langmuir isotherms fitting the adsorption results of PAHs on C035PM10

5.4.4 Impact of Isotherm Models on the Transport of PAHs under Different Initial Concentrations of the Contaminant

In an urban area, the concentration of PAHs source is usually under 1 mg/L (Bojes and Pope, 2007). Because naphthalene can have a relatively high solubility under certain extreme conditions (e.g. 80.9 mg/L at 50 ℃), such as a high road surface temperature, 20 mg/L and 100 mg/L were chosen as different concentrations of the PAHs source for comparison and evaluation. Simulation results of PAHs remediation and transport onsite under certain time intervals with different source concentrations are presented in **Fig. 5.13** (a) and **Fig. 5.13** (b). In **Fig. 5.13** (a), if the PAHs source concentration is at the higher level (100 mg/L), the plume shape of the linear isotherm is relatively smaller than the other two, which indicated that the linear isotherm overestimated the sorption capacity of MGPC in long-term service. And the plume sizes of Freundlich and Langmuir isotherms are similar. The Freundlich isotherm can be used to fit the multilayer adsorption while the Langmuir isotherm basically describes the monolayer adsorption by the finite localized sizes on a sorbent (Foo and Hameed, 2010). The microstructure of the organoclay used in MGPC is a paraffin bilayer, and the simulation results indicated that both Freundlich and Langmuir isotherms well fit the MGPC at a high PAHs source concentration.

Fig. 5.13 (b) presented simulation results based on the three isotherms with lower PAHs source concentration. The increment concentration of the plume is 20 mg/L. By comparison, the plume size of the linear isotherm is a little smaller than those of the other two, but their concentrations are on the same order of magnitude. Key parameters for the linear isotherm model can be readily determined from laboratory tests. Meanwhile, under most circumstances, the concentration of stormwater induced PAHs is much lower than

those used in this study. Therefore, the linear isotherm is an appropriate and reliable option for evaluating the PAHs removal by MGPC pavement and onsite transport in most cases. Results show that the types of isotherm models would influence the long-term simulation results. Therefore, the adsorption isotherm model type should be carefully selected before design. The removal efficiency of PAHs by MGPC was initial concentration-dependent while the desorption occurred at a high source concentration, which is in agreement with the findings of the batch sorption tests and other experimental studies (Braida et al., 2001; DiVincenzo and Sparks, 1997; Giannakopoulou et al., 2012).

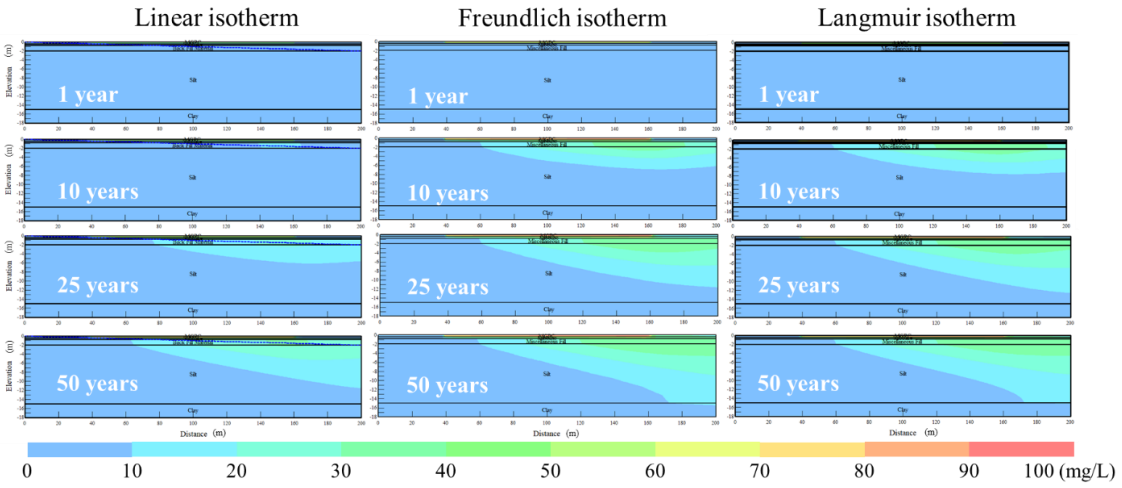

(a)

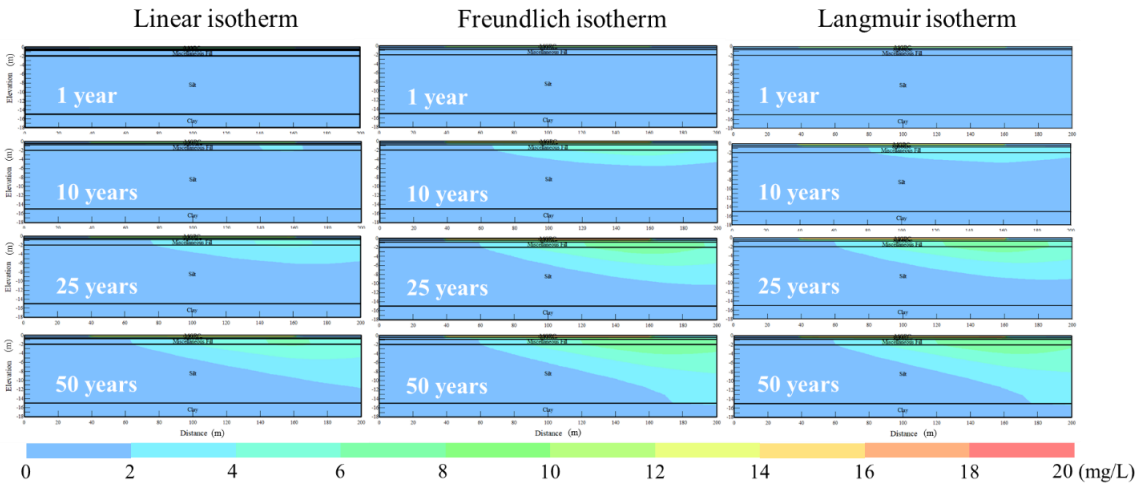

(b)

Fig. 5.13. Results for PAHs remediation and transport analysis with (a) 100 mg/L PAHs source vs. (b) 20 mg/L PAHs source and moderate permeability of subbase under different isotherm models

The transport analysis results of PAHs with different time intervals and source concentrations are further presented in **Fig. 5.14** (a) and (b). It should be noted that the MGPC pavement had higher efficiency on the PAHs remediation when the source concentration was lower. For the initial PAHs concentration of 20 mg/L, MGPC pavement would remove most of the contaminants in 10 years. The PAHs would start to influence the shallow soil stratum after 25 years (see **Fig. 5.14** (a)). However, for 100 mg/L concentration, PAHs source would begin to impact the beneath layer of pavement just after 1 year in service. After 10-year transport of the water through the pavement, the PAHs concentration adjacent to the pavement tended to reach a near-equilibrium level and the concentration after 25 years simulation would finally become stable (see **Fig. 5.14** (b)).

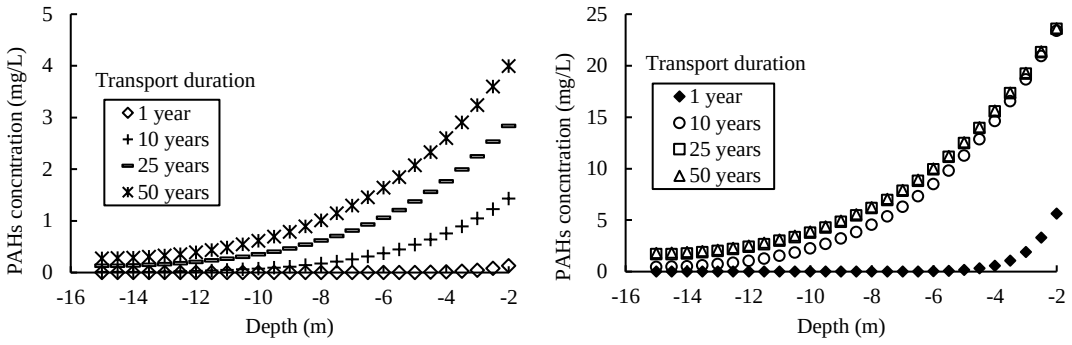

(a) (b)

Fig. 5.14. PAHs concentration vs. soil stratum depth as the middle of the site with (a) 20 mg/L source or (b) 100 mg/L source and different transport durations in years

5.5 Summaries and Conclusions

This chapter evaluates the key parameters which would impact the long-term performance of PAHs removal by MGPC pavement. A mass transport model with *in-situ* conditions is developed for the numerical simulation to bring some beneficial outcomes for potential applications and future design. Based on the results presented here, important conclusions can be drawn as presented below:

1. 10-years simulation results of the onsite advection-dispersion-retardation analysis indicates that the MGPC pavement has a remarkable capability of the PAHs removal for a moderate permeability (3×10-6 m/s) of the subbase compared with the conventional pervious concrete pavement;

2. 50-years simulation results of the MGPC pavement performance with variable permeability have proved that the permeability of subbase plays an important role in the PAHs removal efficiency of the MGPC pavement. An appropriate permeability of subbase

can ensure enough adsorption time for PAHs removal while guaranteeing a sufficient flow rate for runoff infiltration;

3. 50-years simulation results of moderately permeable MGPC pavement performance showed that the initial concentration of contaminant source would influence the PAH removal efficiency by the proposed MGPC pavement. MGPC had higher removal efficiency at a lower initial PAHs concentration;

4. After the 50-years simulation of MGPC pavement, it can be concluded that under lower concentrations of PAHs source all the 3 used sorption isotherm models (linear, Freundlich, and Langmuir) would adequately describe the long-term PAHs sorption performance of MGPC pavement. However, under the higher concentrations of PAHs source, the linear model would overestimate the sorption capacity of MGPC pavement.

CHAPTER 6 LIFE CYCLE ASSESSMENT (LCA) OF MULTI-FUNCTIONAL GREEN PERVIOUS CONCRETE (MGPC) PAVEMENT

6.1 Introduction

Pavements are crucial for the US because the national economy and activities of daily living highly depend on the road transportation system (National Economic et al., 2014). In the US, pavements annually support more than three trillion ton-miles of freight since 2015 (Worth et al., 2016). Sustainability requires a better understanding of the environmental footprint of the Multi-functional Green Pervious Concrete (MGPC) pavement throughout its whole life cycle because the MGPC aims to serve as an alternative and innovative construction material with the stormwater runoff purification functions. Recently, the life cycle assessment (LCA) increasingly has become a useful tool for evaluating the environmental impacts of a specific product and gained public attention for environmental protection and sustainable developments. LCA is a standard and comprehensive approach involves in the perspectives from the phases of raw materials extraction to the end-of-life according to the ISO 14.040 and ISO 14.044 (ISO, 2006a, b). However, the MGPC pavement has its unique properties and broad potential implementations compared to the general pavement. Thus, a specific LCA approach for the MGPC pavement is in demand for evaluating the environmental impact and design purpose.

A lot of research efforts have been done in order to standardize and formalize a fundamental framework for quantitatively evaluating the environmental impacts of pavement (Harvey et al., 2010; Harvey et al., 2016; Loijos et al., 2013; Santero et al., 2011a; Yu and Lu, 2012; Yu et al., 2013). Typically, the entire life cycle of concrete pavement consists of five phases that are materials, construction, use, maintenance and end-of-life (Loijos et al., 2013; Santero et al., 2011b). Since the pavement structure is rich in cementitious materials, and the production and transportation processes do not include a significant amount of other toxic gas emissions, thus, the most adverse impact on the environment is the greenhouse gas emission in terms of Carbon Dioxide Equivalent (CO_2 e) (Marceau et al., 2007; Santero et al., 2011b; Yu and Lu, 2012).

Selecting appropriate indicators are crucial for establishing an effective and efficient performance assessment system. Comparing with the general LCA ideas of the pavement, the MGPC pavement is intensively focused on the impacts of stormwater quality. Thus, one must put emphasis on the water purifying functions when evaluating the MGPC pavement. Following this path, a Pavement Environment and Performance Index (PEPI) is proposed to quantitatively evaluate the environmental impacts and environment-related performance of the MGPC pavement. Several impact indicators are considered in this chapter for PEPI calculation. The carbon dioxide equivalent (CO_2 e) is a significant indicator of greenhouse emission involving in raw materials production, transportation demand, extra fuel cost due to surface deflection and roughness, and concrete carbonation (Gajda, 2001; Haselbach, 2009; Lagerblad, 2005). PAHs removal efficiency is a new indicator that only uses for evaluating the positive environmental impact of the MGPC

pavement. Pervious concrete and MGPC pavements can reduce the Urban Heat Island effect so the Albedo would also be evaluated (Marceau and Van Geem, 2007; Pomerantz, 1997). Permeability is essential to reduce the stormwater runoff and ponding issues so it would also be considered. Some other indicators like lighting associated with the energy cost of illumination would be used. The PAHs removal efficiency and permeability are the primary data sources gained from the lab experiment. However, due to the gap in data collection and time consumption, it is hard to monitor a whole life cycle correlated to every process for a certain project. Other life cycle processes data are collected from software databases such as OpenLCA, Gabi or SimPRO.

The objective of this chapter is to develop an LCA approach of MGPC pavement for potential future design. To develop the LCA approach the study specifically compares three different types of concrete pavements (the conventional impervious concrete pavement, the conventional pervious concrete pavement, and the developed MGPC pavement) to evaluate the life cycle environmental performance. The LCA approach for MGPC pavement can be divided into 1) identify the key parameters of the MGPC pavement that can be analyzed thought out its whole life cycle chain based on the environmental impact considerations; 2) collect the input and output data for all the life cycle phases of the MGPC pavement and define the functional units and system boundaries based on the data collection; 3) develop a PEPI to translate the collected data into impact categories indicators by normalization and weighting methods; and 4) make interpretation of environmental impacts by the proposed type of pavement with the developed PEPI and clarify the limitations. The approach developed for this chapter is expected to be repeatable and practicable to other MGPC pavement with different projected dimensions and mix design.

6.2 Materials and Methods

The materials used for the LCA are impervious concrete pavement, conventional pervious concrete pavement, and MGPC pavement. The mix designs for these three types of pavements are summarized in **Table 6.1**. The corresponding raw materials for making one tone of the concrete are listed, and bulk density and porosity are also shown for the functional unit translations. The assessment methods follow the standard LCA approaches presented by the ISO 14.040 and ISO 14.044 series (ISO, 2006a, b). The mix design of the impervious concrete pavement is obtained by targeting a compressive strength of 38 MPa (5500 psi) that meets the requirement of highway pavement design (Freeseman et al., 2016; GDOT, 2013).

Table 6.1 Mix design for three types of pavements and raw materials needed for casting one ton of the certain concrete

Specimen name	w/c (or w/b)	s/c	a/c (or a/b)	Raw materials for casting one-ton concrete						Bulk density (kg/m^3)	Porosity
				Cement (kg)	PM-199 (kg)	Water (kg)	Sand (kg)	Aggregates (kg)	PM-199 replacement ratio of cement (%)		
Impervious concrete pavement	0.4	1.35	2.3	198.0	0.0	79.2	267.3	455.4	0	2440	0.015
Conventional pervious concrete pavement	0.35	0	5	157.5	0.0	55.1	0	787.4	0	1900	0.29
MGPC pavement	0.35	0	5	141.7	15.7	55.1	0	787.4	10	1900	0.28

6.2.1 Goal and Scope

The phase of goal and scope is the first part of the LCA methodology. This phase provides a specific limit for the MGPC pavement with the considerations of environmental impacts (ISO, 1998). The pavement system is a complicated composition that includes the pavement structure, the subbase, and the compacted subgrade soil. The LCA approach for this chapter only focuses on the pavement structure because the underlying parts are almost the same between different types of pavements. The goal is to prove that the MGPC pavement can provide positive environmental impacts compared with the impervious concrete pavement and conventional pervious concrete pavement by the LCA approach.

The system boundary and all the concerned parameters are shown in **Fig. 6.1**. The whole life cycle of pavement is divided into five phases that are materials, construction, use, maintenance, and end-of-life. Besides the general phases above, the scope also considers the PAHs removal function and the infiltration capacity of the MGPC pavement.

For the goal and comparison purpose, one kilometer with two lanes (3.7m per lane) and 30 cm depth (12 inches) is used as the functional unit for the three types of pavements. The raw materials and some physical properties used for the functional unit are listed in **Table. 6.2**. The mass of each component of the three types of pavements is calculated based on the total volume of the functional unit and the mix designs listed in **Table 6.1**. All the LCA results will be presented based on this functional unit. The analysis period is the whole life cycle (typically 50 years for pavement service) and only landfilling would be considered as the end-of-life process in order to simplify the LCA approach.

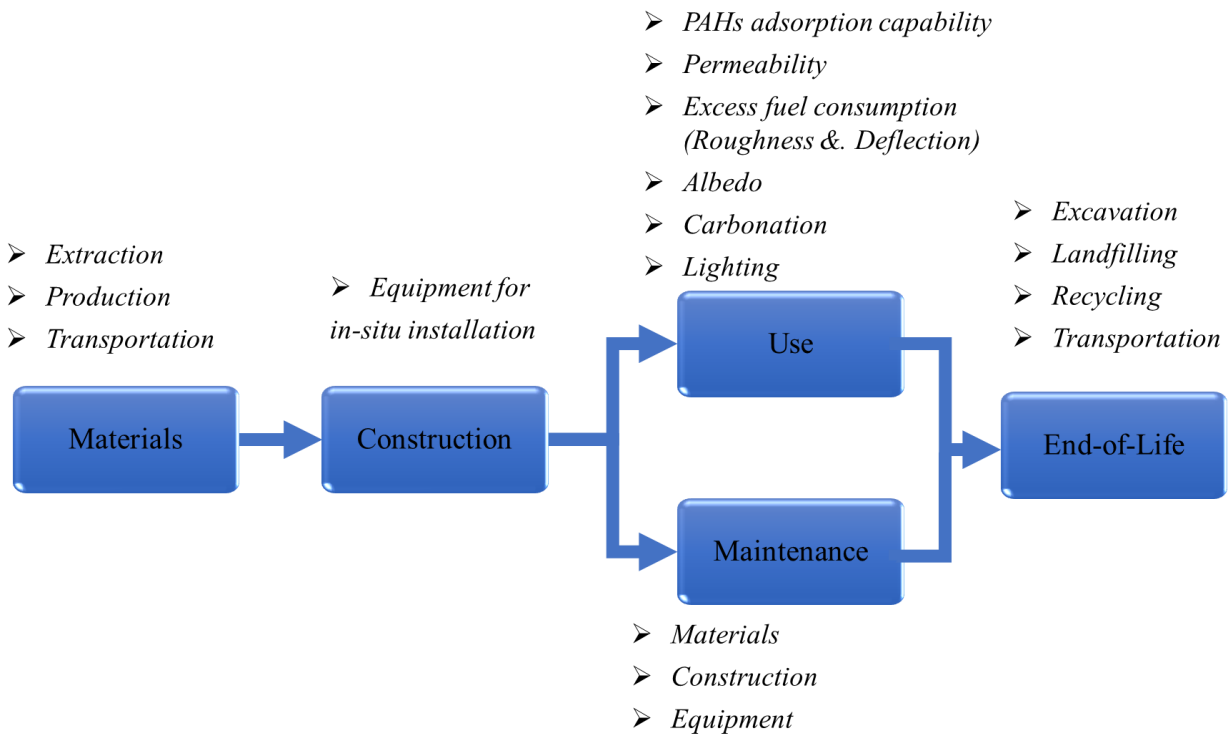

Fig. 6.1. System boundary for MGPC pavement LCA adapted from Noshadravan et al. (2013) and Loijos et al. (2013)

Table 6.2 Functional unit -- one kilometer with two lanes (3.7m per lane) and 30 cm depth (12 inches) and corresponding raw materials for the three types of pavements

Pavement types	Bulk density (kg/m^3)	Porosity	Total Volume (m^3)	Total Mass (kg/km)	Cement (kg/km)	PM-199 (kg/km)	Water (kg/km)	Sand (kg/km)	Aggregates (kg/km)
Impervious concrete	2435	0.015	2220	5.41E+06	1.07E+06	0	4.28E+05	1.45E+06	2.46E+06
Conventional pervious concrete	1900	0.29	2220	4.22E+06	6.64E+05	0	2.32E+05	0	3.32E+06
MGPC	1900	0.28	2220	4.22E+06	5.98E+05	6.64E+04	2.32E+05	0	3.32E+06

6.2.2 Life Cycle Inventory (LCI) Analysis

The Life Cycle Inventory (LCI) Analysis is the second phase of the LCA approach of the MGPC pavement. The necessary data of certain environmental indicators is collected in this phase to serve the goal and scope. LCI is defined by ISO 14.040 as "the phase of life-cycle assessment involving the compilation and quantification of inputs and outputs for a product throughout its life cycle" (ISO, 2006a). The general flow work is shown in **Fig. 6.2**. The main outputs of the LCI results are summarized in **Table 6.3**. Among them, PAHs removal function and the infiltration are primary data that are needed to be gained from the lab experiments. Other LCI data are secondary data that can be collected from commercial and/or public databases and literature. In this chapter, the secondary data are mainly from the public Environmental Footprint database associated with the OpenLCA software and literature.

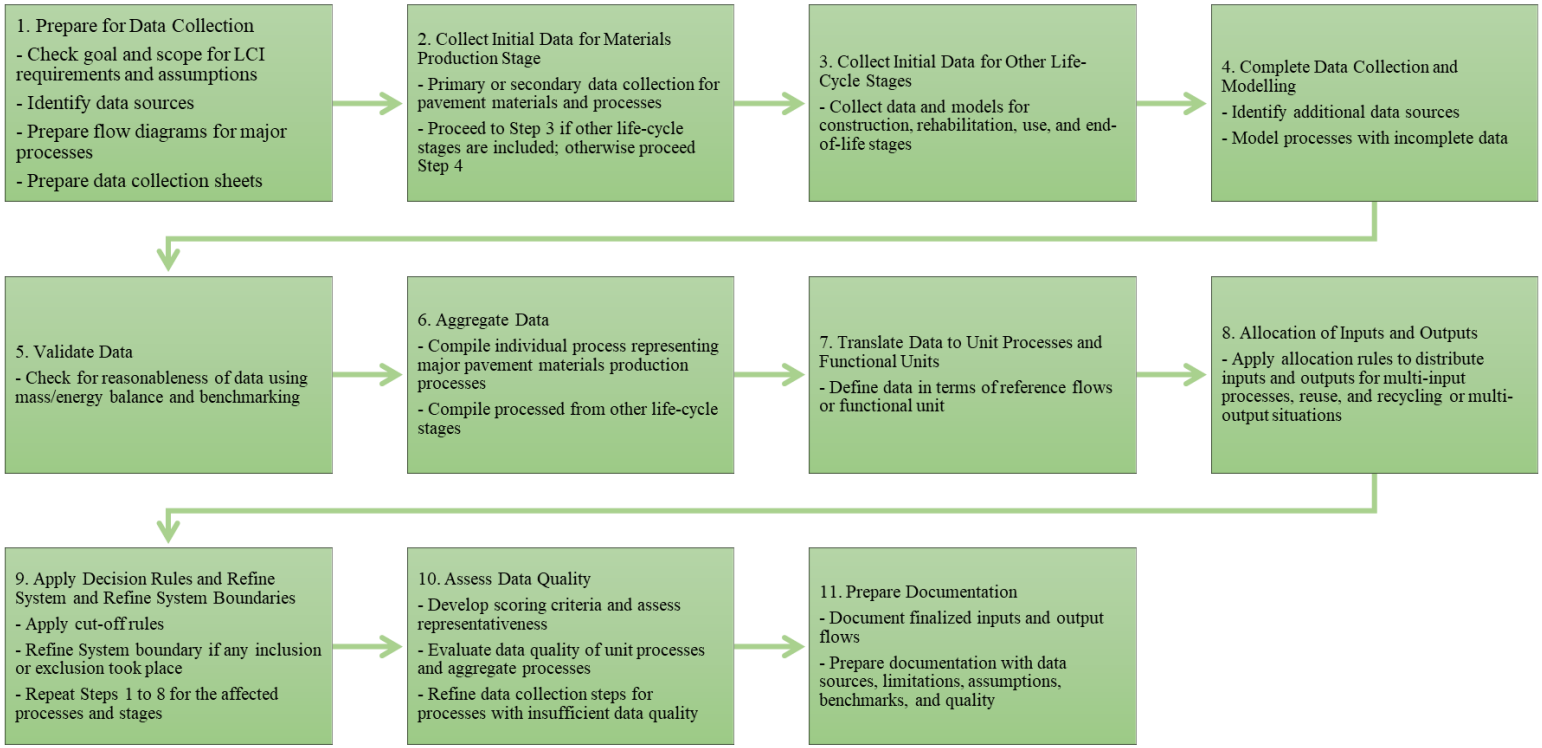

Fig. 6.2. Flow work and key procedures for Life Cycle Inventory (LCI) Analysis (Harvey et al., 2016)

Table 6.3 All the phases and LCI parameters for MGPC pavement LCA

Phases	Process	LCI Parameters	Unit	Data source
Materials	Extraction	CO_2e (Carbon Dioxide Equivalent)	kg/km	Secondary
	Production	CO_2e	kg/km	Secondary
	Transportation	CO_2e	kg/km	Secondary
Construction	Equipment	Energy	kWh/km	Secondary
Use	PAHs adsorption	K_de Partitioning Coefficient Equivalent	L/kg·km	Primary
	Excess fuel consumption	CO_2e	kg/km	Secondary
	Albedo	%	%	Secondary
	Carbonation	Sequestered CO_2e	kg/km	Secondary
	Lighting	Energy	kWh/km	Secondary
	Permeability	Hydraulic conductivity	cm/s	Primary
Maintenance	Materials	CO_2e	kg/km	Secondary
	Construction	CO_2e	kg/km	Secondary
	Equipment	CO_2e	kg/km	Secondary
End-of-life	Excavation	CO_2e	kg/km	Secondary
	Landfilling	CO_2e	kg/km	Secondary
	Recycling	CO_2e	kg/km	Secondary
	Transportation	CO_2e	kg/km	Secondary

6.2.3 Life Cycle Impact Assessment (LCIA)

Life Cycle Impact Assessment (LCIA) is the third phase of the LCA approach. It translates the LCI results into environmental impacts by certain indicators. ISO 14040 states that the purpose of the LCIA is “understanding and evaluating the magnitude and significance of the potential environmental impacts for a product system throughout the life cycle of the product” (ISO, 2006a). The typical LCIA flowchart is illustrated in **Fig. 6.3**.

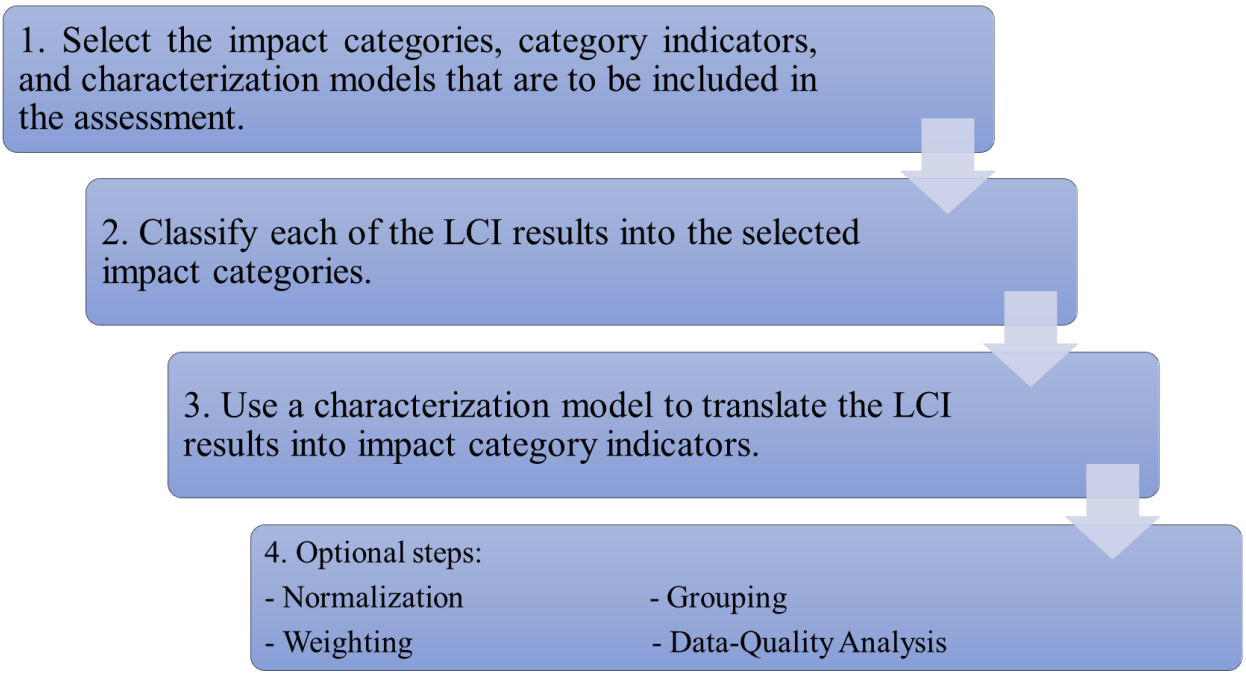

Fig. 6.3. Flowchart of the Life Cycle Impact Assessment (LCIA) (Harvey et al., 2016)

To study the environmental impact of pavements using the LCA approach, the chosen environmental indicators are carbon dioxide emission, energy consumption, PAHs removal function, Albedo and stormwater infiltration capacity. The processes in different phases with the same indicators are grouped together as one LCI result for the subsequent LCIA. Among them, PAHs removal function and stormwater infiltration capacity can provide positive environmental impacts while others would result in adverse environmental influences. A Pavement Environment and Performance Index (PEPI) is proposed to convert these environmental indicators of the pavement into a numerical expression with magnitude ranges between 0 and 1 by weighted normalization method. The value 0 indicates that the type of pavement has no negative environmental impacts while the value 1 stands for the extreme condition of pavement with all negative environmental impacts.

The lower the PEPI is the more environmentally friendly the type of pavement is. The equations for calculating the PEPI, weight value and the normalization of the certain environmental indicator are as follow:

$$PEPI = \sum_{i=1}^{n} W_i \cdot N_i \qquad (6-1)$$

$$W_i = \frac{w_i}{\sum_{i=1}^{n} w_i} \qquad (6-2)$$

$$N_i = \frac{Indicator\ value}{Standard\ indicator\ value} \qquad (6-3)$$

$$or \quad N_i = \frac{(Standard\ indicator\ value - Indicator\ value)}{Standard\ indicator\ value} \qquad (6-4)$$

where the *PEPI* (unitless) is Pavement Environmental Performance Index; n is the number of indicators; w_i (unitless) is an assigned weight with the scale from 1 to 5 by the importance of certain environmental indicator; W_i (unitless) is relative weight value; N_i is the normalized value of a certain environmental indicator, the equation $(6-3)$ expresses the environmental impact of the adverse indicators while the $(6-4)$ expresses the environmental impact of the positive indicators, respectively.

6.2.4 Life Cycle Assessment Interpretation

The Life Cycle Assessment Interpretation is the final phase of the LCA approach. According to the goal and scope of LCA the findings from LCI and LCIA are evaluated to

give the conclusions, limitations, and recommendations (see **Fig. 6.4**) (ISO, 2006b). The purpose of this phase is to convey a transparent and clear result to the decision-makers or certain audiences by transforming the complexity from LCI and LCIA.

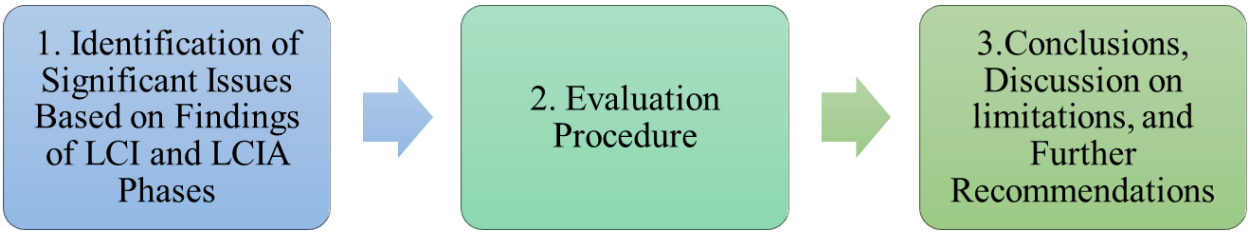

Fig. 6.4. Flowchart of the Life Cycle Interpretation (Harvey et al., 2016)

6.3 Results and Discussions

6.3.1 Greenhouse Gas Emission Results

Greenhouse gas emissions in terms of Carbon Dioxide Equivalent (CO_2e) of the whole life cycle of the three types of pavements are estimated and summarized in **Table 6.4**. In this table, mass (kg) stands for the mass of the material related to certain corresponding process of the three types of pavement (see **Table 6.2**), and CO_2 emission (kg) is the product of the mass and CO_2 emission rate (kg/kg) of each process listed in the table. It is noted that the cement production process is the main contribution of CO_2 emission due to the kilning. The organoclay (PM-199) production is also energy costly. However, the total amount of organoclay usage is small so it does not have significant environmental impacts. Other CO_2 emissions attributed to other raw materials production are not in the same order of magnitude as that of cement production.

By comparison, the pervious concrete pavement and the MGPC pavement have relatively lower CO_2 emission due to less cement usage. Since the cement production is very standard and energy-intensive reducing the cement usage can significantly decrease greenhouse gas emission in order to prevent climate change.

To simplify the LCA, this chapter only considers landfilling as the only option of the End-of-Life phase. It is assumed that all the pavement structures are transported to a landfill 50 km away. It can be seen that transportation would provide a large amount of CO_2 emission in the same order of magnitude as the total quantity before End-of-Life. Therefore, onsite recycling treatment of the construction waste can largely avoid the potential CO_2 emission.

Table 6.4 Greenhouse gas emission of the main processes of the three types of pavements through the whole life cycles

Phase	Process	CO_2 emission rate (kg/kg)	Impervious concrete pavement		Conventional pervious concrete pavement		MGPC pavement	
			Mass (kg/km)	CO_2 emission (kg)	Mass (kg/km)	CO_2 emission (kg)	Mass (kg/km)	CO_2 emission (kg)
Materials	Cement production	0.82255	1.07E+06	8.80E+05	6.64E+05	5.46E+05	5.98E+05	4.92E+05
	Sand production	0.03703	1.45E+06	5.35E+04	0	0.00E+00	0	0.00E+00
	Aggregate production	0.00444	2.46E+06	1.09E+04	3.32E+06	1.47E+04	3.32E+06	1.47E+04
	PM-199 production	0.38503	0	0.00E+00	0	0.00E+00	6.64E+04	2.56E+04
Use	Carbonation	-0.1645	1.07E+06	-1.76E+05	6.64E+05	-1.09E+05	5.98E+05	-9.83E+04
End-of-life	Landfilling	-0.02546	5.41E+06	-1.38E+05	4.22E+06	-1.07E+05	4.22E+06	-1.07E+05
	Transportation	0.0989	5.41E+06	5.34E+05	4.22E+06	4.17E+05	4.22E+06	4.17E+05
Carbon dioxide emission before End-of-life (kg/km)			/	7.69E+05	/	4.52E+05	/	4.34E+05
Carbon dioxide equivalent (kg/km)			/	1.17E+06	/	7.61E+05	/	7.43E+05

6.3.2 Energy Consumption Results of the Three Types of Pavements

Energy consumptions during the whole life cycle for these three types of pavements are estimated in **Table 6.5**. For the production phase, the energy consumption is the product of the fossil fuel consumption rate for production phase and the mass listed in each process. For the construction phase the energy consumption is the product of the power and the mass listed in each process. And for the end-of-life phase the energy consumption is the product of the Crude oil consumption rate for transportation and the mass listed in each process. It can be seen in the table that the traditional impervious concrete pavement requires the largest amount of energy cost comparing to the conventional pervious concrete pavement and MGPC pavement. It is because the other two types of pavement are porous structures that use fewer construction materials than the impervious pavement and the total energy cost is basically weight dependent.

In the production phase cement contributes most of the energy cost even if the consumption rate of PM-199 is higher. In the construction phase, the aggregate provides the most energy cost due to its larger mass. The construction phase will cost several folds of the energy than the material phase. Thus, the better control and management of the construction phase are much more urged to lower the environmental impact for all three types of pavements.

It is also noted that the transportation process in the end-of-life phase occupies the majority part of the total energy consumption. The transportation distance is assumed to be 50 km away. The crude oil consumption rate is determined by the transportation method. If the vehicle type is chosen, the crude oil consumption rate is fixed. And the energy cost for the end-of-life is only dependent on the transportation distance between the job field and landfill position. However, dumping away is not the only choice of the end-of-life phase

of the three types of pavement. For example, the concrete can be recycled as the aggregates for subbase or new concrete. Therefore, rational planning of the end-of-life phase can significantly reduce the total energy consumption for all the three types of pavements.

Table 6.5 Energy consumption results of the main processes of the life cycle for the three types of pavements

Phase	Process	Power (kWh/kg)	Fossil fuel consumption rate for production (MJ/kg)	Crude oil consumption rate for transportation (MJ/kg·km)	Impervious concrete pavement		Conventional pervious concrete pavement		MGPC pavement	
					Mass (kg/km)	Energy (kWh)	Mass (kg/km)	Energy (kWh)	Mass (kg/km)	Energy (kWh)
Production	Cement	/	3.2365	/	1.07E+06	9.62E+05	6.64E+05	5.97E+05	5.98E+05	5.38E+05
	Sand	/	0.64108	/	1.45E+06	2.57E+05	0	0	0	0
	Aggregate	/	0.0596	/	2.46E+06	4.08E+04	3.32E+06	5.50E+04	3.32E+06	5.50E+04
	PM-199	/	11.04423	/	0	0	0	0	6.64E+04	2.04E+05
Construction	Cement	1.3779	/	/	1.07E+06	1.47E+06	6.64E+05	9.15E+05	5.98E+05	8.24E+05
	Sand	1.100141	/	/	1.45E+06	1.59E+06	0	0	0	0
	Aggregate	1.100141	/	/	2.46E+06	2.71E+06	3.32E+06	3.65E+06	3.32E+06	3.65E+06
	PM-199	1.3779	/	/	0	0	0	0	6.64E+04	9.15E+04
End-of-life	Transportation of concrete	/	/	0.75704914	5.41E+06	5.68E+07	4.22E+06	4.44E+07	4.22E+06	4.44E+07
Energy equivalent before end-of-life (kWh/km)					/	7.03E+06	/	5.22E+06	/	5.37E+06
Total energy equivalent (kWh/km)					/	6.39E+07	/	4.96E+07	/	4.97E+07

Assume that the landfill site is 50 km away from the service site and the transportation method is by articulated lorry transport with total weight >32 t

1 MJ = 0.2778 kWh

6.3.3 PAHs Removal Functions for LCI of Three Types of Pavements

PAHs removal function is a new LCI result for the MGPC pavement evaluation. From chapter three it is known that the organoclay plays the key role of PAHs adsorption. The sorption test shows that the partitioning coefficient (K_d) for cement paste is 14.91, while for PM-199, the tested K_d value equals 2370.54. Based on these tested results, the calculated PAHs removal functions of each type of pavement are described by the partitioning coefficient equivalent $K_d\ e$ (L/kg·km) calculated as the weighted average value of K_d (see **Table 6.6**). For the impervious concrete pavement, a depth of 0.67 mm (the average size of the organoclay particle, and the cement paste coating of the pervious concrete and the MGPC) is assumed as the penetrating distance of the stormwater for comparing purpose. Therefore, the mass of cement paste of the impervious concrete pavement is only calculated for the assumptive depth. The partitioning coefficient equivalent is the weighted average value of K_d on mass. The unit of the numbers in the last row of this table is L/kg·km. By comparison, the MGPC pavement has apparently higher $K_d\ e$ than the other two types of pavements. This is because of the organoclay PM-199 having significantly higher PAHs sorption capacity than the cement paste. Only a small replacement proportion can give MGPC better environmental performance on PAHs removal from stormwater runoff. The $K_d\ e$ of conventional pervious concrete pavement is approximately one order of magnitude smaller than that of the MGPC pavement but about two orders of magnitude larger than that of the impervious concrete pavement. It shows that the conventional pervious concrete keeps partial PAHs removal feasibility while the performance of impervious concrete can be negligible.

Table 6.6 PAHs removal functions of three types of pavements

Concrete component	Partitioning coefficient K_d (L/kg)	Impervious concrete pavement		Conventional pervious concrete pavement		MGPC pavement	
		Mass (kg/km)	K_d·Mass (L·kg/kg)	Mass (kg/km)	K_d·Mass (L·kg/kg)	Mass (kg/km)	K_d·Mass (L·kg/kg)
Cement paste	14.91	1.24E+04*	1.85E+05	8.97E+05	1.34E+07	8.30E+05	1.24E+07
Aggregate	0	2.46E+06	0	3.32E+06	0	3.32E+06	0.00E+00
PM-199	2370.54	0	0	0	0	6.64E+04	1.57E+08
Total concrete mass (kg)		5.41E+06	/	4.22E+06	/	4.22E+06	/
Partitioning coefficient equivalent $K_d e$ (L/kg·km)		/	3.42E-02	/	3.17	/	40.27

*Assume that the stormwater can percolate through 0.67 mm depth (equals the cement paste coating of the pervious concrete and MGPC) of the surface cement paste

6.3.4 Other Indicators of Three Types of Pavements

Other indicators of three types of pavements are discussed in this subsection. In order to study the impact of pavement type on the heat island effect, the Albedo of the three types of pavement is listed in **Table 6.7**. The Albedo of impervious concrete pavement is 60% which is a common value of concrete pavement (Levinson and Akbari, 2002). The Albedo of conventional pervious concrete pavement and the MGPC pavement are calculated based on the porosity when assuming the pervious part has no reflection ability. Albedo is defined as the measure of the diffuse reflection of solar radiation out of the total solar radiation. It is used here to describe how much solar energy is reflected by the pavement surface and is considered as a critical factor that is related to the Urban Heat Island (UHI) issue. It was found that the albedo value of concrete pavement is highly related to the cement color and

will be smaller as the surface aging and erosion (Levinson and Akbari, 2002). Some researchers translated the change value of albedo into the CO_2 emission and energy consumption change (Akbari et al., 2009). For this chapter since the albedo is not considered as the main indicator so only a single value for each type of pavement is given based on the different levels of porosities. From the table, it can be seen that the albedo values for conventional pervious concrete and MGPC pavements are very similar due to their similar surface texture. The Albedo of impervious concrete is the largest so that it means that the impervious concrete pavement can reflect more solar energy and has less impact on the environment than the conventional pervious concrete pavement and the MGPC pavement. However, the UHI effect is a more complex issue involves albedo, heat capacities of the pavement and surrounding structure, local weather, etc. Even though the conventional pervious concrete and MGPC pavements have relatively lower Albedo value than the impervious concrete pavement, they can still be considered as the cool pavement option due to the higher heat capacity especially after storing the stormwater (Haselbach et al., 2011).

The infiltration capacity of pavement is essential for reducing the stormwater runoff and preventing the urban ponding issues. The permeabilities of three types of pavements are tested and listed in **Table 6.7** too. The permeability of impervious concrete pavement is obtained from Ollivier and Massat (1992) while the numbers for the conventional pervious concrete pavement and the MGPC pavement are tested in section 2.3.5. As one can see that both pervious pavements have much higher infiltration capacity compared to the impervious pavement. This not only indicates the capability of reducing surface ponding

but also consistent with the lower values of Albedo, which is due to a rough surface texture caused by connected voids.

Table 6.7 Albedo and permeability of three types of pavements

Indicator name	Unit	Impervious concrete pavement	Conventional pervious concrete pavement	MGPC pavement
Albedo	%	60	43.25	43.86
Permeability (k)	cm/s	1.00E-12*	2.05	1.59

*Ollivier and Massat (1992);

6.3.5 Pavement Environment and Performance Index (PEPI)

In order to assist the decision-makers or pavement designers to rationally arrange the strategy for pavement construction plan based on the purpose of sustainable development, the Pavement Environment and Performance Index (PEPI) is proposed as a dimensionless index (range from 0 to 1) that considers various environmental impacts of a pavement. A lower value of PEPI indicates an environmentally friendly behavior, while a larger value of PEPI indicates an adverse environmental impact. The PEPI for the three types of pavements is calculated according to equation $(6-1)$ and they are summarized in **Table 6.8**.

For all three types of pavements, the PEPI is calculated by the normalization method. In this method, all the environmental indicators are assigned a weight (w_i) from 1 to 5 according to the importance of environmental influence and focus strategy from decision-

makers on the consideration of pavement environmental impacts. For this research, since the PAHs adsorption capacity is considered as the most important properties for environment protection so the w_i for the partitioning coefficient equivalent ($K_d\ e$) is assigned as 5. Based on this consideration w_i is assigned as 4 for carbon dioxide equivalent ($CO_2\ e$), 3 for energy equivalent, 3 for permeability, and 1 for Albedo. The relative weight value W_i of each indicator is calculated as the weighted average of the corresponding w_i based on equation $(6-2)$. The standard indicator values are determined by considering some extreme conditions. For the CO_2 emission and energy cost, the pavement structure is assumed to be built only by cement paste due to its higher adverse environmental impact. For PAHs removal, a MGPC with a 20% replacement level of cement by organoclay is used as a standard value for normalizing the PAHs removal functions of the three types of pavements. The standard value of permeability is chosen as 3 cm/s that is close to the superior limit of pervious concrete hydraulic conductivity from literature (Haselbach et al., 2006; Neithalath et al., 2010; Tennis et al., 2004). In the table the indicator values are from the **Table 6.4** to **Table 6.7**. The normalized value N_i is calculated by equation $(6-3)$ or $(6-4)$. And the PEPI for each type of pavement is the summation of $W_i \cdot N_i$ based on equation $(6-1)$.

Since the MGPC pavement mainly focuses on the PAHs removal capacity in this study this indicator is assigned the highest weight value. From the PEPI result in **Table 6.8**, it is shown that the normalization values in the row of CO_2 emission are all relatively lower. It does not mean that the three types of pavement have fewer impacts on climate change. It is because the greenhouse emission is not the key issue when evaluating the MGPC environmental performance. However, by comparison, it is still clear that the MGPC and

pervious concrete pavement have considerably lower greenhouse gas emission than the impervious concrete pavement.

To make the comparisons much more visual, the PEPI results of these three types of pavements are elaborated in **Fig. 6.5**. The colors stand for different environmental indicators. The absolute values of certain color columns cannot be only used as the environmental evaluation basis because they are also related to the w_i values. However, the horizontal comparisons in the identical color can be used for comparing the environmental impacts under the same environmental indicator. By comparisons of the three types of pavements, the conventional pervious concrete pavement and MGPC pavement have relatively lower environmental impacts under all the indicators. The MGPC pavement has better performance on PAHs removal but being a little weaker on infiltration than the conventional pervious concrete. It is because of the organoclay has lower bulk density and occupies partial inter-connected voids of the MGPC.

Table 6.8 Summary of normalization and Pavement Environment and Performance Index (PEPI) of three types of pavements

Indicator name	Indicator unit	Standard indicator value	w_i	W_i	Impervious concrete pavement			Conventional pervious concrete pavement			MGPC pavement		
					Indicator value	N_i	$W_i \cdot N_i$	Indicator value	N_i	$W_i \cdot N_i$	Indicator value	N_i	$W_i \cdot N_i$
Carbon dioxide equivalent ($CO_2 e$)	kg/km	2.40E+06	4	0.25	1.17E+06	0.49	0.12	7.61E+05	0.32	0.08	7.43E+05	0.31	0.08
Energy equivalent	kWh/km	6.56E+07	3	0.19	6.39E+07	0.97	0.18	4.96E+07	0.76	0.14	4.97E+07	0.76	0.14
Albedo	%	100.00	1	0.06	60.00	0.40	0.03	43.25	0.57	0.04	43.86	0.56	0.04
Partitioning coefficient equivalent ($K_d e$)	L/kg·km	77.20	5	0.31	3.42E-02	1.00	0.31	3.17	0.96	0.30	40.27	0.48	0.15
Permeability (k)	cm/s	3.00	3	0.19	1.00E-12	1.00	0.19	2.05	0.32	0.06	1.59	0.47	0.09
Pavement Environment and Performance Index (PEPI)			∑	1.00	∑		0.83	∑		0.62	∑		0.49

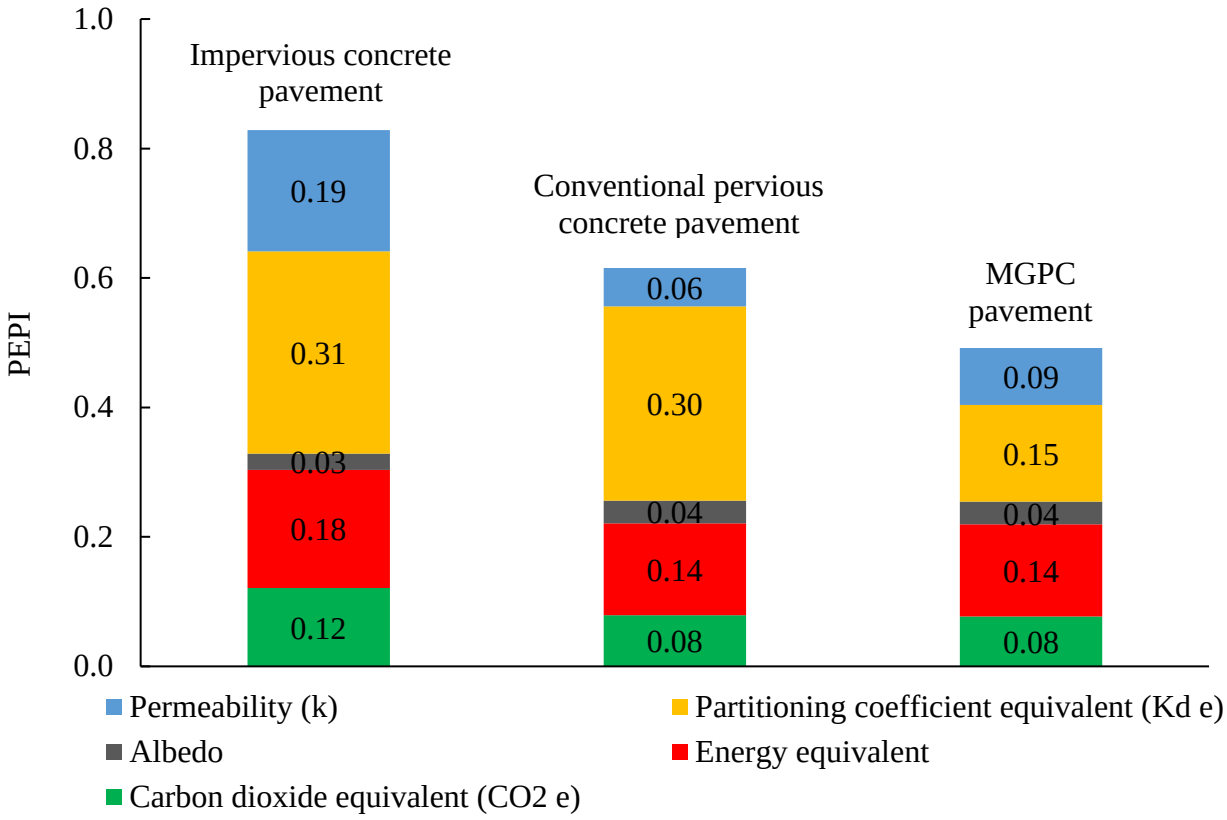

Fig. 6.5. Environmental impacts of three types of pavements by the PEPI

6.4 Summaries and Conclusions

In this chapter, the Life Cycle Assessment (LCA) is applied to three types of concrete pavements including MGPC to evaluate the environmental impacts. A Pavement Environment and Performance Index (PEPI) is proposed to quantify the environmental impact by considering CO_2 emission, water contamination remediation, urban heat island effect, surface ponding reducing, etc. The proposed approach to develop PEPI can be summarized as the following steps:

1. Determining the scope and goal of the LCA and the system boundaries for the pavement by considering the available parameters that can be analyzed in the whole life cycle;

2. Selecting appropriate environmental indicators based on the LCA goal and scope and categorizing the indicators with the same units;

3. Obtaining the initial data from the lab experiments and LCA database and quantifying the environmental impacts by each group of indicators;

4. Developing and calculating the PEPI by normalizing the environmental indicator values by the specific standard values;

5. Identifying the significant issues based on the finding from LCI and LCIA phases and discussing limitations for evaluating the environmental impacts of the pavement by using the PEPI.

After the LCA of the three types of pavements, the conclusions can be drawn as:

1. As the PEPI indicates that the Multi-functional Green Pervious Concrete (MGPC) pavement is more environmentally friendly compared with the traditional impervious concrete pavement and conventional pervious concrete pavement;

2. MGPC pavement has much larger PAHs removal capacity comparing to the other two types of pavements;

3. Energy consumption provides the main contribution to the PEPI score of all the three types of pavements. The majority part of energy consumption is attributed to the

transportation process in the end-of-life phase. If the landfilling can be substituted by the onsite recycling process the adverse environmental impacts can be significantly reduced;

4. The cement production process mainly affects the CO_2 emission of the whole LCA. Comparing with the traditional impervious concrete pavement the pervious concrete pavement and MGPC pavement have a much lower level of CO_2 emission.

CHAPTER 7 CONCLUSIONS AND FUTURE WORK

7.1 Conclusions

In this dissertation, an innovative construction material named Multi-functional Green Pervious Concrete (MGPC) is developed as an alternative material with stormwater runoff-induced PAHs purification function for pavement design. Partial cement power of the pervious concrete is replaced by the organoclay. The mechanical and hydraulic properties are evaluated to find an appropriate cement replaced level by organoclay. After that, the batch sorption test is firstly applied to investigate the PAHs sorption capacity of the cement paste. The column test is then utilized to check the feasibility, in-situ workability, stability and reusability by mimicking the real onsite conditions. Numerical simulation is conducted to assess the long-term performance of MPGC on PAHs removal as a pavement structure. At last, a Life Cycle Assessment (LCA) approach is proposed to make sure that this new type of pavement would not have additional adverse environmental impacts. Based on these studies and results, the conclusions of this research can be drawn as follows:

7.1.1 Organoclay Addition for Cement Paste

1. The organoclay is relatively isolated in the cement paste and would not affect the cement hydration. And the blending energy would not affect the integrity of the organoclay particle;

2. 5% and 10% organoclay replacement of cement had little impact on the mechanical and hydraulic properties of MGPC. Compared to the conventional pervious concrete, the compressive strength of MGPC slightly increased, and the hydraulic conductivity of MGPC moderately decreased.

7.1.2 Preliminary Study of MGPC Feasibility on Stormwater Runoff-induced PAHs Removal

1. The isothermal batch test revealed that with a small amount of organoclay amendment, the cement paste adsorption capacity of PAHs contaminants has been substantially improved;

2. The column test indicated that under a fast flow rate, the retardation factors of the two MGPCs has been dramatically increased compared to that of the conventional pervious concrete;

3. Cement hydration induced alkalinity can additionally improve the adsorption capacity and retardation behavior of the developed concrete, which indicate long-term stability of the material on contaminant remediation.

7.1.3 Applicability and Reusability of MGPC Pavement on PAHs Removal by Mimicking the Real onsite conditions

1. The adsorption efficiency of MGPC pavement increases when the initial concentration of the synthetic PAHs solution decreases;

2. The sorption effect of MGPC pavement substantially improves as the flow rate of the penetration liquid tends to be slow. And the increasing retardation factor R_d also indicates that the MGPC pavement performs better on PAHs removal under the slower stormwater flow rate;

3. FT-IR spectra provide additional evidence that the PAHs molecules are sorbed by the surfactant hydrocarbon chains of the organoclay and lead to an increased bending and torsion;

4. Long-term repeated breakthrough column tests (50 adsorption cycles; 1000 pore volumes synthetic contaminant liquid and water) demonstrate that MGPC pavement can still maintain the capacity of PAHs removal comparing to the conventional pervious concrete.

7.1.4 Simulating the PAHs Removal Properties of MGPC Pavement

1. 10-years simulation results of the onsite advection-dispersion-retardation analysis indicates that the MGPC pavement has a remarkable capability of the PAHs removal for a moderate permeability (3×10-6 m/s) of the subbase compared with the conventional pervious concrete pavement;

2. 50-years simulation results of the MGPC pavement performance with variable permeability have proved that the permeability of subbase plays an important role in the PAHs removal efficiency of the MGPC pavement. An appropriate permeability of subbase can ensure enough adsorption time for PAHs removal while guaranteeing a sufficient flow rate for runoff infiltration;

3. 50-years simulation results of moderately permeable MGPC pavement performance showed that the initial concentration of contaminant source would influence the PAH removal efficiency by the proposed MGPC pavement. MGPC had higher removal efficiency at a lower initial PAHs concentration;

4. After the 50-years simulation of MGPC pavement, it can be drawn that under lower concentrations of PAHs source all the 3 used sorption isotherm models (linear, Freundlich, and Langmuir) would adequately describe the long-term PAHs sorption performance of MGPC pavement. However, under the higher concentrations of PAHs source, the linear model would overestimate the sorption capacity of MGPC pavement.

7.1.5 LCA of MGPC Pavement

1. As the PEPI indicates that the Multi-functional Green Pervious Concrete (MGPC) pavement is more environmentally friendly with relatively lower adverse environmental impacts and emissions comparing with the impervious concrete pavement and conventional pervious concrete pavement;

2. PAHs removal function is a new LCI result for the LCA of the MGPC pavement. MGPC pavement has larger PAHs removal capacity comparing to the other two types of pavements;

3. Energy consumption provides the main contribution to the PEPI score of all the three types of pavements. The majority part of energy consumption is attributed to the transportation process in the end-of-life phase. If the landfilling can be substituted by the onsite recycling process the adverse environmental impacts can be significantly reduced;

4. The cement production process mainly affects the CO_2 emission of the whole LCA. Comparing with the impervious concrete pavement the pervious concrete pavement and MGPC pavement have a lower level of CO_2 emission.

7.2 Future Work

This study suggests MGPC an efficient construction material for pavement in stormwater runoff-induced PAHs removal. Some future work on this topic can be further investigated:

1. PAHs removal function of using various sizes of PM-199 (e.g. fine powders of PM-199) in MGPC can be investigated. If fine powders of PM-199 can be adopted, then the missing protocol of MGPC can be simplified;

2. Further lab tests should be expanded to include other types of PAHs or co-solvent as contaminants and other types of organoclay as additives;

3. Further studies on enhancing the compressive strength of MGPC is needed. The compatibility among the used organoclay and other commonly used chemical additives (e.g. water reducer) need to be further investigated;

4. A pilot field application of MGPC as a parking lot pavement or community road surface can be helpful to further study its water purification function, load capacity, durability, and other long-term serviceability;

5. Life Cycle Cost Analysis (LCCA) can be further refined by collecting enough information of construction and maintenance associated with the price of raw materials.

6. An advanced optimistic LCA approach can be used to improve the proposed approach in chapter 6 by including the maintenance data of MGPC pavement.

REFERENCES

ACI 522R-10, 2010. Report on Pervious Concrete. Farmington Hills, Michigan: American Concrete Institude.

Adams, M.P., Ideker, J.H., 2015. Pore Solution Chemistry of Calcium Aluminate Cement Systems Undergoing Accelerated Conversion, The 14th International Congress on the Chemistry of Cement. Beijing, China.

Akbari, H., Menon, S., Rosenfeld, A., 2009. Global cooling: increasing world-wide urban albedos to offset CO 2. Climatic change 94(3-4), 275-286.

Alkaram, U.F., Mukhlis, A.A., Al-Dujaili, A.H., 2009. The removal of phenol from aqueous solutions by adsorption using surfactant-modified bentonite and kaolinite. Journal of Hazardous Materials 169(1-3), 324-332.

Altare, C.R., Bowman, R.S.B., Katz, L.E., Kinney, K.A., Sullivan, E.J., 2007. Regeneration and long-term stability of surfactant-modified zeolite for removal of volatile organic compounds from produced water. Microporous and Mesoporous Materials 105(3), 305-316.

Altin, O., Ozbelge, O.H., Dogu, T., 1999. Effect of pH, flow rate and concentration on the sorption of Pb and Cd on montmorillonite: I. Experimental. Journal of Chemical Technology & Biotechnology 74(12), 1131-1138.

Anbalagan, G., Prabakaran, A., Gunasekaran, S., 2010. Spectroscopic characterization of Indian standard sand. Journal of applied spectroscopy 77(1), 86-94.

Aoki, Y., Sri Ravindrarajah, R., Khabbaz, H., 2012. Properties of pervious concrete containing fly ash. Road materials and pavement design 13(1), 1-11.

Arnold Jr, C.L., Gibbons, C.J., 1996. Impervious surface coverage: the emergence of a key environmental indicator. Journal of the American planning Association 62(2), 243-258.

Arroyo, M., Lopez-Manchado, M., Herrero, B., 2003. Organo-montmorillonite as substitute of carbon black in natural rubber compounds. Polymer 44(8), 2447-2453.

Association, C.C.R.M.C., 2009. Specifier's Guide for Pervious Concrete Pavement Design–Version 1.2. 24p.

ASTM C31 / C31M - 18a, 2018. Standard Practice for Making and Curing Concrete Test Specimens in the Field. ASTM International, West Conshohocken, PA.

ASTM C39 / C39M-17b, 2017. Standard Test Method for Compressive Strength of Cylindrical Concrete Specimens. ASTM International, West Conshohocken, PA.

ASTM C109 / C109M-16a, 2016. Standard Test Method for Compressive Strength of Hydraulic Cement Mortars (Using 2-in. or [50-mm] Cube Specimens). ASTM International, West Conshohocken, PA.

ASTM C128-15, 2015. Standard Test Method for Relative Density (Specific Gravity) and Absorption of Fine Aggregate. ASTM International, West Conshohocken, PA.

ASTM C136/C136M-14, 2014. Standard Test Method for Sieve Analysis of Fine and Coarse Aggregates. ASTM International, West Conshohocken, PA.

ASTM C188-16, 2016. Standard Test Method for Density of Hydraulic Cement. ASTM International, West Conshohocken, PA.

ASTM C191-13, 2013. Standard Test Methods for Time of Setting of Hydraulic Cement by Vicat Needle. ASTM International, West Conshohocken, PA.

ASTM C204-16, 2016. Standard Test Method for Fineness of Hydraulic Cement by Air-Permeability Apparatus. ASTM International, West Conshohocken, PA.

ASTM C305 - 14, 2014. Standard Practice for Mechanical Mixing of Hydraulic Cement Pastes and Mortars of Plastic Consistency. ASTM International, West Conshohocken, PA.

ASTM C430-08(2015), 2015. Standard Test Method for Fineness of Hydraulic Cement by the 45-μm (No. 325) Sieve. ASTM International, West Conshohocken, PA.

ASTM C837-14, 2014. Standard Test Method for Methylene Blue Index of Clay. ASTM International, West Conshohocken, PA.

ASTM C1754M-12, 2012. Standard Test Method for Density and Void Content of Hardened Pervious Concrete. ASTM International, West Conshohocken, PA.

ASTM D854-14, 2014. Standard test methods for specific gravity of soil solids by water pycnometer. ASTM International, West Conshohocken, PA.

Bartelt-Hunt, S.L., Burns, S.E., Smith, J.A., 2003. Nonionic organic solute sorption onto two organobentonites as a function of organic-carbon content. Journal of Colloid and Interface Science 266(2), 251-258.

Benson, C., Lee, S., Ören, A., 2008. Evaluation of three organoclays for an adsorptive barrier to manage DNAPL and dissolved-phase polycyclic aromatic hydrocarbons (PAHs) in ground water. Geo Engineering Rep. No. 08 24.

Bhutta, M.A.R., Tsuruta, K., Mirza, J., 2012. Evaluation of high-performance porous concrete properties. Construction and Building Materials 31, 67-73.

Bogue, R.H., 1955. The chemistry of Portland cement. LWW.

Bojes, H.K., Pope, P.G., 2007. Characterization of EPA's 16 priority pollutant polycyclic aromatic hydrocarbons (PAHs) in tank bottom solids and associated contaminated soils at oil exploration and production sites in Texas. Regulatory Toxicology and Pharmacology 47(3), 288-295.

Bornstein, R.D., 1968. Observations of the urban heat island effect in New York City. Journal of Applied Meteorology 7(4), 575-582.

Bowman, R.S., Haggerty, G.M., Huddleston, R.G., Neel, D., Flynn, M.M., 1995. Sorption of nonpolar organic compounds, inorganic cations, and inorganic oxyanions by surfactant-modified zeolites, ACS symposium series (USA).

Braida, W.J., White, J.C., Ferrandino, F.J., Pignatello, J.J., 2001. Effect of solute concentration on sorption of polyaromatic hydrocarbons in soil: uptake rates. Environmental science & technology 35(13), 2765-2772.

Brattebo, B.O., Booth, D.B., 2003. Long-term stormwater quantity and quality performance of permeable pavement systems. Water research 37(18), 4369-4376.

Chandrappa, A.K., Biligiri, K.P., 2016a. Comprehensive investigation of permeability characteristics of pervious concrete: A hydrodynamic approach. Construction and Building Materials 123, 627-637.

Chandrappa, A.K., Biligiri, K.P., 2016b. Pervious concrete as a sustainable pavement material–Research findings and future prospects: A state-of-the-art review. Construction and Building Materials 111, 262-274.

Chang, G.C., Parrish, J.H., Soeur, C., 1990. The first flush of runoff and its effects on control structure design. Environmental and Conservation Services Department, Austin, TX, US.

Chang, K.-F., Fang, G.-C., Chen, J.-C., Wu, Y.-S., 2006. Atmospheric polycyclic aromatic hydrocarbons (PAHs) in Asia: a review from 1999 to 2004. Environmental pollution 142(3), 388-396.

Chindaprasirt, P., Hatanaka, S., Chareerat, T., Mishima, N., Yuasa, Y., 2008. Cement paste characteristics and porous concrete properties. Construction and Building materials 22(5), 894-901.

Ćosić, K., Korat, L., Ducman, V., Netinger, I., 2015. Influence of aggregate type and size on properties of pervious concrete. Construction and Building Materials 78, 69-76.

Damodaram, C., Giacomoni, M.H., Prakash Khedun, C., Holmes, H., Ryan, A., Saour, W., Zechman, E.M., 2010. Simulation of Combined Best Management Practices and Low Impact Development for Sustainable Stormwater Management. JAWRA Journal of the American Water Resources Association 46(5), 907-918.

Debnath, B., Sarkar, P.P., 2018. Pervious concrete as an alternative pavement strategy: a state-of-the-art review. International Journal of Pavement Engineering.

Deo, O., Neithalath, N., 2010. Compressive behavior of pervious concretes and a quantification of the influence of random pore structure features. Materials Science and Engineering: A 528(1), 402-412.

Dietz, M.E., 2007. Low impact development practices: A review of current research and recommendations for future directions. Water, air, and soil pollution 186(1-4), 351-363.

DiVincenzo, J.P., Sparks, D.L., 1997. Slow sorption kinetics of pentachlorophenol on soil: concentration effects. Environmental science & technology 31(4), 977-983.

Field, R., Tafuri, A.N., 2006. The use of best management practices (BMPs) in urban watersheds. DEStech Publications, Inc, Lancaster, Pennsylvania.

Foo, K.Y., Hameed, B.H., 2010. Insights into the modeling of adsorption isotherm systems. Chemical engineering journal 156(1), 2-10.

Freeseman, K., Hoegh, K., Khazanovich, L., 2016. Concrete Strength Required to Open to Traffic.

Freeze, R., Cherry, J., 1979. Groundwater. Englewood Cliffs, New Jersey: Prentice-Hall.

Froehlich, D.C., 2009. Graphical calculation of first-flush flow rates for storm-water quality control. Journal of irrigation and drainage engineering 135(1), 68-75.

Gajda, J., 2001. Absorption of atmospheric carbon dioxide by portland cement concrete. Portland Cement Association.

GDOT, 2013. Standard specifications: Construction of transportation systems.

Gehle, K., 2009. Toxicity of polycyclic aromatic hydrocarbons (PAHs). US Department of Health and Human Services, Agency for Toxic Substances and Disease Registry, Centers for Disease Control, Atlanta, GA, pp. 1-68.

Giannakopoulou, F., Gasparatos, D., Haidouti, C., Massas, I., 2012. Sorption behavior of cesium in two greek soils: effects of Cs initial concentration, clay mineralogy, and particle-size fraction. Soil and Sediment Contamination: An International Journal 21(8), 937-950.

Göbel, P., Dierkes, C., Coldewey, W., 2007. Storm water runoff concentration matrix for urban areas. Journal of contaminant hydrology 91(1-2), 26-42.

Greish, S., Rinnan, A.s., Marcussen, H., Holm, P.E., Christensen, J.H., 2018. Interaction mechanisms between polycyclic aromatic hydrocarbons (PAHs) and organic soil washing agents. Environmental Science and Pollution Research 25(1), 299-311.

Guo, A., Aamiri, O.B., Satyavolu, J., Sun, Z., 2019a. Impact of thermally modified wood on mechanical properties of mortar. Construction and Building Materials 208, 413-420.

Guo, A., Sun, Z., Qi, C., Sathitsuksanoh, N., 2020a. Hydration of Portland Cement Pastes Containing Untreated and Treated Hemp Powders. Journal of Materials in Civil Engineering 32(6), 04020148.

Guo, A., Sun, Z., Sathitsuksanoh, N., Feng, H., 2020b. A Review on the Application of Nanocellulose in Cementitious Materials. Nanomaterials 10(12), 2476.

Guo, A., Sun, Z., Satyavolu, J., 2019b. Impact of chemical treatment on the physiochemical and mechanical properties of kenaf fibers. Industrial Crops and Products 141, 111726.

Guo, A., Sun, Z., Satyavolu, J., 2020c. Impact of modified kenaf fibers on shrinkage and cracking of cement pastes. Construction and Building Materials 264, 120230.

Harvey, J., Kendall, A., Lee, I., Santero, N., Dam, T., Wang, T., 2010. Pavement life cycle assessment workshop: discussion summary and guidelines, University of California Pavement Research Center, California.

Harvey, J., Meijer, J., Ozer, H., Al-Qadi, I.L., Saboori, A., Kendall, A., 2016. Pavement Life Cycle Assessment Framework. United States. Federal Highway Administration.

Haselbach, L., 2009. Potential for carbon dioxide absorption in concrete. Journal of Environmental Engineering 135(6), 465-472.

Haselbach, L., Boyer, M., Kevern, J.T., Schaefer, V.R., 2011. Cyclic heat island impacts on traditional versus pervious concrete pavement systems. Transportation research record 2240(1), 107-115.

Haselbach, L.M., Valavala, S., Montes, F., 2006. Permeability predictions for sand-clogged Portland cement pervious concrete pavement systems. Journal of environmental management 81(1), 42-49.

Hernández-Crespo, C., Fernández-Gonzalvo, M., Martín, M., Andrés-Doménech, I., 2019. Influence of rainfall intensity and pollution build-up levels on water quality and

quantity response of permeable pavements. Science of The Total Environment 684, 303-313.

Hrachová, J., Madejová, J., Billik, P., Komadel, P., Fajnor, V.Š., 2007. Dry grinding of Ca and octadecyltrimethylammonium montmorillonite. Journal of colloid and interface science 316(2), 589-595.

Huang, B., Mohammad, L.N., Chris Abadie, P., 1999. Fundamentals of Penneability in Aspbalt Mixtures, The Annual Meeting of the Association of Asphalt Paving Technologist.

Huang, B., Wu, H., Shu, X., Burdette, E.G., 2010. Laboratory evaluation of permeability and strength of polymer-modified pervious concrete. Construction and Building Materials 24(5), 818-823.

Ibrahim, A., Mahmoud, E., Yamin, M., Patibandla, V.C., 2014. Experimental study on Portland cement pervious concrete mechanical and hydrological properties. Construction and building materials 50, 524-529.

Imhoff, M.L., Zhang, P., Wolfe, R.E., Bounoua, L., 2010. Remote sensing of the urban heat island effect across biomes in the continental USA. Remote sensing of environment 114(3), 504-513.

ISO, 1998. Environmental Management-Life Cycle Assessment-Goal and Scope Definition and Inventory Analysis

ISO, 2006a. Environmental Management: Life Cycle Assessment; Principles and Framework. International Organization for Standardization.

ISO, 2006b. Environmental management: Life cycle assessment; requirements and guidelines. International Organization for Standardization.

Javadi, S., Ghavami, M., Zhao, Q., Bate, B., 2017. Advection and retardation of non-polar contaminants in compacted clay barrier material with organoclay amendment. Applied Clay Science 142, 30-39.

Joshaghani, A., Ramezanianpour, A.A., Ataei, O., Golroo, A., 2015. Optimizing pervious concrete pavement mixture design by using the Taguchi method. Construction and Building Materials 101, 317-325.

Kah, M., Zhang, X., Jonker, M.T., Hofmann, T., 2011. Measuring and modeling adsorption of PAHs to carbon nanotubes over a six order of magnitude wide concentration range. Environmental science & technology 45(14), 6011-6017.

Kasaraneni, V., Kohm, S.E., Eberle, D., Boving, T., Oyanedel-Craver, V., 2014. Enhanced containment of polycyclic aromatic hydrocarbons through organic modification of soils. Environmental Progress & Sustainable Energy 33(1), 47-54.

Kasaraneni, V.K., 2015. Fate and removal of contaminants in urban environment. University of Rhode Island.

Kaya, E.M.Ö., Özcan, A.S., Gök, Ö., Özcan, A., 2013. Adsorption kinetics and isotherm parameters of naphthalene onto natural-and chemically modified bentonite from aqueous solutions. Adsorption 19(2-4), 879-888.

Keller, G., Sherar, J., 2003. Low-volume road engineering: Best Management Practices: Field Guide.

Kemper, W., Van Schaik, J., 1966. Diffusion of Salts in Clay-Water Systems 1. Soil Science Society of America Journal 30(5), 534-540.

Knox, A., Michael Paller, M., Danny D Reible, D., Ioana G Petrisor, I., 2007. Innovative in-situ remediation of contaminated sediments for simultaneous control of contamination and erosion. SRS.

Krahn, J., 2004a. Seepage modeling with SEEP/W: An engineering methodology. GEO-SLOPE International Ltd. Calgary, Alberta, Canada.

Krahn, J., 2004b. Transport Modeling with CTRAN, W. GEO–SLOPE International Ltd., Canada.

Krahn, J., 2004c. Transport Modeling with CTRAN/W: an engineering methodology. GEO–SLOPE International Ltd., Canada.

Kwiatkowski, M., Welker, A.L., Traver, R.G., Vanacore, M., Ladd, T., 2007. Evaluation of an infiltration best management practice utilizing pervious concrete JAWRA Journal of the American Water Resources Association 43(5), 1208-1222.

Lagaly, G., 1986. Interaction of alkylamines with different types of layered compounds. Solid State Ionics 22(1), 43-51.

Lagerblad, B., 2005. Carbon dioxide uptake during concrete life cycle: State of the art. Swedish Cement and Concrete Research Institute Stockholm.

Lee, S., Ören, A.H., Benson, C.H., Dovantzis, K., 2011. Organoclays as variably permeable reactive barrier media to manage NAPLs in ground water. Journal of Geotechnical and Geoenvironmental Engineering 138(2), 115-127.

Lee, S.M., Tiwari, D., 2012. Organo and inorgano-organo-modified clays in the remediation of aqueous solutions: an overview. Applied Clay Science 59, 84-102.

Levinson, R., Akbari, H., 2002. Effects of composition and exposure on the solar reflectance of portland cement concrete. Cement and Concrete Research 32(11), 1679-1698.

Li, H., Kayhanian, M., Harvey, J.T., 2013. Comparative field permeability measurement of permeable pavements using ASTM C1701 and NCAT permeameter methods. Journal of Environmental Management 118, 144-152.

Liu, F., Sun, Z., 2016. Study of Hydration Process of Cement Paste with Chemical Mapping. ACI Materials Journal 113(5), 1-12.

Loijos, A., Santero, N., Ochsendorf, J., 2013. Life cycle climate impacts of the US concrete pavement network. Resources, Conservation and Recycling 72, 76-83.

López-Carrasquillo, V., Hwang, S., 2017. Comparative assessment of pervious concrete mixtures containing fly ash and nanomaterials for compressive strength, physical durability, permeability, water quality performance and production cost. Construction and Building Materials 139, 148-158.

Lowenthal, D.H., Zielinska, B., Chow, J.C., Watson, J.G., Gautam, M., Ferguson, D.H., Neuroth, G.R., Stevens, K.D., 1994. Characterization of heavy-duty diesel vehicle emissions. Atmospheric Environment 28(4), 731-743.

Marceau, M., Nisbet, M.A., Van Geem, M.G., 2007. Life cycle inventory of portland cement concrete. Portland Cement Association.

Marceau, M., Van Geem, M.G., 2007. Solar reflectance of concretes for LEED sustainable sites credit: heat island effect. Portland Cement Association.

Marr, L.C., Kirchstetter, T.W., Harley, R.A., Miguel, A.H., Hering, S.V., Hammond, S.K., 1999. Characterization of polycyclic aromatic hydrocarbons in motor vehicle fuels and exhaust emissions. Environmental science & technology 33(18), 3091-3099.

Matos, C., Sá, A.B., Bentes, I., Pereira, S., Bento, R., 2019. An approach to the implementation of Low Impact Development measures towards an EcoCampus classification. Journal of environmental management 232, 654-659.

Miguel, A.H., Kirchstetter, T.W., Harley, R.A., Hering, S.V., 1998. On-road emissions of particulate polycyclic aromatic hydrocarbons and black carbon from gasoline and diesel vehicles. Environmental Science & Technology 32(4), 450-455.

Mikkelsen, P., Häfliger, M., Ochs, M., Jacobsen, P., Tjell, J., Boller, M., 1997. Pollution of soil and groundwater from infiltration of highly contaminated stormwater-a case study. Water Science and Technology 36(8-9), 325-330.

Mikkelsen, P.S., Weyer, G., Berry, C., Waldent, Y., Colandini, V., Poulsen, S., Grotehusmann, D., Rohlfing, R., 1994. Pollution from urban stormwater infiltration. Water Science and Technology 29(1-2), 293-302.

Miller, D.A., White, R.A., 1998. A conterminous United States multilayer soil characteristics dataset for regional climate and hydrology modeling. Earth interactions 2(2), 1-26.

Montes, F., Valavala, S., Haselbach, L.M., 2005. A new test method for porosity measurements of Portland cement pervious concrete. Journal of ASTM International 2(1), 1-13.

National Economic, C., Council of Economic, A., United States. White House, O., 2014. An economic analysis of transportation infrastructure investment. White House, Washington.

Neithalath, N., Sumanasooriya, M.S., Deo, O., 2010. Characterizing pore volume, sizes, and connectivity in pervious concretes for permeability prediction. Materials characterization 61(8), 802-813.

Nguyen, D.H., Sebaibi, N., Boutouil, M., Leleyter, L., Baraud, F., 2014. A modified method for the design of pervious concrete mix. Construction and Building Materials 73, 271-282.

Noshadravan, A., Wildnauer, M., Gregory, J., Kirchain, R., 2013. Comparative pavement life cycle assessment with parameter uncertainty. Transportation Research Part D: Transport and Environment 25, 131-138.

Nourmoradi, H., Nikaeen, M., Khiadani, M., 2012. Removal of benzene, toluene, ethylbenzene and xylene (BTEX) from aqueous solutions by montmorillonite modified with nonionic surfactant: Equilibrium, kinetic and thermodynamic study. Chemical Engineering Journal 191, 341-348.

Nzengung, V.A., Nkedi-Kizza, P., Jessup, R.E., Voudrias, E.A., 1997. Organic cosolvent effects on sorption kinetics of hydrophobic organic chemicals by organoclays. Environmental science & technology 31(5), 1470-1475.

Obla, K.H., 2010. Pervious concrete—An overview. Indian Concrete Journal 84(8), 9-18.

Ollivier, J., Massat, M., 1992. Permeability and microstructure of concrete: a review of modelling. Cement and concrete research 22(2-3), 503-514.

Owabor, C.N., Ono, U.M., Isuekevbo, A., 2012. Enhanced sorption of naphthalene onto a modified clay adsorbent: effect of acid, base and salt modifications of clay on sorption kinetics. Advances in Chemical Engineering and Science 2(03), 330-335.

Pitt, R., Clark, S., Field, R., 1999. Groundwater contamination potential from stormwater infiltration practices. Urban water 1(3), 217-236.

Pitt, R.E., 1996. Groundwater contamination from stormwater infiltration. CRC Press.

Pomerantz, M., 1997. Paving materials for heat island mitigation.

Ramezani, M., Kim, Y.H., Sun, Z., 2019. Modeling the mechanical properties of cementitious materials containing CNTs. Cement and Concrete Composites 104, 103347.

Reddy, K.R., Xie, T., Dastgheibi, S., 2013. PAHs removal from urban storm water runoff by different filter materials. Journal of Hazardous, Toxic, and Radioactive Waste 18(2), 04014008.

Reddy, K.R., Xie, T., Dastgheibi, S., 2014a. Evaluation of biochar as a potential filter media for the removal of mixed contaminants from urban storm water runoff. Journal of Environmental Engineering 140(12), 04014043.

Reddy, K.R., Xie, T., Dastgheibi, S., 2014b. Mixed-media filter system for removal of multiple contaminants from urban storm water: large-scale laboratory testing.

Journal of Hazardous, Toxic, and Radioactive Waste 18(3), 04014011-04014011-04014018.

Reible, D.D., Lu, X., Galjour, J., Qi, Y., 2008. The use of organoclay in managing dissolved contaminants relevant to contaminated sediments. Technical Rep 840.

Ringler, S., 2007. First Flush Characterization of Storm Water Runoff. University of New Orleans, Louisiana, US.

Rothermich, M.M., Hayes, L.A., Lovley, D.R., 2002. Anaerobic, sulfate-dependent degradation of polycyclic aromatic hydrocarbons in petroleum-contaminated harbor sediment. Environmental science & technology 36(22), 4811-4817.

Saba, B., Hashmi, I., Awan, M.A., Nasir, H., Khan, S.J., 2012. Distribution, toxicity level, and concentration of polycyclic aromatic hydrocarbons (PAHs) in surface soil and groundwater of Rawalpindi, Pakistan. Desalination and water treatment 49(1-3), 240-247.

Santamarina, J.C., Klein, K.A., Wang, Y.H., Prencke, E., 2002. Specific surface: determination and relevance. Canadian Geotechnical Journal 39(1), 233-241.

Santero, N.J., Harvey, J., Horvath, A., 2011a. Environmental policy for long-life pavements. Transportation Research Part D: Transport and Environment 16(2), 129-136.

Santero, N.J., Masanet, E., Horvath, A., 2011b. Life-cycle assessment of pavements. Part I: Critical review. Resources, Conservation and Recycling 55(9-10), 801-809.

Schaefer, V.R., Wang, K., Suleiman, M.T., Kevern, J.T., 2006. Mix design development for pervious concrete in cold weather climates.

Schueler, T.R., 1994. First flush of stormwater pollutants investigated in Texas. Watershed Protection Techniques 1(2), 88.

Schuetzle, D., 1983. Sampling of vehicle emissions for chemical analysis and biological testing. Environmental Health Perspectives 47, 65-80.

Shackelford, C.D., 1994. Critical concepts for column testing. Journal of Geotechnical Engineering 120(10), 1804-1828.

Shang, H., 2015. Geotechnical laboratory characterization of sand-zeolite mixtures. University of Louisville, Kentucky, U.S.

Shang, H., Javadi, S., Zhao, Q., 2017. Organic Surfactant Modified Zeolite as a Permeable Reactive Barrier Component—A Laboratory Study, Geotechnical Frontiers 2017. pp. 443-449.

Shang, H., Sun, Z., 2019. PAHs (naphthalene) removal from stormwater runoff by organoclay amended pervious concrete. Construction and Building Materials 200, 170-180.

Shang, H., Sun, Z., 2021. Laboratory evaluation of PAHs removal by multi-functional green pervious concrete (MGPC) pavement. Journal of Cleaner Production, 128032.

Shang, H., Sun, Z., Bhaskar, N.R., 2020. Simulating the Long-Term Performance of Multifunctional Green-Pervious Concrete Pavement in Stormwater Runoff–Induced PAHs Remediation. Journal of Environmental Engineering 146(6), 04020033.

Shen, S., Burton, M., Jobson, B., Haselbach, L., 2012. Pervious concrete with titanium dioxide as a photocatalyst compound for a greener urban road environment. Construction and building materials 35, 874-883.

Shu, Y., Li, L., Zhang, Q., Wu, H., 2010. Equilibrium, kinetics and thermodynamic studies for sorption of chlorobenzenes on CTMAB modified bentonite and kaolinite. Journal of hazardous materials 173(1), 47-53.

Simpson, J.A., Bowman, R.S., 2009. Nonequilibrium sorption and transport of volatile petroleum hydrocarbons in surfactant-modified zeolite. J Contam Hydrol 108(1-2), 1-11.

Sivapullaiah, P., Prasad, B.G., Allam, M., 2008. Methylene blue surface area method to correlate with specific soil properties.

Sonebi, M., Bassuoni, M., 2013. Investigating the effect of mixture design parameters on pervious concrete by statistical modelling. Construction and Building Materials 38, 147-154.

Tennis, P.D., Leming, M.L., Akers, D.J., 2004. Pervious concrete pavements. Portland Cement Association Skokie, IL.

Terzaghi, K., Peck, R.B., Mesri, G., 1996. Soil mechanics in engineering practice. John Wiley & Sons, New York.

Todd, D., Mays, L., 2004. Groundwater Hydrology. Jhon Willy and Sons. Inc., New York.

Torres, A., Hu, J., Ramos, A., 2015. The effect of the cementitious paste thickness on the performance of pervious concrete. Construction and Building Materials 95, 850-859.

Tsai, W., Lai, C., Hsien, K., 2003. Effect of particle size of activated clay on the adsorption of paraquat from aqueous solution. Journal of colloid and interface science 263(1), 29-34.

Vaia, R.A., Teukolsky, R.K., Giannelis, E.P., 1994. Interlayer structure and molecular environment of alkylammonium layered silicates. Chemistry of Materials 6(7), 1017-1022.

Valocchi, A.J., 1985. Validity of the Local Equilibrium Assumption for Modeling Sorbing Solute Transport through Homogeneous Soils. Water Resour Res 21(6), 808-820.

van Genuchten, M.T., Leij, F.J., Skaggs, T.H., Toride, N., Bradford, S.A., Pontedeiro, E.M., 2013. Exact analytical solutions for contaminant transport in rivers 1. The equilibrium advection-dispersion equation. Journal of Hydrology and Hydromechanics 61(2), 146-160.

Wilcke, W., 2007. Global patterns of polycyclic aromatic hydrocarbons (PAHs) in soil. Geoderma 141(3), 157-166.

Worth, M., Guerrero, S., Meyers, A., 2016. 2016 Freight Quick Facts Report. United States. Federal Highway Administration.

Xie, T., Reddy, K.R., Wang, C., Yargicoglu, E., Spokas, K., 2015a. Characteristics and applications of biochar for environmental remediation: a review. Critical Reviews in Environmental Science and Technology 45(9), 939-969.

Xie, T., Sadasivam, B.Y., Reddy, K.R., Wang, C., Spokas, K., 2015b. Review of the effects of biochar amendment on soil properties and carbon sequestration. Journal of Hazardous, Toxic, and Radioactive Waste 20(1), 04015013.

Xu, M., Eckstein, Y., 1995. Use of weighted least-squares method in evaluation of the relationship between dispersivity and field scale. Ground Water 33(6), 905-908.

Yahia, A., Kabagire, K.D., 2014. New approach to proportion pervious concrete. Construction and Building Materials 62, 38-46.

Yan, J., Wang, L., Fu, P.P., Yu, H., 2004. Photomutagenicity of 16 polycyclic aromatic hydrocarbons from the US EPA priority pollutant list. Mutation Research/Genetic Toxicology and Environmental Mutagenesis 557(1), 99-108.

Yang, J., Jiang, G., 2003. Experimental study on properties of pervious concrete pavement materials. Cement and Concrete Research 33(3), 381-386.

Yu, B., Lu, Q., 2012. Life cycle assessment of pavement: Methodology and case study. Transportation Research Part D: Transport and Environment 17(5), 380-388.

Yu, B., Lu, Q., Xu, J., 2013. An improved pavement maintenance optimization methodology: Integrating LCA and LCCA. Transportation Research Part A: Policy and Practice 55, 1-11.

Zheng, C., Bennett, G.D., 2002. Applied contaminant transport modeling. Wiley-Interscience, New York.

Zhong, R., Leng, Z., Poon, C.-s., 2018. Research and application of pervious concrete as a sustainable pavement material: A state-of-the-art and state-of-the-practice review. Construction and Building Materials 183, 544-553.

Zhong, R., Wille, K., 2015. Material design and characterization of high performance pervious concrete. Construction and Building Materials 98, 51-60.

Zielinska, B., Sagebiel, J., Arnott, W., Rogers, C., Kelly, K., Wagner, D., Lighty, J., Sarofim, A., Palmer, G., 2004. Phase and size distribution of polycyclic aromatic hydrocarbons in diesel and gasoline vehicle emissions. Environmental Science & Technology 38(9), 2557-2567.

Zobrist, J., Müller, S., Ammann, A., Bucheli, T., Mottier, V., Ochs, M., Schoenenberger, R., Eugster, J., Boller, M., 2000. Quality of roof runoff for groundwater infiltration. Water research 34(5), 1455-1462.

CURRICULUM VITA

Hong "Rocky" Shang, P.E.

1238 Inverary Ct
Louisville, KY, 40222

Phone: (502)-206-3688
Email: hong.shang@louisville.edu

EDUCATION

- **Ph.D. candidate** in Civil and Environmental Engineering, *University of Louisville, Louisville*, KY, US, Aug. 2015 – Expected May. 2020 (GPA:3.97/4.0)
  Dissertation Title: Develop A Multi-Functional Green Pervious Concrete (MGPC) Pavement with Mitigate Polycyclic Aromatic Hydrocarbons (PAHs) Removal Function

- **M.Sc.** in Civil and Environmental Engineering, *University of Louisville, Louisville*, KY, US, Aug. 2014 – Aug. 2015 (GPA:3.68/4.0)
  Thesis Title: Geotechnical Laboratory Characterization of Sand-Zeolite Mixtures

- **B.Sc.** in Civil and Environmental Engineering, *Tongji University, Shanghai*, China, Sep. 2002 – Jul. 2006
  (Total Semester Credit Hours Earned: 147, Credential Evaluation by NCEES)
  Thesis Title: Dewatering Design for Yishanlu Station of Metro Line 9 in Shanghai

PROFESSIONAL EXPERIENCE

- **P.E.** License No. **35040** (KY)

- **Geotechnical Engineer** (2006-2014), China Institute of Geotechnical Investigation &. Surveying (CIGIS) Co. Ltd., Beijing, China
  - Site investigation and In-situ soil sampling and analysis
  - Geotechnical laboratory test and analysis
  - Survey and field measurement
  - Pipe jacking and trenchless technology design and construction supervision
  - Pile foundation design
  - Retaining wall and protection structure design for deep excavation
  - Construction scheme and geotechnical report writing

- **Projects**
  - Design and construction supervision for the electrical substation of the Beijing Olympic Beach Volleyball Court, $3M (2006-2007)
  - Site investigation of Xisanqi Residential District for over 30 buildings, which is the first price-fixed housing project in China, scheme and report writing supervision of lab analysis and this project was rewarded as The First Award of survey and design in CIGIS., Ltd, China, $260K (2008)
  - Cement fly-ash gravel (CFG) pile foundation design and construction supervision for over 50 buildings locating in Chaoyang District, Beijing, which is one of the largest affordable housing projects in China), $10M (2006-2009)
  - 3 miles, $6^{3/4}$"× 60" concrete sewer pipes, design and construction supervision with complex suburban engineering geological condition for Changping District in Beijing, China. It is a newly built sewage pipe system by using pipe jacking, the trenchless technology with TBM, jacking force 14000 kN, $20M (2009-2010)
  - 560 meters, $11^{3/4}$"× 120" concrete sewer pipes, design and construction supervision with complex coastal engineering geological condition for Tianjin Binhai New Area in Tianjin, China, one range pipe jacking with two segmental relays, jacking force 24000 kN, $12M (2010-2012).

COMPUTER SKILLS

- GeoStudio
- AutoCAD
- ABAQUS
- GIS
- MODFLOW
- OpenLCA
- SAP
- REVIT
- Microsoft Office Suite (Access, Excel, FrontPage, PowerPoint, Visio, Word)

PROFESSIONAL ACTIVITIES

- Student Member of American Society of Civil Engineering (ASCE)
- CEE departmental representative in Graduate Student Council in UofL – Fall 2017 – Summer 2019
- Committee member and reviewer of the Graduate Student Council Research Grants in UofL – Fall 2017 – Summer 2019

HONORS AND AWARDS

- Graduate Dean's Citation Award (May 2020, Ph.D. degree)
- Doctoral Dissertation Completion Award – (2020 – recent)
- Graduate Teaching Assistant Scholarship – University of Louisville – (2015 – recent)
- Graduate Research Fund – University of Louisville – (2018)
- Terracon Scholarship – Terracon – (2014 – 2015)
- The First Award of survey and design in CIGIS., Ltd, China – (2008)
- The First Prize Scholarship – Tongji University – (2005 – 2006)

TEACHING ASSISTANCE EXPERIENCES

- Construction Materials – CEE530 – UofL – Spring 2017-2019 (Instructed by: Dr. Zhihui Sun (2017) Mr. David Kessinger P.E. (2018-2019))
- Construction Materials Laboratory – CEE531 – UofL – Spring 2017-2019 (Instructed by Dr. Zhihui Sun (2017), Mr. David Kessinger P.E. (2018-2019) and Hong Shang (2017-2019))
- Field Measurements – CEE260 – UofL – Fall 2018-2019 (Instructed by Dr. Robert Kluger)
- Field Measurements Laboratory – CEE261 – UofL – Fall 2018-2019 (Instructed by Dr. Robert Kluger and Hong Shang)
- Introduction of Environmental Engineering – CEE309 – UofL – Sumer 2016, 2018-2019 (Instructed by Dr. Qian Zhao (2016) and Dr. Nageshwar Bhaskar (2017-2018))
- Statics – CEE205 – UofL – Fall 2016-2017 (Instructed by Dr. Qian Zhao (2016) Dr. Nageshwar Bhaskar (2017))
- Geomechanics Laboratory – CEE451 –UofL – Fall 2015, 2016, 2019 (Instructed by Dr. Qian Zhao (2015-2016), Omid Ghasemi Fare (2019), and Hong Shang (2015-2016, 2019))

ADDITIONAL RESEARCH PROJECTS

- Geotechnical characterization of natural and organic surfactant modified zeolite
- Adsorption and retardation behavior of organic surfactant modified zeolite on non-polar contaminant remediation
- Investigation of organo-zeolite using as a filter material for Permeable Reactive Barriers (PRBs)
- Numerical modeling of Permeable Reactive Barriers (PRBs) for long-term onsite service

PUBLICATIONS

- Shang, H., and Sun, Z. (2020). "Life Cycle Assessment (LCA) for Multi-functional Green Pervious Concrete (MGPC) Pavement" In process.
- Shang, H., and Sun, Z. (2020). "Laboratory Evaluation of PAHs Removal by Multi-functional Green Pervious Concrete (MGPC) Pavement" Submitted to Journal of Environmental Management.
- Shang, H., Sun, Z., and Bhaskar, N. R. (2020). "Simulating the Long-Term Performance of Multifunctional Green-Pervious Concrete Pavement in Stormwater Runoff–Induced PAHs Remediation." Journal of Environmental Engineering, 146(6), 04020033.
- Shang, H., and Sun, Z. (2019). "Multi-functional Green Pervious Concrete (MGPC) Pavement with Stormwater Runoff Purifying Functions" Abstract submitted to 2019 Annual Water Resources Conference.
- Shang, H., and Sun, Z. (2019). "PAHs (naphthalene) removal from stormwater runoff by organoclay amended pervious concrete." Construction and Building Materials, 200, 170-180.
- Shang, H., Javadi, S., and Zhao, Q. (2017). "Organic Surfactant Modified Zeolite as a Permeable Reactive Barrier Component—A Laboratory Study." Geotechnical Frontiers 2017, 443-449.
- Shang, H. (2015). "Geotechnical laboratory characterization of sand-zeolite mixtures," M.S. thesis, University of Louisville, Kentucky, U.S.

GRADUATE COURSES

Earth Pressures and Retaining Structures, Advanced Mechanics of Solids, Non-destructive Testing, Groundwater Hydrology, Fundamentals of Prestressed Concrete, Masonry Design, Environmental Geotechnics, Green Engineering & Sustainable Design, Finite Element Analysis for Structural Engineers, Structural Dynamics, Advanced Foundation Design, Entrepreneurship in Civil and Environmental Engineering, Numerical Methods Civil Engineering, Earthquake Engineering

REFERENCE

Dr. Zhihui Sun (Dissertation Director)
Winna Professor, Dept. Chair,
Civil & Environmental Engineering
The University of Louisville.
Email: z.sun@louisville.edu
Phone: (502) 852-4583

Dr. Nageshwar R. Bhaskar, P.E.
(Dissertation Committee member)
Professor, Director of Grad. Study,
Civil & Environmental Engineering
The University of Louisville.
Email: nageshwar.bhaskar@louisville.edu
Phone: (502) 852-4547

Dr. Tom Rockaway, P.E.
(Dissertation Committee member)
Professor, Civil & Environmental Engineering
The University of Louisville.
Email: tdrock01@louisville.edu
Phone: (502) 852-3272

Dr. Noppadon (Tik) Sathitsuksanoh
(Dissertation Committee member)
Assistant Professor, Chemical Engineering
The University of Louisville.
Email: n0sath01@louisville.edu
Phone: (502) 852-6737

Dr. Yao Zhang, P.E.
Senior Geotechnical Engineer
AECOM, Sacramento, California
The University of Michigan
Email: zhyao@umich.edu
Phone: (734) 730-1956

Mr. David Kessinger, P.E
Construction services manager
Michael Baker International
Lecturer, Civil & Environmental Engineering
The University of Louisville.
Email: dav.kessinger@mbakerintl.com
Phone: (502) 339-5877

Dr. Omid Ghasemi Fare
Assistant Professor,
Civil & Environmental Engineering
University of Louisville.
Email: o0ghas01@louisville.edu
Phone: 502-852-4616

Dr. Robert Kluger, P.E.
Assistant Professor,
Civil & Environmental Engineering
University of Louisville.
Email: robert.kluger@louisville.edu
Phone: (502) 852-4561